

**Seed Development in *Phaseolus vulgaris* L.,
Populus nigra L., and *Ranunculus sceleratus* L.
with Special Reference to the
Microtubular Cytoskeleton**

Ontvangen

31 MEI 1995

UB-CARDEX

Xu XuHan

CENTRALE LANDBOUWCATALOGUS



0000 0577 3300

40951

Promotoren: dr. M.T.M. Willemse
hoogleraar in de plantkunde
dr. A. Souvré
hoogleraar in de plantencytologie en biotechnologie
ENSAT-Toulouse

Co-promotor: dr. A.A.M. van Lammeren
universitair hoofddocent plantencytologie en morfologie

NN08201, 1944

**Seed Development in *Phaseolus vulgaris* L.,
Populus nigra L., and *Ranunculus sceleratus* L.
with Special Reference to the
Microtubular Cytoskeleton**

Xu XuHan

Proefschrift
ter verkrijging van de graad van doctor
in de landbouw- en milieuwetenschappen
op gezag van de rector magnificus,
dr. C.M. Karssen,
in het openbaar te verdedigen
op woensdag 7 juni 1995
des namiddags te vier uur in de Aula
van de Landbouwwuniversiteit te Wageningen

ISBN 9039782

CIP-GEGEVENS KONINKLIJKE BIBLIOTHEEK, DEN HAAG

Xu XuHan

ISBN 90-5485-403-0

Seed Development in *Phaseolus vulgaris* L., *Populus nigra* L., and
Ranunculus sceleratus L. with Special Reference to the Microtubular
Cytoskeleton

Cover figure: Seed (Chinese handwriting, by Hui Yu)

BIBLIOTHEEK
LANDEBOUWUNIVERSITEIT
WAGENINGEN

Stellingen

1. The shaping and elongation of endosperm alveoli is conditioned by a physical equilibrium system of microtubules at growing wall ends in the contact region of three neighbouring alveoli.

This thesis

2. The occurrence of a phragmoplast system in coenocytes required the definition of an alveolar phragmoplast.

This thesis

3. The presence, number, and position of wall ingrowths in the embryo suspensor cells of bean are indications for the direction, pathway, and intensity of the nutrient flux from the surrounding tissue via the basal part to the embryo proper.

This thesis

4. Alveolation and subsequent mitosis-derived cytokinesis are important processes in the cellularization of coenocytic endosperm. This is expected to be true also for cellularization processes occurring in the nuclear part of Helobial endosperm and in the Gymnosperm female gametophyte.

This thesis

5. What we find with natural science are only interactions between nature and the methods used.

6. The spirit of joint development should be based on an ancient Chinese proverb which runs "Qiu Tong Cun Yi" or "Seek common ground while preserving differences".

Hui Yu, 1992, *Asian Yearbook of International Law* 2: 87-112

7. "The fundamental cause of the development of a thing is not external but internal; it lies in the contradictoriness within the thing. This internal contradiction exists in every single thing, hence its motion and development. Contradictoriness within a thing is the fundamental cause of its development while its interrelations and interactions with other things are secondary causes."

Ze-Dong Mao, 1937, *On Contradiction*.

8. "Sustainable development is development that meets the needs of the present generation without compromising the ability of future generations to meet their own needs."

The World Commission on Environment and Development, 1987,
Our Common Future, p. 43.

9. Human's damaging nature is in fact the evolution of nature itself.

10. Only by writing the family name twice, Chinese preserve their identity in the west.

Stellingen behorende bij het proefschrift getiteld

"Seed Development in *Phaseolus vulgaris* L., *Populus nigra* L., and *Ranunculus sceleratus* L. with Special Reference to the Microtubular Cytoskeleton"

te verdedigen door X. XuHan op woensdag 7 juni 1995 te Wageningen

Contents

| | | |
|-----------|---|-----|
| Chapter 1 | General introduction | 7 |
| Chapter 2 | Structural analysis of embryogenesis in celery-leafed buttercup (<i>Ranunculus sceleratus</i> L.) | 17 |
| Chapter 3 | Ultrastructural and immunofluorescence studies on bean (<i>Phaseolus vulgaris</i> L.) embryogenesis with particular reference to growth patterning and microtubular configurations | 33 |
| Chapter 4 | The ultrastructure of seed coat development in <i>Ranunculus sceleratus</i> | 49 |
| Chapter 5 | Microtubular configurations during the cellularization of coenocytic endosperm in <i>Ranunculus sceleratus</i> L. | 65 |
| Chapter 6 | Microtubular configurations during endosperm development in <i>Phaseolus vulgaris</i> | 77 |
| Chapter 7 | An improved immunolabelling method for the microtubular cytoskeleton in poplar (<i>Populus nigra</i> L.) free nuclear endosperm | 91 |
| Chapter 8 | Development of coenocytic endosperm in poplar (<i>Populus nigra</i> L.): Two kinds of microtubular configurations constitute one alveolar phragmoplast during alveolation | 103 |
| Chapter 9 | General discussion | 125 |
| | Acknowledgements | 137 |
| | Samenvatting, Summary, Résumé, Chinese Summary | 139 |
| | Curriculum vitae | 150 |

Chapter 1

General Introduction

Xu XuHan

Plant Cytology and Morphology Department, Wageningen Agricultural
University, Arboretumlann 4, 6703 BD Wageningen, The Netherlands

1. SCOPE OF THIS THESIS

In this thesis, seed development is investigated in celery-leafed buttercup (*Ranunculus sceleratus* L.), bean (*Phaseolus vulgaris* L.) and poplar (*Populus nigra* L.). Developing embryos, endosperms and seed coats are investigated. The comparative study of seed morphology, anatomy and development gives insight into the different types of seed differentiation in relation to its function. A main goal of the thesis is to study the role of the microtubular cytoskeleton in plant reproduction processes. Special attention has been paid to configurations of microtubular cytoskeleton during cellularization of the endosperm. Functions of the microtubular cytoskeleton in relation to the particular organizations of microtubular populations have been analyzed based on the studies of the overall developmental patterning of tissues and organs. Cytomorphogenesis during seed development is investigated at histological and cytological levels using combined techniques of conventional light microscopy, scanning and transmission electron microscopy, and immunofluorescence light microscopy.

2. SEED MORPHOLOGY, ANATOMY, AND DEVELOPMENT

Seed

The seed is a unit of dispersal and a final phase of Spermatophytes (seed plants) reproduction, which links the successive generations. It originates from the fertilized ovule.

As a general feature of Angiosperms, mature pollen grains germinate on the stigma of the pistil, and one of the pollen tubes enters the embryo sac releasing two sperms into a synergid. One of the male gametes fuses with the egg cell forming the zygote, while the other male gamete fuses with the central cell forming the primary endosperm cell. Seed development starts immediately after the double fertilization. Angiospermic seeds exhibit a great

morphological and structural diversity (Boesewinkel and Bouman 1984). In general, a typical Angiosperm seed consists of three components: the embryo, the endosperm and the seed coat, which can be schematically drawn as in Fig. 1. The endosperm is often absent in the mature seed.

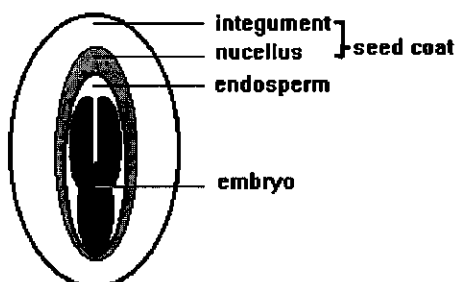


Fig. 1. A diagrammatic representation of an Angiosperm seed.

Zygotic embryo

The zygotic embryo is the main part of the seed from the reproduction point of view. It is the individual plant at the initial phase of the new generation. The development of the embryo starts in the embryo sac (Willemse and van Went 1984) after gamete fusion between the haploid egg cell and a haploid sperm cell. The fused cell is the diploid zygote (van Went and Willemse 1984), which represents the first cell of the next generation. In most cases, with exception of Paeoniaceae (Johri et al. 1992), the zygote divides to give rise to the embryo. In dicots, the embryo develops, via proglobular, globular, heart-shaped, torpedo-shaped and cotyledonary stages, to the mature stage. Recently the molecular and cytological events of embryogenesis get more attention (de Jong *et al.* 1993). In this thesis, embryo development and especially the cytological aspects involved, are investigated in *R. sceleratus* and *Ph. vulgaris*, as discussed in Chapters 2 and 3. Based on previous embryological descriptions on the two species, *R. sceleratus* has small sized embryos and *Ph. vulgaris* has large sized ones. The differentiation

of the various parts of the embryo, i.e. suspensor, embryo axis and cotyledons varies in the two species. Thus, using the two species for the present work helps to understand the embryogenesis in a comparative way. At the same time, it provides information on general developmental patterns and relations between embryogenesis and endosperm ontogeny.

Endosperm

In Angiosperms, the endosperm is the tissue derived from the fertilized central cell after fusion between one sperm and the central cell. The sperm nucleus fuses with the two polar nuclei or, more often, with the fused product of the two polar nuclei, the secondary nucleus. The endosperm is an Angiosperm-specific tissue and because the primary nucleus of the endosperm is formed by the fusion of three nuclei, its nuclear condition is often triploid at its early developmental stages (Vijayaraghavan and Prabhakar 1984). Concerning the evolutionary origin of the endosperm, two models are in discussion (Friedman 1994).

There are three types of endosperm development: Cellular Type, Free Nuclear Type and Helobial Type (Vijayaraghavan and Prabhakar 1984). In the Cellular Type, the first nuclear division is followed by cytokinesis whereas in the Free Nuclear Type, the first cycles of nuclear divisions are not followed by cytokinesis, thus, resulting in a multinuclear structure, a coenocyte. The Helobial Type is an intermediate of the types mentioned above. The free nuclear type is subject to the present studies. Endosperm development and involved cytological events are investigated in *R. sceleratus* (Chapter 5), *Ph. vulgaris* (Chapter 6) and *P. nigra* (Chapters 7 and 8). Although they belong to different taxa, i.e. Ranunculaceae, Leguminosae and Salicaceae, respectively, these species are chosen because the developmental patterns of their endosperm all belong to the Free Nuclear Type (Johri et al. 1992). Besides, in *R. sceleratus* the endosperm persists in the mature seed, in *Ph. vulgaris* and *P. nigra*, the endosperms are already used to nourish the embryos. In *P. nigra* and *R. sceleratus*, endosperm cellularization differs from that found in *Ph. vulgaris*.

Seed coat

The seed coat is the envelope of the seed and serves mostly as a protective layer. During seed development, the outer layers of the ovule, *i.e.*, integuments sometimes with nucellus, differentiate to the seed coat.

Depending on the species, the developing seed coat exhibits various patterns of structural and morphological differentiation and can be characterized by the different contribution of the nucellus and integument (Boesewinkel and Bouman 1984). Seed coat development and ultrastructural characteristics are studied in *R. sceleratus*, as described in Chapter 4.

3. MICROTUBULAR CYTOSKELETON

There are three major classes of cytoskeletal elements in eukaryotic cells: microtubules, intermediate filaments and microfilaments. They function in spatial shaping of the cell. Although with many molecular varieties, all these cytoskeletal elements are present in plant cells, and play important roles in cytomorphogenesis (Lloyd 1982, 1991). The present study pays special attention to the microtubular cytoskeleton during seed development.

Microtubules and tubulins

A microtubule is an unbranched cylinder, about 25 nm in external diameter, with an open central channel of about 15 nm. It is assembled from heterodimers containing one α -tubulin polypeptide and one β -tubulin polypeptide. Each of the tubulins has a molecular weight near 50 kD and about 450 amino acids. A third tubulin type, γ -tubulin, generally forms a part of the organizing region rather than assembling into microtubules, and will not be subject to the present work. A microtubule is generally made up by 13 protofilaments each of which contains a chain of about 8 nm long, α - β tubulin heterodimers. The heterodimers are asymmetrical and oriented in one direction. The α -tubulin side is termed plus side/end and the β -tubulin side the minus side/end. Fig. 2 shows the construction of a microtubule. A

microtubule is a polar and dynamic structure that assembles and disassembles during the whole cell cycle in living cells, *i.e.* tubulin heterodimers are constantly added to or released from both ends. In certain cases they are added more to the plus end and released more from the minus end. The assembly is initiated by the microtubule organizing center (MTOC), or by self-assembly. Through microtubule-associated proteins (MAPs), microtubules can interact with other cytoskeletal elements and organelles. In the present work as reported in Chapters 5, 6 and 8, microtubules are analyzed with respect to their mechanical function as a part of the integrated dynamic framework in the cytoplasm.

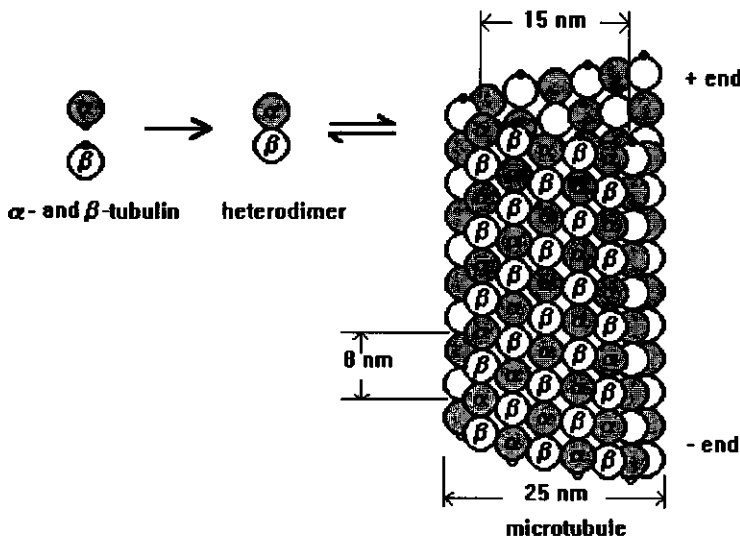


Fig. 2. Schematic representation of the architecture of a microtubule and its components.

Visualization of microtubules

Like other structural elements of the cell, microtubules can be preserved by chemical fixation, *e.g.* they are fixed by aldehyde-based fixatives. For transmission electron microscopy, post-fixation with osmium tetroxide is

recommended. Microtubules can also be studied immunocytochemically based on the biochemical characteristics of the proteinous α - and β -tubulins. These polypeptides can be fixed for a proper time length by formaldehyde without loss of antigenicity, and labeled by polyclonal or monoclonal antibodies, e.g. anti- α -tubulin and anti- β -tubulin. The primary antibody reacts with a secondary antibody that is conjugated with either a fluorescent marker that can be observed by fluorescence light microscopy, or heavy metal particles such as gold, to be detected with conventional light microscopy and electron microscopy.

Sectioning samples sets free the cellular elements, and enhances antibody penetration by diffusion. Proper *in situ* immunochemical reactions still depend on optimizing various parameters during processing. Fixation plays an important role in the preservation of microtubular antigenicity and structural integrity. The biochemical characteristics of microtubules in relation to the *in situ* preservation of the integrity of the microtubular network and the antigenicity of tubulin are studied in Chapter 7, in which an improved immunolabelling method for the microtubular cytoskeleton in *P. nigra* nuclear endosperm is described and discussed. Furthermore, it is of great importance to combine conventional light microscopy with immunocytochemistry and electron microscopy on properly fixed, oriented and sectioned material, and to follow development chronologically. Serial sections are also necessary to get a proper 3-dimensional insight into the developing structures. The analysis of successive microtubular configurations will result in a better understanding of the development of the microtubular cytoskeleton. In the present work, based on the utilization of electron microscopy, conventional light microscopy and immunocytochemical staining procedures, the subcellular structures and histological events leading to seed development are analyzed

Microtubular configurations and general functions in plant cells

According to Derksen *et al.* (1990) and Goddard *et al.* (1994), five major classes of microtubular organizations are distinguished based on their

collective configurations in higher plant cells: cortical array, radiating array, preprophase band, spindle and phragmoplast. The microtubular cytoskeleton functions in cytomorphogenesis, especially in the mechanical support and the maintenance of polarity in all living plant cells. The cortical microtubules are generally positioned in the peripheral areas of plant cells. Microfibre deposition sometimes is highly related to the orientation of the cortical microtubules. Cell elongation and enlargement also coincide with the configurational change of the cortical microtubules. The radiating arrays of microtubules are the population that run from the surface of nucleus into the cytoplasm and appear both in plant cells and in animal cells. This population of microtubules forms and maintains a nuclear domain and regulates nuclear positioning. The preprophase band, spindle and phragmoplast microtubular populations are related to karyokinesis and/or cytokinesis. The preprophase band in the mononuclear cell of the plant determines the division plane of the nucleus. The spindle microtubules function in chromosome movement both in plant cell and in animal cell division. The phragmoplast microtubules are responsible for the cell plate formation during cytokinesis in plant cells. In some algae a phycoplast appears with microtubules parallel to the cell plate. Fig. 3 shows configurations and generally believed functions of microtubules in higher plant cells. Whenever possible, these microtubular configurations and functions will be compared in each chapter of this thesis.

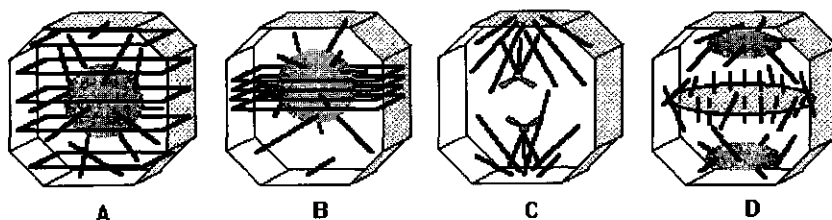


Fig. 3. A Schematic overview of microtubular configurations commonly occurring in higher plant cells. (A) Interphase, cortical and radiating microtubular arrays. (B) Preprophase, Preprophase microtubule band. (C) Karyokinesis, spindle. (D) Cytokinesis, phragmoplast.

Phragmoplast microtubules

From the point of view of developmental and reproduction biology, cell division is an important event. A major function of microtubules, therefore, is the role they play in cell divisions. Among the three configurations of microtubules associated with plant cell division, *i.e.* preprophase band, spindle and phragmoplast, only the spindle configuration exists both in animal and plant cells. In the Chapters 5, 6 and 8, microtubular organizations, mainly phragmoplasts, are investigated during endosperm development. Endosperms of all the three species used in this thesis, *i.e.* *R. sceleratus*, *Ph. vulgaris* and *P. nigra*, belong to the Free Nuclear Type. In these species, there are few data on cytoskeletons in the endosperm, and on the detailed roles of the cytoskeletons in endosperm cellularization. Studies addressed to the process of endosperm cellularization initially provide an approach to microtubular function in cell wall formation. Particularly, in Chapter 5, the phragmoplast in *R. sceleratus* is investigated and the phragmoplast microtubular configurations are modeled. In Chapters 6, phragmoplast microtubular configurations are studied in *Ph. vulgaris*, and the origin of the axial phragmoplast microtubular configuration is revealed. Followed by an improvement of immunolabelling, which is described in Chapter 7, the characteristic types of phragmoplasts are modeled in Chapter 8.

Finally, in the general discussion (Chapter 9), the embryogeny and endosperm formation of the *R. sceleratus*, *Ph. vulgaris* and *P. nigra* are compared in the perspective of organogenesis, cellularization, nutrition, and the role of the microtubular cytoskeleton involved.

REFERENCES

- Boesewinkel, F.D., and Bouman, F. (1984) The seed: Structure. *In*: Johri, B.M. (ed.) *Embryology of Angiosperms*. Springer-Verlag, Berlin, Heidelberg, pp. 567-610.
- de Jong, A.J., Schmidt, E.D.L., and de Vries, S. (1993) Early events in higher-plant embryogenesis. *Plant Molecul. Biol.* **22**:367-377.
- Derksen, J., Wilms, F.H.A., and Pierson, E.S. (1990) The plant cytoskeleton: its significance in plant development. *Acta Bot. Neerl.* **39**:1-18.

Chapter 1. General introduction

- Friedman, W. (1994) The evolution of embryogeny in seed plants and the developmental origin and early history of endosperm. *Am. J. Bot.* **81**: 1468-1486.
- Goddard, R.H., Wick, S.M., Silflow, C.D., and Snustad, D.P. (1994) Microtubule components of the plant cell cytoskeleton. *Plant Physiol.* **104**:1-6.
- Johri, B.M., Ambegaokar, K.B., and Srivastava, P.S. (1992) Paeoniaceae. In: Johri, B.M., Ambegaokar, K.B., and Srivastava, P.S. (eds.) *Comparative Embryology of Angiosperms*. Springer-Verlag, Berlin. Vol. 1. pp. 325-328.
- Lloyd, C.W. (1982) *The Cytoskeleton in Plant Growth and Development*. Academic Press, London.
- Lloyd, C.W. (1991) *The Cytoskeletal Basis of Plant Growth and Form*. Academic Press, London.
- van Went, J.L., and Willemse, M.T.M. (1984) Fertilization. In: Johri, B.M. (ed.) *Embryology of Angiosperms*. Springer-Verlag, Berlin, Heidelberg. pp. 273-317.
- Vijayaraghavan, M.R., and Prabhakar, K. (1984) The endosperm. In: Johri, B.M. (ed.) *Embryology of Angiosperms*. Springer-Verlag, Berlin, Heidelberg, pp. 319-376.
- Willemse, M.T.M., and van Went, J.L. (1984) The female gametophyte. In: Johri, B.M. (ed.) *Embryology of Angiosperms*. Springer-Verlag, Berlin, Heidelberg, pp. 159-196.

Chapter 2

Structural Analysis of Embryogenesis in Celery-leafed Buttercup (*Ranunculus sceleratus* L.)

X. XuHan and A.A.M. van Lammeren

Department of Plant Cytology and Morphology, Wageningen Agricultural
University, Arboretumlaan 4, 6703 BD Wageningen, The Netherlands

Abstract. The embryo development and seed formation of *Ranunculus sceleratus* was investigated by light and electron microscopy. The pollen tube entered the embryo sac one day after pollination. The division of the zygote was transversal. From three-celled proembryo, the basal cell gave rise to a multicellular suspensor, and the middle and upper cells formed the embryo proper. Therefore, we conclude that the embryogeny in *R. sceleratus* deviates from the Onagrad Type. The suspensor exhibited limited development until 8-cell stage, and persists in the mature seed. Cellularization of the nuclear endosperm coincides with accumulation of storage products. Multivesicular structures were observed in the endosperm. They were probably involved in metabolite transport between the apoplast and the symplast. The endosperm occupied the greater part of the mature seed, and was filled with lipid and starch. Endosperm cells surrounding the embryo suspensor persisted whereas those surrounding the embryo proper degenerated, indicating a site-specific interaction with the embryo.

Key words: embryo, endosperm, multivesicular structure, *Ranunculus sceleratus*, seed

INTRODUCTION

Embryological data of *Ranunculus sceleratus* L. have long been recorded (Souèges 1913, Singh 1936, Vijayaraghavan and Bhat 1982, Cardemil and Jordan 1982, Bhandari and Chitralkha 1989, also see Johri *et al.* 1992 for review). The embryogeny is described to belong to the Onagrad Type in which the zygote divides transversally first. Then, the basal cell gives rise to the suspensor by repeated transversal divisions in the first cycles of cytokinesis, whereas the apical cell forms the embryo proper by the first cycles with longitudinal divisions (Johansen 1950, Natesh and Rau 1984). In such type of embryogeny, the basal cell will not contribute to the formation of the embryo proper. During the embryogeny, the endosperm development is characterized by the transition from the free nuclear, to the alveolar, and finally to the cellular phase (XuHan and Van Lammeren 1994). The interaction between the embryo and the endosperm is, however, not studied in detail yet, although of major importance for the understanding of sexual reproduction of *R. sceleratus* as analyzed in, *e.g.* maize (Schel *et al.* 1984). In this paper, we present structural data of the embryogenesis, and analyze the interaction with the endosperm surrounding the embryo proper and the suspensor.

MATERIALS AND METHODS

Wild plants of *Ranunculus sceleratus* L. (Ranunculaceae) were collected in the field and transplanted to the greenhouse. For scanning electron microscopy whole ovaries were directly observed with a Yeol scanning electron microscope. Callose containing pollen tubes were visualized in hand-cut sections of fresh ovaries stained with 1% aniline blue in phosphate buffered saline (PBS), pH 9, and observed with a UV microscope. Light and transmission electron microscopy was the same as described previously (XuHan and Van Lammeren 1993, 1994). Briefly, developing seeds were excised from achenes and were fixed in 4% glutaraldehyde for 6h and then in 1% osmium tetroxide for 6h, both in PBS, pH 7. Samples were dehydrated, and embedded in low viscosity resin (Spurr 1969). Semithin sections were stained with Toluidine Blue O and examined with light microscope. Ultrathin

sections were stained with uranyl acetate followed by lead citrate and examined with a JEM-1200 EXII transmission electron microscope operating at 80 kV.

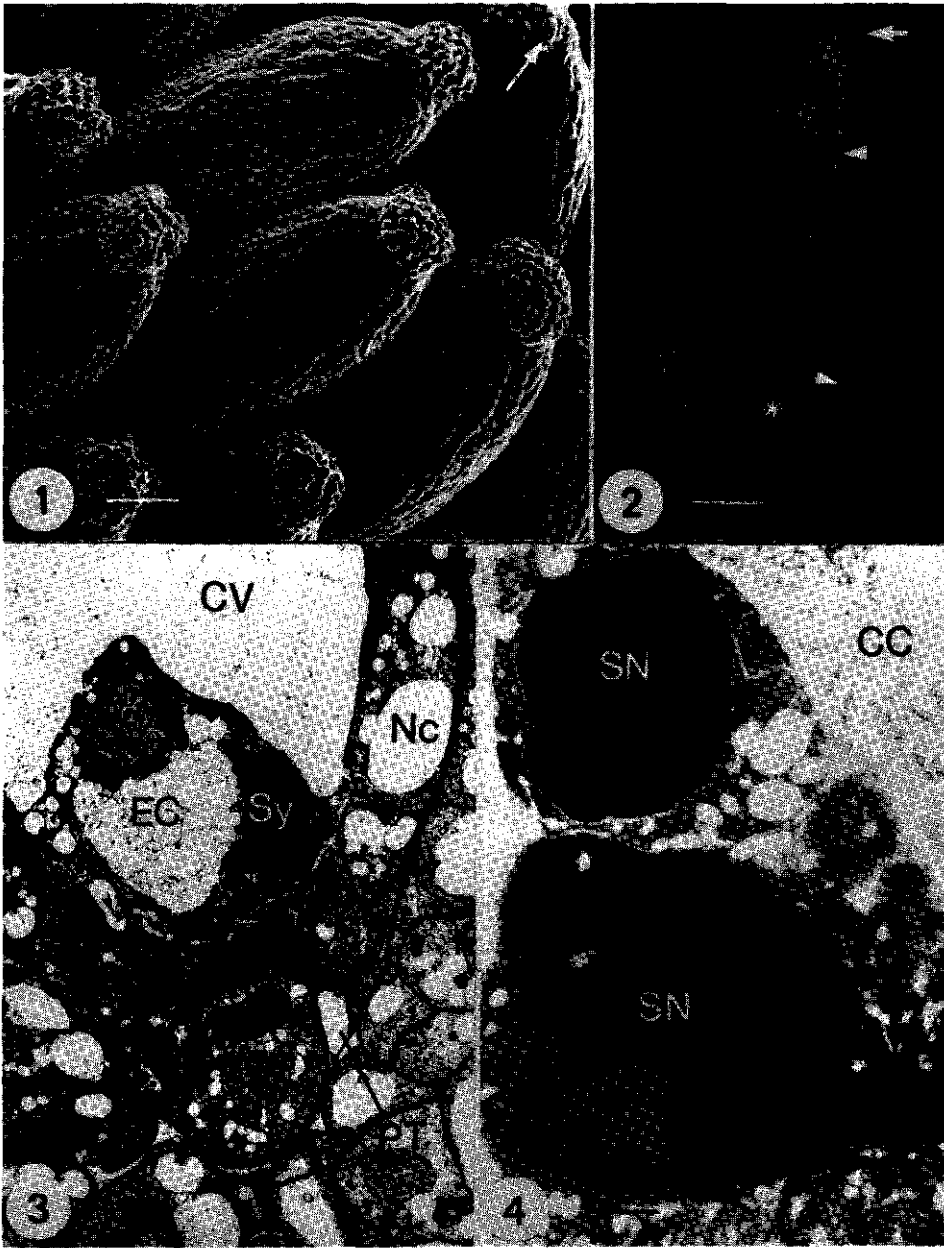
RESULTS

1. Progamic phase

When flowers of *R. sceleratus* bloomed, pistils showed embryo sacs at the seven-celled stage with either fused or unfused polar nuclei. Receptive stigmas exhibited papillate cells (Fig. 1). Pollen grains germinated on the receptive stigma within 30 min after shedding and pollen tubes grew into the ovary along the ovary cavity towards the basal funicular tissue of the single ovule (Fig. 2). One pollen tube passed the micropyle, grew through the nucellus, entered a synergid and released its contents (Fig. 3). Serial sectioning of the same ovule revealed that the two sperms were released in the middle area of the synergid (Fig. 4), whereas two x-bodies (the vegetative nucleus and synergid nucleus) were positioned in the micropylar part of the synergid. The cytoplasm of all female gametophyte cells contained large arrays of endoplasmic reticulum (ER).

The microtubular cytoskeleton was visualized around the time of fertilization. No difference in MT configurations were observed in nucellus cells before and after arrival of the pollen tube. MTs were also present throughout the cytoplasm in all the cells in the embryo sac. Before the pollen tube entered a synergid, cortical MTs were present in both synergids, and near

Fig. 1. Scanning electron micrograph of a *R. sceleratus* flower showing pistils with papillate dry stigmas. The arrow points to a pollen grain. Bar = 100 μm . **Fig. 2.** Fluorescence micrograph showing a longitudinal section of pistil with pollen grains (arrow) germinated on the stigma. The pollen tubes (arrowheads), stained with aniline blue, grow through the style into the ovary loculus towards the micropyle (*). Additional fluorescence was caused by chloroplasts and xylem. Bar = 100 μm . **Fig. 3.** Electron micrograph showing the growth of the pollen tube (PT) through the micropyle and its entrance into a synergid (Sy). It releases its contents into that synergid. CV, central vacuole; EC, egg cell; Nc, nucellus. Bar = 5 μm . **Fig. 4.** Electron micrograph of an adjacent section of Fig. 3 showing two released sperms in the synergid. Note the thin layer of cytoplasm around the sperm nuclei (SN). The lower sperm shows a tail-like structure (arrow). CC, central cell. Bar = 1 μm .

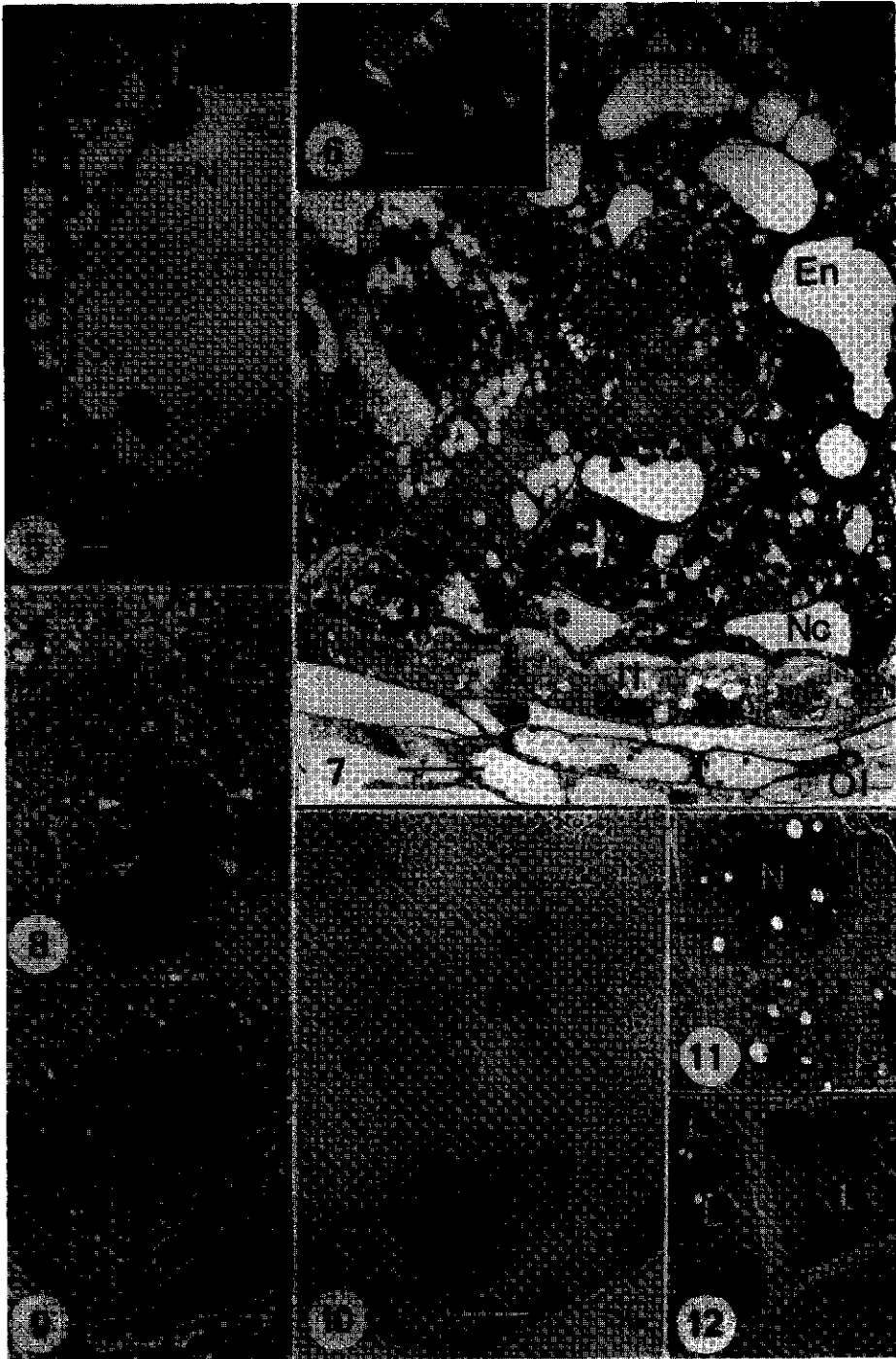


the micropylar part they were found approximately parallel to the profiles of the filiform apparatus. After the pollen tube released its contents into the synergid, MTs were no longer detectable in the entire synergid. At this stage, the three antipodal cells contained few randomly oriented MTs. Wall ingrowths of the transfer cell type were present in the antipodal cell walls bordering the hypostase (see Fig. 18).

2. Embryo

After fertilization, the zygote still had its nucleus positioned at the chalazal side (Fig. 5). At 32 h after pollination (HAP), when the primary endosperm had divided for two cycles, the zygote divided transversally, giving rise to a large basal cell and a small apical cell. At 3 days after pollination (DAP), a 3-celled linear embryo was formed with an apical cell, a small middle cell, and a vacuolated large basal cell (Fig. 6). At 5 DAP, the 3-celled embryo had turned into a 5-celled embryo by longitudinal division of the upper two cells. At 6 DAP, the apical cells of the embryo had divided longitudinally once more, and the basal cell divided once. At 7 DAP, the upper cells of the embryo continued longitudinal division, and the suspensor contained 4 cells (Fig. 7). The middle cell of the former three celled embryo now had divided

Fig. 5. Longitudinal section of ovule showing the zygote (Zy), a free endosperm nucleus (EN) and antipodal cells (AC) in the embryo sac. The persistent synergid (Sy) adjacent to the zygote is still visible. CV, central vacuole. Bar = 10 μ m. Fig. 6. Low magnification micrograph of longitudinal section through a three-celled proembryo. Note the vacuolated basal cell (arrow), and the smaller middle and apical cells. Arrowheads point to the two transversal walls. Bar = 10 μ m. Fig. 7. Proglobular embryo, showing the embryo proper and the 4-celled suspensor. Note the longitudinal division in the upper cells of the embryo proper. Chromosomes are indicated by an arrow. Endosperm (En) surrounding the apical part of the embryo has not yet degenerated. Arrowheads point to the two transversal walls of the former 3-celled embryo. II, inner integument; Nc, nucellus; OI, outer integument. Bar = 10 μ m. Fig. 8. Globular embryo and cellular endosperm (En). Note the degeneration of the cellular endosperm (arrow) surrounding the embryo, and the 8-celled embryo suspensor. Arrowheads point to the two transversal walls of the former 3-celled embryo. Bar = 200 μ m. Fig. 9. Older stage of globular embryo. Note the accumulation of reserve materials in the endosperm cells. Bar = 20 μ m. Fig. 10. Mature seed. The embryo was at cotyledonary stage with a small suspensor (arrow). The persistent endosperm (En) occupied the largest part of the seed and accumulated many lipid droplets. Note the absence of storage products and the degeneration of the endosperm cells (DE) near the embryo (Em). Co, cotyledon; E, epistase; SC, seed coat. Bar = 100 μ m. Fig. 11. Electron micrograph of cotyledon cells of the embryo shown in Fig. 10. Note the accumulation of starch, lipid droplets, and vesicles. N, nucleus. Bar = 5 μ m. Fig. 12. Electron micrograph of endosperm cells of the seed shown in Fig. 10. Detail at the transition area from the lipid (L) accumulating endosperm cells to the empty endosperm cells (*) surrounding the embryo. Arrows indicate the thin layer of degenerating cytoplasm. Bar = 5 μ m.



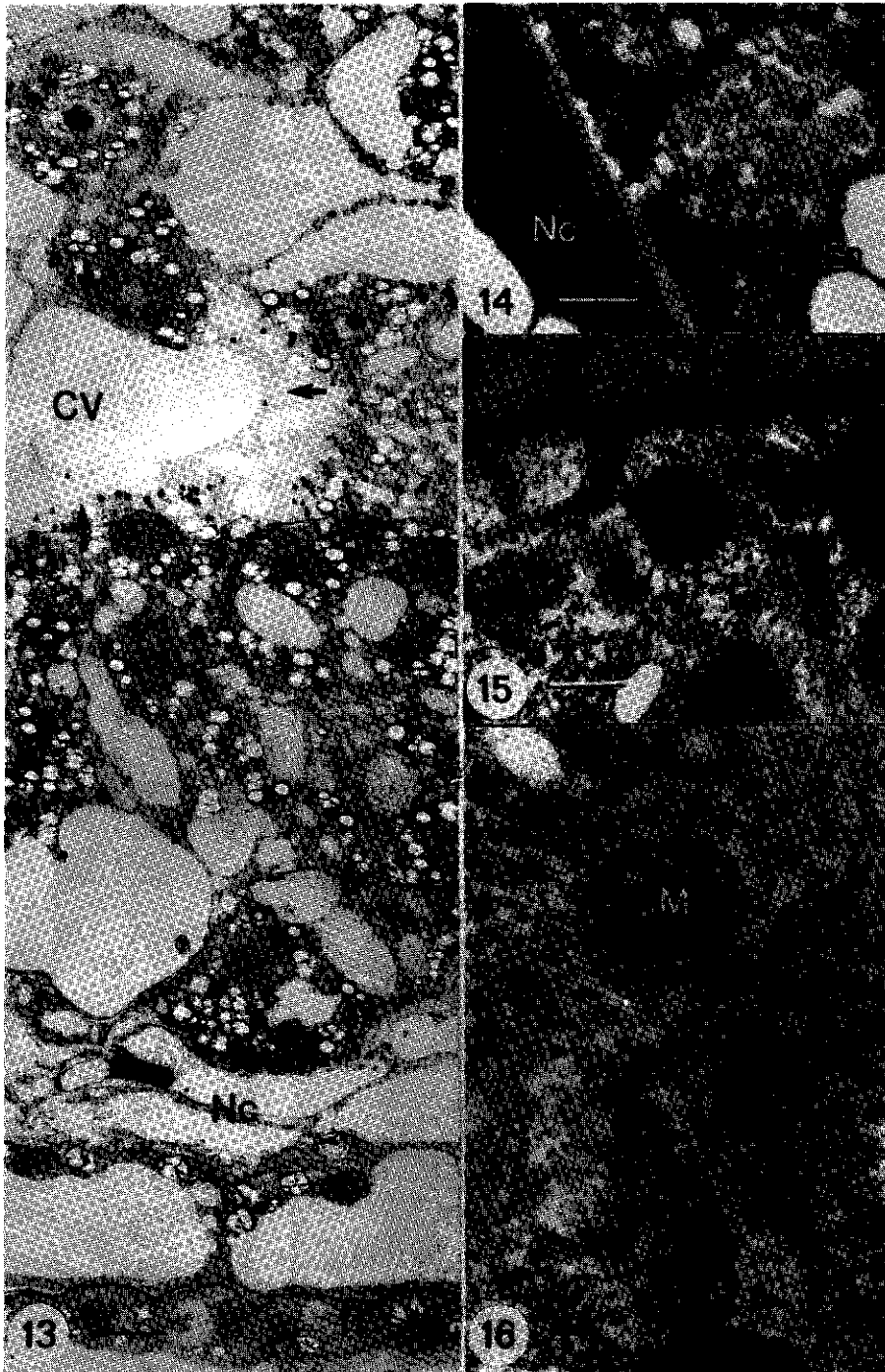
longitudinally and transversely, forming the lower part of the embryo proper (Fig. 7). The basal cell exhibited transversal divisions and formed a file of 4 suspensor cells, in which the upper cell was the hypophysis. During the early development, very few and small starch grains and lipid droplets were found in both the embryo proper cells and the suspensor cells. (Fig. 7). Extensive MTs and a dense population of ribosomes were found in all embryo cells.

The embryo proper cells exhibited more cell divisions than the suspensor cells, and the size of the embryo proper rapidly enlarged at the globular stage. Comparing embryos of 10 DAP with younger stages, the original cell lineage was still recognized (Fig. 8). At the same time, the four suspensor cells had divided once longitudinally, and had formed a two-cell-thick 8-celled suspensor (Fig. 8). The suspensor exhibited neither elongation nor enlargement. Further cell divisions of the outer cells of the globular embryo proper resulted in the development of the protoderm and the enlargement of the embryo proper around which the endosperm degenerated (Fig. 9). In the mature seed (25 DAP, Fig. 10), a small sized embryo remained at the cotyledonary stage. The cotyledon cells contained many lipid droplets (Fig. 11). The small suspensor, with two files of four or five cells each, persisted in the mature seed (Fig. 10). The length of the embryo was about 1/3 of the seed length. Each ovary contained one seed. In 200 ovaries sampled, no aborted seeds were found.

3. Endosperm

Initially the endosperm was free nuclear (Fig. 5). Nuclei became regularly spaced in the cytoplasm surrounding the central vacuole of the central cell. Cellularization of the free nuclear endosperm started at the pro-globular embryo stage. The process of the cellularization was preceded by alveolation

Fig. 13. Electron micrograph of the middle part of the seed at the final stage of endosperm cellularization showing the accumulation of reserve materials. Note that the front edge of alveolation (arrows) is about to fuse with the edge of the opposite side. Arrows point to the directions of endosperm cellularization. CV, central vacuole; Nc, nucellus; II, inner integument. Bar = 10 μ m. **Fig. 14.** Electron micrograph of a multivesicular structure of an endosperm cell (En) bordering the nucellus (Nc) The multivesicular structure is attached to the embryo sac wall. Bar = 500 nm. **Fig. 15.** Electron micrograph showing a multivesicular structure (arrow) in the endosperm cell (En) bordering the embryo (Em). Bar = 500 nm. **Fig. 16.** Electron micrograph of endosperm alveoli showing the vesicles (arrows) in the newly formed wall (W). Note the connection of a mitochondrion (M) to the wall. Bar = 200 nm.



of the free nuclear endosperm. Alveoli surrounding the central vacuole of the endosperm had lateral walls anticlinal to the embryo sac wall. These walls maintained a freely growing pattern and the wall ends were directed to the central vacuole. When the lateral walls of the alveoli grew to the central area of the embryo sac, their wall ends pushed against the tonoplast of the central vacuole and they eventually met and fused in the central area, replacing the central vacuole (Fig. 13).

The endosperm started to accumulate storage materials as starch grains and lipid droplets at the late free nuclear stage, and the accumulation continued during further development. Before cellularization had completed, more starch grains were found than lipid droplets (Fig. 13). After cellularization had finished, however, more lipid droplets were found than starch grains (Fig. 7). In mature endosperm, large lipid droplets were accumulated in all the endosperm cells. However, no reserve materials were present in the endosperm cells surrounding the embryo proper (Figs. 10, 12).

The endosperm cells close to the embryo started to be used by the embryo at the globular stage (Fig. 8). This process was further enhanced in the later developmental stages (Figs. 9, 10). In the mature seed, significant degeneration occurred in the endosperm cells close to the embryo proper that already occupied a part of the space originally filled by the endosperm (Figs. 10, 12). The endosperm cells adjacent to the suspensor did not exhibit degeneration (Figs. 8, 10).

During endosperm cellularization, many multivesicular structures were observed in the endosperm. These structures consisted of many membranous vesicles which gathered apoplasmically into groups enveloped by a membrane (Fig. 14). Sometimes parts of the envelope exhibited a double membrane appearance. Multivesicular structures were frequently found in the endosperm cells bordering the nucellus (Fig. 14) and the embryo (Fig. 15), and especially between endosperm alveoli or between endosperm cells (Fig. 16). Darkly stained materials, likely from degenerating nucellus cells, were found in the embryo sac wall and connected with the multivesicular structures. Golgi bodies, ER, plastids and mitochondria were often observed close to the multivesicular structure. We observed that mitochondria were

connected to the cell membrane where vesicles of the multivesicular structure seemed to accumulate (Fig. 16).

3. Antipodal cells

Three antipodal cells bordered the chalazal side of the embryo sac (Fig. 5). They were about 10 times larger than the nucellus cells in the chalazal area (Fig. 17). At the mature embryo sac stage, wall ingrowths were already formed on their cell walls sheared with the hypostase cells. They remained well developed during early stages of embryo development and extended deep into the cytoplasm of the antipodals (Fig. 18). Some wall ingrowths were also developed on the common walls between the antipodal cells. Cortical MTs ran along or between the profiles of the wall ingrowths. Initially the antipodal cells contained large numbers of mitochondria and extensive flattened ER. Later, ER exhibited swelling (Fig. 18), and during next development stages, many lipid droplets accumulated, but almost no starch grains appeared. The antipodal cells degenerated from the globular embryo stage onwards (Fig. 17).

4. Epistase, hypostase and nucellar stalk

In the micropylar region the ovules of *R. sceleratus* formed a poorly developed epistase, the cells of which differed from the neighbouring nucellus cells in having smaller vacuoles, more densely stained cytoplasm and accumulation of lipid droplets (Figs. 5, 7). In the mature seed, the epistase cells had degenerated (Fig. 10). The chalazal part of the nucellus differentiated a hypostase consisting of a few cells with thick walls bordering the antipodal cells, and a nucellar stalk running from the hypostase to the attachment site of the nucellus in the ovule (Fig. 17). The cells of the hypostase exhibited disintegration of the cytoplasm and contained no storage materials at the early globular embryo stage (Figs. 17, 18). Compared with other nucellus cells in its surrounding area, the cells of the nucellar stalk contained less starch grains. Lipid droplets in the nucellar stalk exhibited polar distribution: less lipid accumulation occurred near the hypostase and more near the attachment site of the nucellus (Fig. 17).

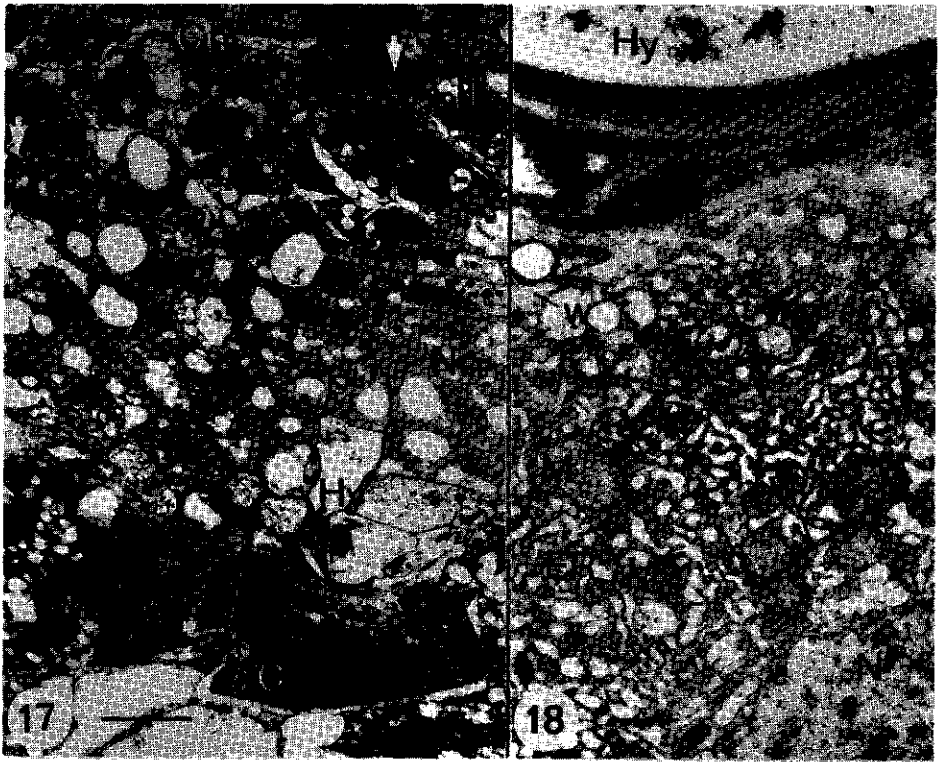


Fig. 17. Electron micrograph of hypostase and antipodal cells at the pro-globular embryo stage as shown in Fig. 7. Arrows point to cuticles of the integuments bordering the nucellus (Nc) attachment sites. Note the gradient of accumulation of lipids along the nucellar stalk towards the antipodal cells (AC). Ch, chalaza; Hy, hypostase; II, inner integument. Bar = 10 μm . **Fig. 18.** Electron micrograph of antipodal cell bordering the nucellus. Note the wall ingrowth (W) and extensive ER. Hy, hypostase; M, mitochondrion; N, nucleus. Bar = 1 μm .

DISCUSSION

1. Embryo developmental type

According to Souèges (1913, 1914) and Singh (1936) the embryogeny in *Ranunculus* proceeds through the Onograd Type (also see Johri *et al.* 1992). In that type, as represented by *Myosurus minimus* (Johansen 1950), the apical cell of the two-celled embryo divides longitudinally and the basal cell divides transversally. The embryo proper is formed by the apical cell for the greatest part, and the very basal end of the embryo proper is formed by the hypophysis which on its turn is derived from the basal cell of the two-celled embryo. In the present work, we observed three-celled embryos in which the two upper cells seemed to be formed by transversal division of the apical cell. The upper cell gave rise to the upper part of the embryo proper whereas only the sub-apical cell of the three-celled embryo gave rise to the middle part of the embryo proper. At the very basal end of the embryo proper, the hypophysis is derived from the basal cell of the former three-celled embryo (Fig. 19). Apparently, the developmental pattern in *R. sceleratus* deviates from the pattern described, though Johansen (1950) mentions that the proembryo stages are very irregular.

2. Nutrient transport pathways

In the developing seed of *R. sceleratus*, reserve materials have been previously investigated (Vijayaraghavan and Bhat 1982). The results from the present research are similar to those findings, but add further information at the ultrastructural level. Micropylar and chalazal pathways are proposed for the early and later transport of nutrients into the embryo sac. Based on the structural data, the transport through the chalazal zone is probably the main nutrient supply pathway in *R. sceleratus*. The nutrients are transported apoplasmically to the antipodal cells via the nucellar-stalk and hypostase and finally through the wall ingrowths of the antipodal cells. Such wall ingrowths, which enhance the short-distance transport of metabolites (Gunning and Pate 1969), have been described recently for *R. sceleratus* (Chitrlekha and Bhandari 1991). Along the pathway in the nucellar stalk, a change of storage

products from starch to lipid and the eventual absence of storage products points to a gradient, likely caused by the turn over and transport of metabolites. Because the hypostase cells degenerate and the cell wall ingrowths of the antipodals develop from a very early stage onwards, we propose that the apoplasmic transport of nutrients exists from early postgamic phase onwards. Based on the structure of the micropylar nucellus forming the epistase (whose dense cytoplasm forms a striking contrast to the degeneration of cytoplasm in the hypostase), and the limited development of the suspensor, we assume that embryo sac directed nutrient transport via the micropylar nucellus only occurs in a limited scale. Additionally, the limited development of the suspensor and the persistence of its surrounding endosperm do neither point to important functions in the transport of nutrients through the suspensor towards the embryo proper, nor to a major influence of the suspensor on the positioning of the embryo proper.

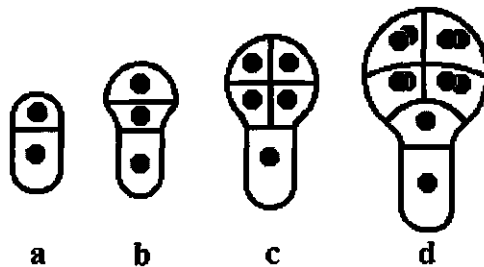


Fig. 19. Schematic representation of the early stages of the embryony of *R. sceleratus* showing the middle cell of the 3-celled embryo is involved in the formation of the embryo proper. (a) 32 HAP. (b) 3 DAP. (c) 5 DAP. (d) 6 DAP.

Membranous multivesicular structures are observed in almost all newly formed endosperm cell walls, and in some parts of the embryo sac wall. Similar structures, named *multivesicular bodies*, *multivesicular endosomes*, *paramural bodies*, *plasmalemmasomes* and *lomasomes*, are also reported in cells of other plant and animal species. Their origin is frankly presumed to be from plasma membrane or organelles, and their function is suggested to be related to endocytosis or exocytosis (see review Marchant and Robards 1968, Tanchak and Fowke 1987). Based on electron microscopy in adipose cells of the chick embryo, Ohoue and Makita (1989) reported an ultrastructural proof for the mitochondrion's origin of multivesicular structures.

In *R. sceleratus*, the behavior of the multivesicular structure is different from endocytosis or exocytosis because normally these processes do not involve the translocation of whole vesicles from the apoplast to the symplast or *vice versa*, whereas we observed whole vesicles in or against the cell wall. In our research we also found that the mitochondria connected to the cell membrane close to the places where vesicles of the multivesicular structure accumulated, suggesting that the mitochondrion might be the origin of the multivesicular structure here. This result is in agreement with the findings in animal cells (Ohoue and Makita 1989). The vesicles of the multivesicular structure may function in the apoplasmic transport of materials. On the other hand, it can not be excluded that the vesicles release enzymes to digest apoplast materials. The content of the vesicles has to be elucidated.

Endosperm cells exhibit an interaction with the embryo. At proglobular stage, no protoderm is developed. The endosperm cells surrounding the whole embryo are still intact. At the globular stage, the protoderm has formed, and the endosperm cells surrounding the embryo degenerate. The suspensor does not develop a protoderm-like organization, and it is remarkable that it remains surrounded by endosperm cells which do not degenerate. It has been demonstrated that protoderm cells differ in gene expression from the other embryonic cells in carrot (Sterk *et al.* 1991). The coincidence of the development of the protoderm and the degeneration of its surrounding endosperm in *R. sceleratus* points to a functional differentiation of the outer cell layer of the embryo proper, a differentiation not present in the early phases yet.

Acknowledgments: The authors thank Mr. S. Massalt for photographs and Mr. A. Haasdijk for artwork. The authors also thank Prof. M.T.M. Willemsse for critical reading of the manuscript. This study is granted by a Sandwich Ph.D. Fellowship of Wageningen Agricultural University to X. XuHan.

REFERENCES

- Bhandari, N.N., and Chitralkha, P. (1989) Cellularization of the female gametophyte in *Ranunculus sceleratus* Linn. *Can. J. Bot.* **67**: 1325-1330.
- Cardemil, L., and Jordan, M. (1982) Light and electron microscopic study of *in vitro* cultured female gametophyte of *Araucaria araucana* (Mol.) Koch. *Z. Pflanzenphysiol. Bd.* **107S**: 329-338.
- Chitralkha, P., and Bhandari, N.N. (1991) Post-fertilization development of antipodal cells in *Ranunculus sceleratus* Linn. *Phytomorphology* **41**: 200-212.

Chapter 2. Embryogenesis in *Ranunculus sceleratus*

- Gunning, B., and Pate, J.S. (1969) Transfer cells: Plant cells with wall ingrowths specialized in relation to short distance transport of solutes - their occurrence, structure and development. *Protoplasma* 68: 107-133.
- Johansen, D.A. (1950) *Plant Embryology - Embryogeny of the Spermatophyta*. Chronica Botanica Co. Waltham.
- Johri, B.M., Ambegaokar, K.B., and Srivastava, P.S. (1992) Ranunculaceae. In: Johri, B.M., Ambegaokar, K.B., and Srivastava, P.S. (eds.) *Comparative Embryology of Angiosperms*. Springer-Verlag, Berlin. Vol. 1. pp. 285-291.
- Marchant, R., and Robards, A.W. (1968) Membrane systems associated with the plasmalemma of plant cells. *Ann. Bot.* 32: 457-471.
- Natesh, S., and Rau, M.A. (1984) The embryo. In: Johri, B.M. (ed.) *Embryology of angiosperms*. Springer, Berlin, Heidelberg, New York. pp. 377-443.
- Ohoue, M., and Makita, T. (1989) The formation of multivesicular structures in the adipose cells of chick embryos. *Cell Biol. Int. Report* 13: 927-932.
- Schel, J.H.N., Kieft, H., and Van Lammeren, A.A.M. (1984) Interactions between embryo and endosperm during early developmental stages of maize caryopses (*Zea mays*). *Can. J. Bot.* 62: 2842-2853.
- Singh, B. (1936) The life-history of *Ranunculus sceleratus* L. *Proc. Ind. Acad. Sci.* 4B: 75-91.
- Souèges, R. (1913) Recherches sur l'embryogénie des Renonculacées-Renonculées. Genre *Ranunculus*. *Bull. Soc. Bot. Fr.* 60: 506-514, 542-549, 615-621.
- Souèges, R. (1914) Recherches sur l'embryogénie des Conclusions générales. *Bull. Soc. Bot. Fr.* 61: 27-32.
- Sterk, P., Booiij, H., Schellekens, G.A., van Kammen, A., and de Vries, S. (1991) Cell-specific expression of the carrot EP2 lipid transfer protein. *Plant Cell* 3: 907-921.
- Tanchak, M.A., and Fowke, L.C. (1987) The morphology of multivesicular bodies in soybean protoplasts and their role in endocytosis. *Protoplasma* 138: 173-182.
- Vijayaraghavan, M.R., and Bhat, U. (1982) Localization of macromolecules during achene development in *Ranunculus sceleratus* L. *Beitr. Biol. Pflanzen.* 57: 105-118.
- XuHan, X., and Van Lammeren, A.A.M. (1993) Microtubular configurations during the cellularization of coenocytic endosperm in *Ranunculus sceleratus* L. *Sex. Plant Reprod.* 6: 127-132.
- XuHan, X., and Van Lammeren, A.A.M. (1994) Ultrastructure of seed coat development in *Ranunculus sceleratus*. *Acta Bot. Neerl.* 43: 27-37.

Chapter 3

Ultrastructural and Immunofluorescence Studies on Bean (*Phaseolus vulgaris* L.) Embryogenesis with Particular Reference to Growth Patterning and Microtubular Configurations

X. XuHan and A.A.M. van Lammeren

Department of Plant Cytology and Morphology, Agricultural University
Wageningen, Arboretumlaan 4, 6703 BD Wageningen, The Netherlands.
Fax: (31) 8370 85005

Abstract. An Immunofluorescence and ultrastructural study was conducted on embryo development of the bean plant (*Phaseolus vulgaris* L.). The zygote undergoes transversal asymmetric division by phragmoplast and cell plate formation. The apical cell gives rise to an embryo proper whereas the basal cell forms a hypertrophic, multicellular suspensor that includes a basal zone and a neck zone. These three zones of the embryo exhibit significant differences in cytomorphogenesis, ultrastructure and microtubular configurations. Transfer cells developed in various cells. Wall ingrowths were found in the micropylar part of the central cell, in the outer endosperm cells, in the outer walls of the suspensor cells and at the inner walls of the suspensor cells bordering the neck zone. The presence of wall ingrowths points to transition from symplasmic to apoplasmic transport of nutrients towards the suspensor and from the suspensor towards the embryo proper. Cortical microtubules form parallel bundles in the elongating basal and neck cells of the suspensor, whereas they distribute less ordered in the enlarging suspensor basal part. In both cases, cell wall ingrowths do not influence the overall microtubular configurations. Cells in the elongation areas of the cotyledon exhibit cortical microtubules running perpendicular to the axis of elongation. Thus, microtubular configurations are highly involved in the differentiation of the suspensor and the embryo proper, and the transition from the globular to the cotyledon stage.

Key words: embryo, endosperm, microtubule, *Phaseolus vulgaris*, suspensor, wall ingrowth

INTRODUCTION

The reproduction of the bean (*Phaseolus vulgaris* L.) has been investigated since the beginning of this century (Brown 1917, Weinstein 1926, Öpick 1966a,b, Schnepf and Nagl 1970, 1976, Walbot *et al.* 1972, Sussex *et al.* 1973, Offler and Patrick 1984, Summerfield and Roberts 1985, Yeung and Clutter 1979, Yeung 1980, Yeung and Cavey 1988, Brady and Combs 1988, Sage and Webster 1990). The formation of a large and multicellular suspensor is characteristic for its embryogeny. Its development and ultrastructure have been described in the genus by Yeung and Clutter (1979) and Yeung (1980). We have previously reported the microtubular configurations in relation to endosperm ontogeny (XuHan and Van Lammeren 1994b). In this paper, we focus on the growth patterns during early embryogeny, especially we analyze microtubular configurations during the differentiation of the embryo proper and the suspensor, and during the transition of the embryo from the globular to the cotyledon stage. Additionally, we analyze the development of wall ingrowths in the developing endosperm and embryo in relation to the transport of nutrients.

MATERIAL AND METHODS

Developing seeds were excised from pods of bean plants (*Phaseolus vulgaris* L. var. Groffy) grown in the greenhouse. Light and electron microscopical methods were the same as previously described (Van Lammeren 1988, XuHan and Van Lammeren 1994b). Briefly, seeds were fixed in 4% paraformaldehyde and 4% glutaraldehyde in PBS, rinsed in PBS, and post-fixed in 1% OsO₄, dehydrated, and embedded in Spurr (Spurr 1969). Semithin sections were stained by Toluidine Blue O and were examined with the light microscope. Ultrathin sections, stained by uranyl acetate and lead citrate, were analyzed with a JEM-1200 EXII transmission electron microscope. For the immunocytochemical staining of microtubules, samples were fixed in 4% paraformaldehyde in PBS, rinsed, dehydrated and embedded in polyethylene glycol as described in detail elsewhere (Van Lammeren 1988, XuHan and Van Lammeren 1994b). Fluorescence of immunocytochemically stained microtubules (MTs) was examined either by fluorescence microscopy

or by confocal laser scanning microscopy (Bio-Rad MRC 600). Digitized images from the confocal microscope were printed directly with a Canon laser Jet CLC-300.

RESULTS

1. Progamic phase

One day before anthesis, the female gametophyte reached the mature stage (Fig. 1). Then cleistogamic pollination occurred. In the mature embryo sac, the central cell contained a large central vacuole. Around the moment of pollen tube entry into the synergid, the two polar nuclei fused (Fig. 2). The egg apparatus of the mature embryo sac exhibited a polar distribution of nuclei. The nucleus of the egg cell was positioned at the chalazal side of the egg cell whereas the nuclei of the two synergids were positioned at the micropylar side next to the filiform apparatus (Fig. 2). Microtubular cytoskeleton was observed in all the cells in the mature embryo sac. Cortical MTs were found parallel to the profiles of the filiform apparatus in the synergids.

2. Proembryo and globular embryo

Short after fertilization, the zygote divided, forming an apical cell and a basal cell. The division of the zygote was transversal and in asymmetric position and associated with phragmoplast MTs (Fig. 3a). The basal cell was longer and larger than the apical cell. The nuclei of the apical cell and the basal cell were similar in size. The primary endosperm nucleus divided before zygote division. The division in the fertilized central cell was restricted to karyokinesis. A spindle of MTs was formed, however, it did not give rise to a phragmoplast. Repeated karyokinesis led to the formation of the free nuclear endosperm (Fig. 3b).

The apical and basal cell, formed by the zygote division, gave rise to the embryo proper and the suspensor, respectively. Initiated at the proglobular stage (Fig. 4) and becoming apparent since the globular stage (Figs. 5, 7),

three cytological zones were formed in the embryo: (1) the embryo proper containing small isodiametric cells, (2) the basal part of the suspensor consisting of hypertrophic cells, which elongated and invaded the micropylar integument tissue and enlarged during the globular embryo stage, and (3) the suspensor "neck zone" (*i.e.* the zone between the basal part of the suspensor and the embryo proper) consisting of enlarged isodiametric cells. At the proglobular stage the basal zone of the suspensor was attached to the embryo sac wall, whereas the neck-zone and the embryo proper were surrounded by free nuclear endosperm (Fig. 4).

At the pro-embryo stage, the sizes of the embryo proper and the suspensor was quite similar. The suspensor cells were about twice as long as the embryo proper cells, but the sizes of the nuclei of the embryo proper and suspensor cells were comparable (Fig. 4).

At 5 DAP, the embryo proper cells were filled with cytoplasm and frequently exhibited cell division. The suspensor neck cells were larger and exhibited extensive large DNA-carrying organelles. These organelles were observed by electron microscopy and with the fluorescence microscope after DAPI staining (Figs. 5, 7a,b). The basal cells of the suspensor were the largest ones of the embryo as were their nuclei.

Among the three zones of the embryo, most MTs were found in the embryo proper (Fig. 7a). Preprophase band (PPB), spindle and phragmoplast microtubular configurations were observed frequently in the embryo proper. The formation of the protoderm and sub-epidermal cells was indicated by both anticlinal and periclinal cell divisions (Fig. 8, see also Fig. 5). The neck zone cells were enlarged but remained isodiametric, and sometimes cell divisions were observed in this area. Interphase suspensor neck cells exhibited large bundles of cytoplasmic and cortical MTs which were interwoven (Fig. 9). The neck cells near the basal part of the suspensor exhibited a lower density of MTs, and the connection between the cortical MTs and the cytoplasmic MTs was less obvious (Fig. 10). The basal suspensor cells were enlarged and elongated, and exhibited no cell division. These cells showed a criss-cross configuration of cytoplasmic MTs. In the



Fig. 1. Light micrograph showing an overview of the embryo sac of bean at the mature stage. CV, central vacuole; E, egg cell; I, integument; Nc, nucellus; Ns, nuclei of central cell; Sy, synergid. Bar = 50 μ m. **Fig. 2.** Electron micrograph of the egg apparatus of a mature embryo sac. E, egg cell; FA, filliform apparatus; Sy, synergid. Bar = 5 μ m. **Fig. 3 (a)** Immunofluorescence micrograph of the zygote showing cytokinesis. The cell plate margin, still bearing phragmoplast MTs (arrows), reaches the lateral walls of the zygote. Non-division-related cytoplasmic MTs (arrowhead) reappeared. **(b)** Low magnification overview of the same section stained by DAPI showing the divided zygote (arrow), the positions of its fluorescent daughter nuclei, the large nuclei of the free nuclear endosperm (arrowheads), and the small nuclei of the nucellus. Bar = 5 μ m. **Fig. 4.** Electron micrograph of proembryo showing the embryo proper (EP) and the suspensor (Su). Note the elongation of the basal cells of the suspensor. CV, central vacuole; En, free nuclear endosperm; II, inner integument; Nc, nucellus. Bar = 500 nm.

enlarging areas of the basal cell at the very end of the suspensor, the cortical MTs were randomly distributed but in the elongating areas, the cortical MTs formed about parallel arrays perpendicular to the axis of elongation (Fig. 11).

Cell wall ingrowths of the transfer cell type were already formed in the micropylar part of the central cell and in the synergids when the embryo sac was mature. In the embryo they were initiated in the suspensor at the globular stage (Fig. 5). The wall ingrowths developed in the outer walls of suspensor cells independently whether the

Fig. 5. Electron micrograph of proembryo showing the embryo proper (EP), and the neck zone (NZ) and basal zone (BZ) of the suspensor. Note the enlarged and elongated basal suspensor cells and the enlarged neck suspensor cells. Wall ingrowths (arrows) appeared in all suspensor cells adjacent to the endosperm or integument. Wall ingrowths also developed in the walls between neck and basal suspensor cells (double arrows). En, endosperm; II, inner integument. Bar = 5 μ m. **Fig. 6.** Electron micrograph of the basal cell of the suspensor (Su) at globular stage. Note that wall ingrowths (W) appear in the walls adjacent to the inner integument (II). Bar = 1 μ m.

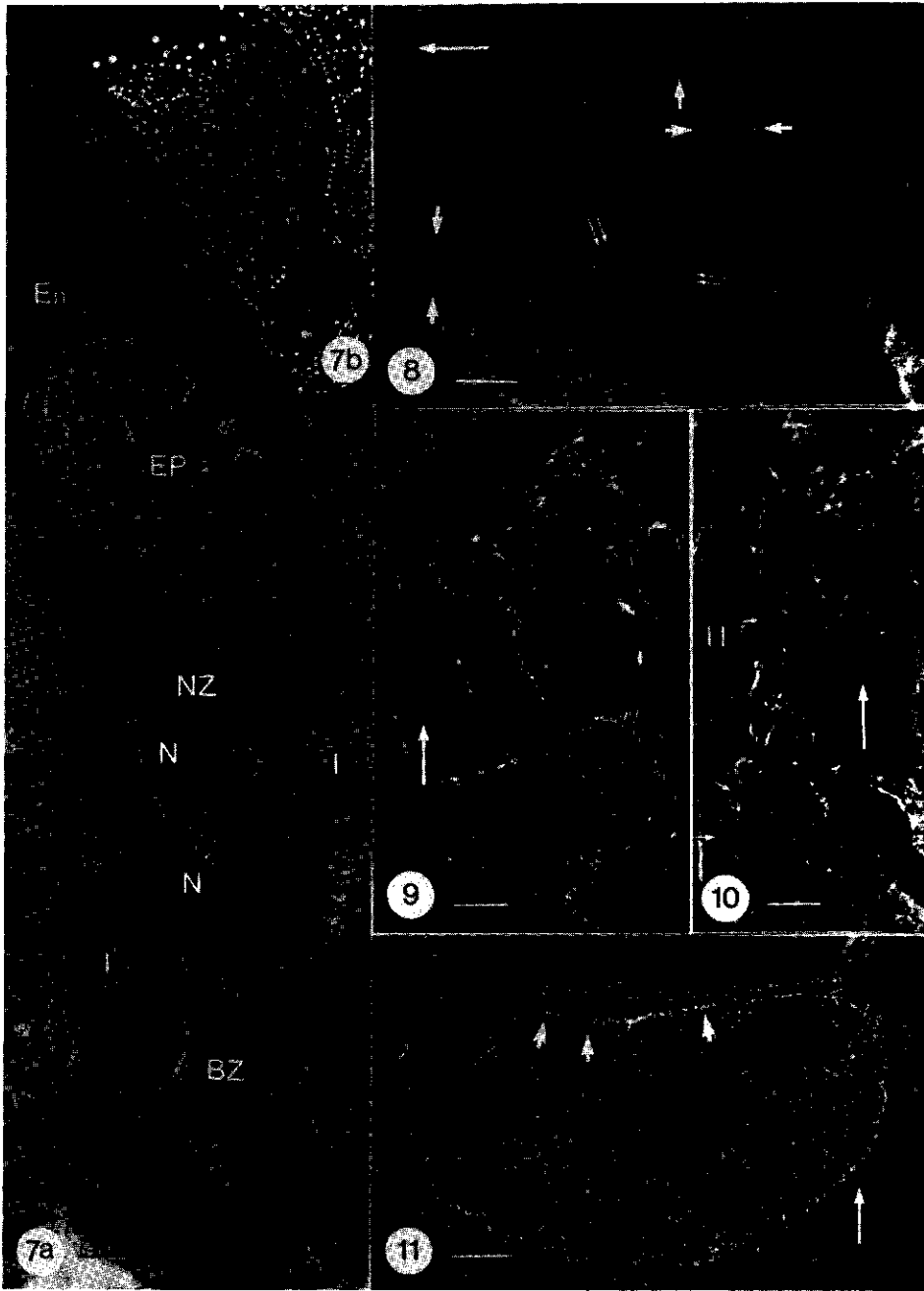


suspensor cells connected to the endosperm, or to the integument (Figs. 5, 6). Wall ingrowths also developed at the inner walls of the suspensor cells in the region where the basal cells bordered the neck cells (Fig. 5). The development of the wall ingrowths was not found to affect the overall configurations of MTs, though randomly oriented arrays of MTs were regularly observed in the interprofile areas of the wall ingrowths (Figs. 10, 11).

3. Heart-shaped and cotyledonary embryo

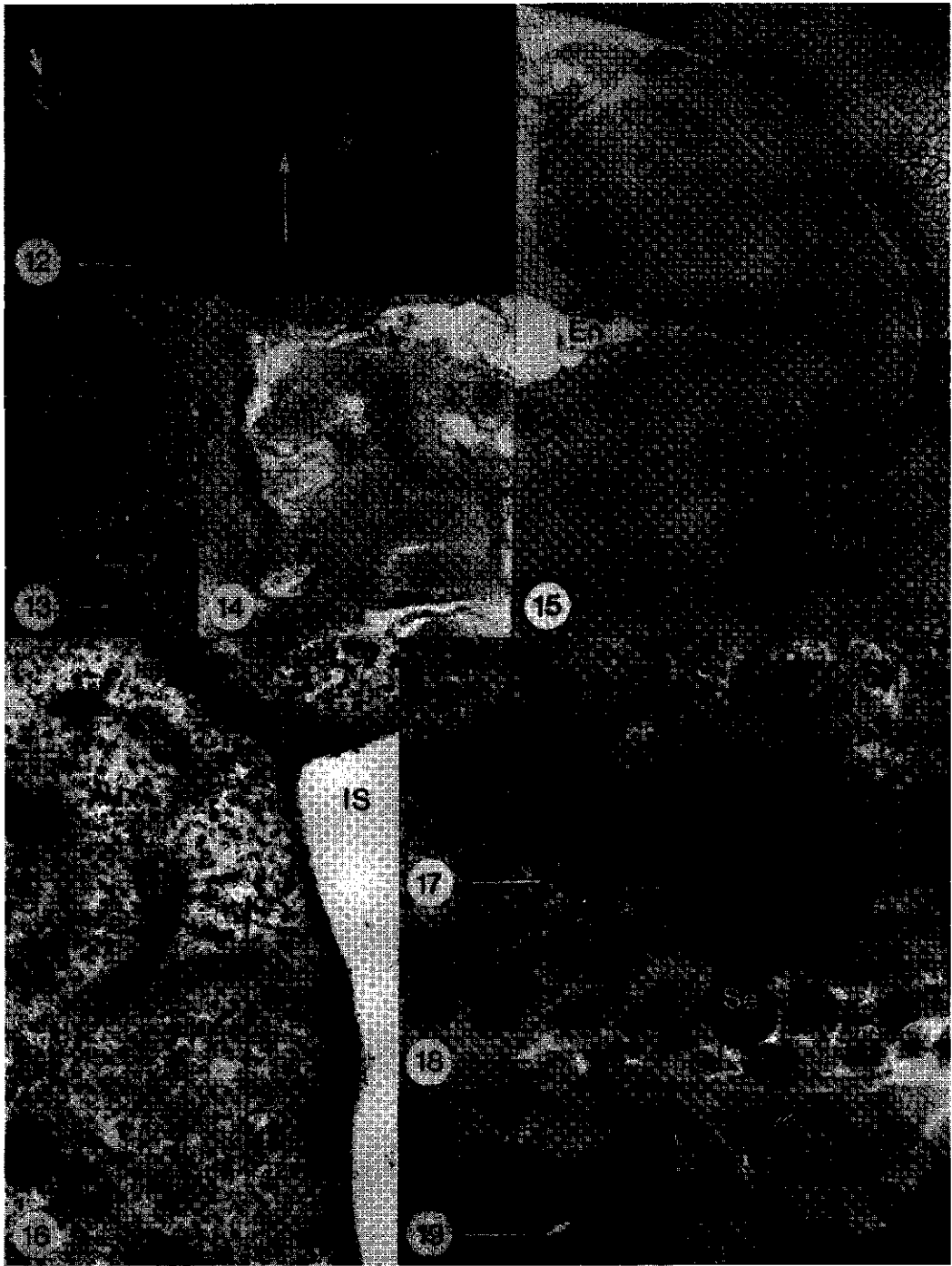
At the heart-shaped stage, primordia of the cotyledons were initiated at the chalazal side of the embryo. Here, MTs were extensively present (Fig. 12). PPB, spindle and phragmoplast MTs were mostly observed in the parts of the forthcoming cotyledon primordia. The development of the cotyledons resulted in the transition of the embryo from globular to heart-shape (Fig. 13). The wall ingrowths in the suspensor cells did not develop further, and cortical MTs were observed in the interprofile spaces of those wall ingrowths (Fig. 14). Cotyledons continued growth and the embryo reached the cotyledonary stage at about two weeks after pollination (Fig. 15). During heart-shaped and early cotyledon stages, both the cell length and nucleus diameter of the basal suspensor cells increased about 10 times compared to those of the embryoproper cells (Figs. 13, 15). In the neck zone, the suspensor cells and nuclei were about 3 times larger than the basal cells and nuclei of the embryo proper, respectively.

Fig. 7. (a) Immunofluorescence micrograph of embryo at globular stage showing fluorescent MTs in the embryo proper and suspensor cells. BZ, suspensor basal zone; En, endosperm; EP, embryo proper; I, integument; N, nucleus; NZ, suspensor neck zone. **(b)** Fluorescence micrograph of the same section at lower magnification showing fluorescent nuclei stained with DAPI. Bar = 10 μm . **Fig. 8.** Immunofluorescence micrograph of the embryo proper showing fluorescent PPB (arrows), spindle (double arrows), and interphase MTs. The embryo axis is indicated by a large arrow. Bar = 5 μm . **Fig. 9.** Confocal fluorescence image of the neck zone cells showing a microtubular network in the central and cortical cytoplasm of the cells. The embryo axis is indicated by a large arrow. Bar = 5 μm . **Fig. 10.** Confocal fluorescence image of the neck zone cells adjacent to the basal cells showing cytoplasmic and cortical MTs. The wall ingrowths are present in the walls (small arrows). II, inner integument. The embryo axis is indicated by a large arrow. Bar = 5 μm . **Fig. 11.** Confocal fluorescence image of a basal cell showing parallel arrays of cortical MTs underneath the wall between two basal cells (short arrows), and the less ordered cortical MTs along the wall between the basal cell and the integument tissue. Also note the criss-cross configuration of the cytoplasmic MTs. The embryo axis is indicated by a large arrow. Bar = 5 μm .



At the cotyledonary stage, cortical MTs were well established in all interphase cells of the embryo (Fig. 17), but extensive in the apex of the embryo axis and in the cotyledons. When cortical MTs formed PPBs, some cytoplasmic MTs ran from the PPB to the nucleus and connected to the nuclear envelope. Figure 16 shows a prophase cell with such a PPB bordering an intercellular space, regularly formed in cotyledons. During the enlargement of intercellular spaces, the cortical MTs in the bordering cells did not exhibit drastic changes in configuration. The orientation of the cortical population of MTs in the inner cells of the cotyledon differed from cell to cell, and within cells there was not a strict parallel organization. Cell growth and multiplication resulted in the formation of about isodiametric cells, and in both widening and elongation of the cotyledon (cf Figs. 15 and 18). In the epidermal cells of the cotyledon, however, an ordered microtubular network was observed. The MTs of individual epidermal cells were strictly ordered perpendicular to the length axis, though the individual cells showed variously oriented length axes. These cells did not develop into isodiametric cells but into flattened long epithelial cells (cf Figs. 15 and 19).

Fig. 12. Immunofluorescence micrograph of embryo at the onset of cotyledon formation. Note fluorescent spindle MTs (double arrows) and phragmoplast MTs (arrow) appearing in the forthcoming cotyledon primordia. The embryo axis is indicated by a large arrow. Bar = 10 μm . **Fig. 13.** Fluorescence micrograph showing DAPI-stained nuclei of a developing seed with a heart-shaped embryo. The embryo proper had surpassed the suspensor in size. Note the large bright nucleus (arrow) of a basal cell of the suspensor. Bar = 100 μm . **Fig. 14.** Electron micrograph of wall ingrowths (W) in the basal suspensor cell bordering the integument at cotyledon stage. Note the cortical MTs (arrows) close to the wall. Bar = 200 nm. **Fig. 15.** Light micrograph of cotyledonary embryo. At this stage the suspensor (Su) ceased growth while the embryo proper enlarges and elongates. Co, cotyledons; En, endosperm; I, integument. Bar = 100 μm . **Fig. 16.** Electron micrograph showing PPB MTs (PPB) in a cotyledonary cell bordering an intercellular space (IS). Note that MTs (arrows) are connected with the nuclear envelope on which nuclear pores are visible (arrowheads). N, nucleus. Bar = 20 nm. **Fig. 17.** Electron micrograph of a common wall of cotyledon cells showing grouped plasmodesmata and extensive cortical MTs. Bar = 500 nm. **Fig. 18.** Immunofluorescence micrograph of the cotyledon of the embryo. Note that subepidermal cells (Se) have criss-cross patterning of fluorescent cortical MTs. The epidermal cells (Ed) are flattened. Bar = 10 μm . **Fig. 19.** Immunofluorescence micrograph of a tangential section of epidermal cells of the embryo cotyledon. Note that MTs often show orientations perpendicular to the length axes of the cells (arrows). Bar = 10 μm .



DISCUSSION

1. Embryo differentiation

Embryo development in bean proceeds from zygote stage to cotyledon stage within two weeks. The differentiation of three zones, each characterized by specific cell features, is analyzed cytologically. The rapid formation of the club-like hypertrophic suspensor has been described previously (Brown 1917, Sussex *et al.* 1973, Nagl 1974, 1976, Yeung and Clutter 1979, Yeung 1980, Lersten 1983, Cionini 1987, Brady and Combs 1988, Yeung and Meinke 1993). Our observations on cell size and nuclear size of the suspensor cells are in agreement with data on the structure and polyteny of chromosomes of the suspensor cells (Nagl 1970, 1974).

In soybean plant, an autoradiographic analysis of water-insoluble photosynthates in developing seed was recently conducted revealing the suspensor being a main pathway of the nutrient transport (Chamberlin and Horner 1993). Results from pod-labeling in bean by ^{14}C -sucrose indicate that the suspensor is the main transport pathway of nutrients from the surrounding tissues to the embryo proper until semi-mature stage (Yeung 1980). Transfer-cell-type wall ingrowths (see Gunning *et al.* 1968, 1974, Pate and Gunning 1972) are widely present in bean plants (*e.g.* see Folsom and Cass 1986). We not only observed them in all the outer walls of the basal suspensor cells but in the neck cells bordering the basal suspensor. Thus, the orientation of the wall ingrowths just matches the direction of the nutrient flux from surrounding tissue via the basal part to the upper embryo proper (see Brady and Combs 1988). It is therefore likely that nutrient transport meets apoplasmic to symplasmic transition in both these areas of wall ingrowths. Additionally, plasmodesmata are present in all the common walls of the embryo cells indicating that there are no symplasmic barriers throughout the embryo. All the features foregoing, therefore, highly agree with the physiological function of the suspensor that it is a very active metabolic organ for synthesis, and an organ for apoplasmic and symplasmic transport of materials to the developing embryo proper.

The transition of the basal suspensor to the neck zone is marked by wall ingrowths. Both DAPI-fluorescent staining and electron microscopy reveal that the DNA-carrying organelles, *i.e.* plastids and mitochondria, are much larger in the suspensor neck cells compared with the cells in the embryo proper and the basal suspensor. On the one hand, the results on wall ingrowth suggest an active apoplasm-symplasm transport of nutrients between suspensor base and neck, and on the other hand, the results on organelle differentiation point to a metabolic difference between the suspensor neck and the embryo proper.

2. Cell morphogenesis and microtubular configurations

In the present work the organization of the microtubular cytoskeleton has been investigated throughout the embryogeny of bean until the cotyledon stage. All cell types exhibited microtubular configurations independent from their type of differentiation, however, the organization of the microtubular cytoskeleton highly depended upon the type of differentiation and the stage in the cell cycle. Knowledge about the microtubular cytoskeleton in higher plant embryogeny is still restricted. In *Arabidopsis*, it is found that MTs are abundant throughout proembryogenesis and cortical MTs form transverse arrays to the length axis of the embryo both in the embryo proper cells and in the suspensor cells during zygote to octant embryo stage (Webb and Gunning 1991). In bean, the transversal asymmetric division of the zygote is a result of phragmoplast positioning and shows the polarity of the embryo in the earliest phase. As a general rule, the organization of the microtubular cytoskeleton at interphase was related to the type of growth observed in those cells, independent from the size of the cells, *e.g.* elongating suspensor cells and cotyledon cells exhibited microtubular arrays perpendicular to the length axes of those cells, whereas isodiametric cells in both suspensor and cotyledon exhibited random microtubular configurations. The results reveal that the organizations of MTs are comparable in the embryo proper, the neck zone and the basal zone, but are strongly related to the developmental fate of the cells. Mitoses were observed from the zygote stage onward until the cotyledon stage. In the early globular stage protoderm and subepidermal cell formation was caused by both anticlinal and periclinal cell division. Periclinal divisions in the outer cell layer of the embryo could be predicted by visualizing the orientation of the cortical interphase MTs. When interphase MTs were in

periclinal position, the PPB would get such position leading to an anticlinal spindle position and then to a periclinal division. During the transition from the globular to the heart shaped stage, no such divisions were observed any more, and most PPB and spindle MTs occur in the areas of the forthcoming cotyledon primordia

Configurations of cortical MTs are studied in developing integument cells of *R. sceleratus* to analyse their function in wall ingrowth formation (XuHan and Van Lammeren 1994a). The integument cells exhibited regular profiles of wall ingrowths of the non-transfer cell type and on top of these profiles bundles of cortical MTs run well parallel to the profiles (XuHan and Van Lammeren 1994a). In that case it was suggested that they functioned in the formation and positioning of those wall profiles which probably function in providing mechanical support to the seed coat. In the suspensor cells of the bean embryo, cortical MTs orient randomly in the interprofile areas of wall ingrowths of transfer cell type. We did not observe co-localization of arrays of MTs and developing wall profiles as observed in the cells of *R. sceleratus*. Thus, the overall microtubular configuration in bean seems to be coupled with the cell shaping rather than with the formation of wall ingrowths.

Acknowledgments. The authors thank Mr. S. Massalt and Mr. A. Haasijk for the artwork, Mr. G. van Geerenstein for greenhouse work, Prof. M.T.M. Willemse for helpful discussion, and Mrs. H. Yu for experimental assistance. This study was granted by a Ph.D. Fellowship of Wageningen Agricultural University.

REFERENCES

- Brady, T., and Combs, S.H. (1988) The suspensor is a major route of nutrients into proembryo, globular and heart stage *Phaseolus vulgaris* embryos. In: Cresti, M., Gori, P., and Pacini, E. (eds.) *Sexual Reproduction in Higher Plants*. Springer-Verlag Berlin Heidelberg. pp. 419-424.
- Brown, M.M. (1917) The development of the embryo-sac and of the embryo in *Phaseolus vulgaris*. *Bull. Torrey Bot. Club* 44: 535-544.
- Chamberlin, M.A., and Horner, H.T. (1993) Nutrition of ovule, embryo sac, and young embryo in soybean: an anatomical and autoradiographic study. *Can. J. Bot.* 71: 1153-1168.
- Cionini, P.G. (1987) The suspensor and its role in embryo development in *Phaseolus* (Papilionaceae): a review. *Atti. Soc. Toscana Sci. Nat. P. V. Mem. Ser. B.* 94: 151-161.
- Gunning, B.E.S. Pate, J.S., and Briarty, L.G. (1968) Specialized "transfer cells" in minor veins of leaves and their possible significance in phloem translocation. *J. Cell Biol.* 37: 7-12.

Chapter 3. Microtubules during embryogeny of bean plant

- Gunning, B.E.S., Pate, J.S., and Briarty, L.G. (1974) Transfer cells. In: Robards, A.W. (ed.) *Dynamic Aspects of Plant Ultrastructure*. Maidenhead McGraw-Hill. pp. 441-480.
- Folsom, M.W., and Cass, D.D. (1986) Changes in transfer cell distribution in the ovule of soybean after fertilization. *Can. J. Bot.* **64**: 965-972.
- Lersten, N.R. (1983) Suspensors in leguminosae. *Bot. Rev.* **49**: 233-257.
- Nagl, W. (1974) The *Phaseolus* suspensor and its polytene chromosomes. *Z. Pflanzenphysiol.* **73**: 1-44.
- Nagl, W. (1976) Ultrastructural and development aspects of autolysis in embryo-suspensors. *Ber. Deutsch. Bot. Ges. Bd.* **89S**: 301-311.
- Offler, E.E., and Patrick, J.W. (1984) Cellular structures, plasma membrane surface areas and plasmodesmatal frequencies of seed coats of *Phaseolus vulgaris* L. in relation to photosynthate transfer. *Aust. J. Plant Physiol.* **11**: 79-99.
- Öpik, H. (1966a) Changes in cell fine structure in the cotyledons of *Phaseolus vulgaris* L. during germination. *J. Exp. Bot.* **17**: 427-439.
- Öpik, H. (1966b) Development of cotyledon cell structure in ripening *Phaseolus vulgaris* seeds. *J. Exp. Bot.* **19**: 64-76.
- Pate, J.S., and Gunning, B.E.S. (1972) Transfer cells. *Ann. Rev. Plant Physiol.* **23**: 173-196.
- Sage, T.L., and Webster, B.D. (1990) Seed abortion in *Phaseolus vulgaris*. *Bot. Gaz.* **151**: 167-175.
- Schnepf, E., and Nagl, W. (1970) Über einige Strukturbesonderheiten der Suspensorzellen von *Phaseolus vulgaris*. *Protoplasma* **69**: 133-143.
- Summerfield, R.J., and Roberts, E.H. (1985) *Phaseolus vulgaris*. In: *Handbook of Flowering*. CRC Press, Boca Raton, Vol. I. pp. 139-148.
- Sussex, I., Clutter, M., Walbot, V. and Brady, T. (1973) Biosynthetic activity of the suspensor of *Phaseolus vulgaris*. *Caryologia* **25** (Suppl.): 261-272.
- Van Lammeren, A.A.M. (1988). Structure and function of the microtubular cytoskeleton during endosperm development in wheat: an immuno-fluorescence study. *Protoplasma* **146**: 18-27.
- Walbot, V., Clutter M., and Sussex, I.M. (1972) Reproductive development and embryogeny in *Phaseolus*. *Phytomorphology* **22**: 59-68.
- Webb, A.C., and Gunning, B.E.S. (1990) The microtubular cytoskeleton during development of the zygote, proembryo and free-nuclear endosperm in *Arabidopsis thaliana* (L.) Heynh. *Planta* **184**: 187-195.
- Weinstein, A.I. (1926) Cytological studies on *Phaseolus vulgaris*. *Am. J. Bot.* **13**: 248-263.
- XuHan, X., and Van Lammeren, A.A.M. (1993) Microtubular configurations during the cellularization of coenocytic endosperm in *Ranunculus sceleratus* L. *Sex. Plant Reprod.* **6**: 127-132.
- XuHan, X., and Van Lammeren, A.A.M. (1994a) The ultrastructure of seed coat development in *Ranunculus sceleratus*. *Acta Bot. Neerl.* **43**: 27-37.
- XuHan, X., and Van Lammeren, A.A.M. (1994b) Microtubular configurations during endosperm development in *Phaseolus vulgaris*. *Can. J. Bot.* **72**: 1489-1495.
- Yeung, E.C. (1980) Embryogeny of *Phaseolus*: the role of the suspensor. *Z. Pflanzenphysiol. Bd.* **96**: 17-28.
- Yeung, E.C., and Cavey, M.J. (1988) Cellular endosperm formation in *Phaseolus vulgaris*. I. Light and scanning electron microscopy. *Can. J. Bot.* **66**: 1209-1216.
- Yeung, E.C., and Clutter, M.E. (1979) Embryogeny of *Phaseolus coccineus*: the ultrastructure and development of the suspensor. *Can. J. Bot.* **57**: 120-136.

Chapter 4

The Ultrastructure of Seed Coat Development in *Ranunulus sceleratus*¹

X. XuHan and A.A.M. Van Lammeren

Department of Plant Cytology and Morphology, Wageningen Agricultural
University, Arboretumlaan 4, 6703 BD Wageningen, The Netherlands

¹ Reprinted, with permission, from *Acta Bot. Neerl.* 43: 27-37 (1994)

Abstract. Seed coat development in *Ranunculus sceleratus* L. has been studied by electron microscopy. Three layers developed from the single integument. The outer epidermis consisted of elongated and flattened cells that were always well attached to each other. The cells were characterized by thin walls, the presence of chloroplasts and small vacuoles. The cells of the middle layer were originally closely packed. Gradually, extensive intercellular spaces were formed. The cells of the inner epidermis elongated initially, until they became cubic and developed a thick wall with numerous wall ingrowths at the side bordering the nucellus. Thus they give rise to a mechanical layer protecting the inner part of the seed.

The elongation of cells, the thickening of cell walls, the formation of wall ridges, and the formation of intercellular spaces each coincided with characteristic configurations of microtubules. Plasmodesmata were originally found between all cells of the integument but their number decreased drastically during development, especially between the three developing seed coat layers. Well-differentiated chloro-amyloplasts, present in all cells of the developing seed coat, pointed to autotrophy during development.

Maturation eventually led to the disappearance of cytoplasm in all cells, the compression of the cells of the outer epidermis and middle layers, and the formation of a mechanical layer from the inner epidermis.

Key words: cell aging, integument, intercellular space, microtubule, plasmodesma, *Ranunculus sceleratus*, seed coat.

INTRODUCTION

Seed coats in angiosperms have been studied from structural as well as physiological points of view (Boesewinkel and Bouman 1984). As the seed of *Ranunculus sceleratus* L. develops, several cytomorphogenic processes occur in the seed coat which eventually lead to cell death and the disappearance of cytoplasm. Thus, the development of the seed coat includes processes of cell growth, differentiation, and cell aging.

Recently, endosperm formation was investigated in *R. sceleratus* (XuHan and Van Lammeren 1993) but no detailed data have been recorded on seed coat development and maturation in the genus *Ranunculus* (Sing 1936; Boesewinkel and Bouman 1984). In the study presented here, the general anatomy as well as the cytology of the developing seed coat was analyzed in ovules and developing seeds. In particular, attention was paid to the distribution of plasmodesmata, the arrangement of microtubules (MTs), the thickening of cell walls, and the formation of cell wall ingrowths. These developmental aspects are of particular importance to cell to cell contact, cell morphogenesis and the mechanical properties, respectively, and thus to the ultimate function of the developing seed coat.

MATERIALS AND METHODS

Plants of *Ranunculus sceleratus* L. were grown in the greenhouse. Developing seeds were excised from ovaries at five developmental stages from 1 day before anthesis (Stage I), when seeds contained a zygote (Stage II), a proembryo (Stage III), a globular to heart-shaped embryo (Stage IV) and a mature embryo (Stage V, *i.e.*, 25 days after anthesis (DAA)). For electron microscopy, the seeds were fixed in 4% glutaraldehyde for 6h and then in 1% osmium tetroxide for 6 h, both in phosphate-buffered saline (PBS), pH 7. Samples were dehydrated, and embedded in low viscosity resin (Spurr 1969). Ultrathin sections were stained with uranyl acetate followed by lead citrate and examined with a JEM-1200 EXII transmission electron microscope operating at 80 kV.

RESULTS

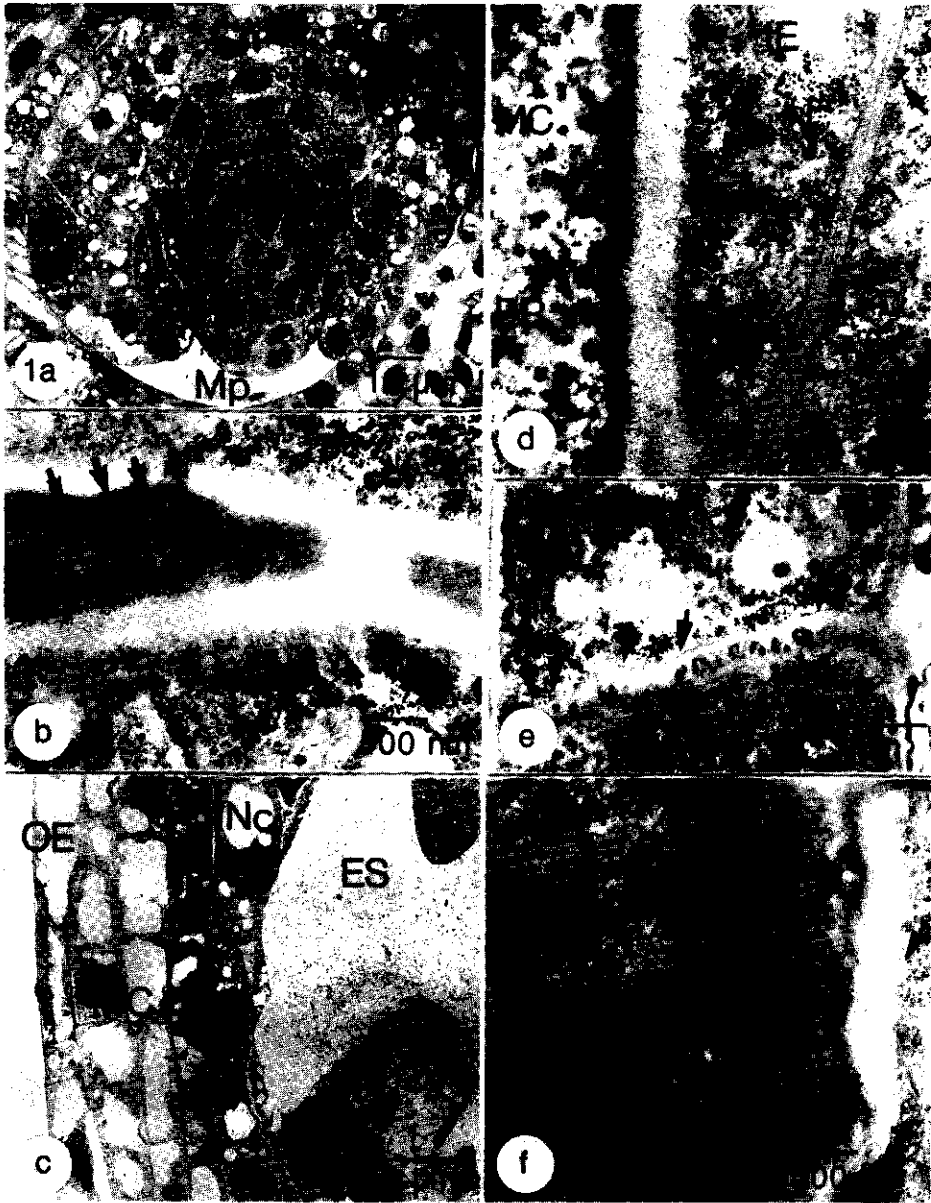
Stage I (-1 DAA)

One day before anthesis, ovules were at the megaspore stage. As shown in Fig. 1a, the single integument grew from the chalazal part of the ovule towards the micropylar part. It consisted of an outer epidermis, one to three middle layers, and an inner epidermis. The cytoplasm of the various cells of the integument had a comparable appearance, but the cell walls of the two epidermis had a cuticle and differed from the middle layer in this respect. The cytoplasm of the integumentary cells contained small and medium-sized vacuoles and numerous organelles, such as mitochondria, plastids, endoplasmic reticulum (ER), dictyosomes and spherosomes. Intercellular spaces were not observed at this stage. All the cells of the integument showed plasmodesmata to adjacent cells. Cortical MTs were observed in all cells. They formed a helical network under the cell membrane of slightly elongated cells (Fig. 1b) and were arranged in more random patterns in isodiametric cells.

Stage II (1 DAA)

The integument of the mature ovule now consisted of three morphologically distinct layers covering the nucellus with the fertilized

Fig. 1. Electron micrographs of *R. sceleratus* ovules from 1 day before (a, b) to 1 day after anthesis (c-f). (a) Longitudinal section of the anatropous ovule surrounded by the pericarp of the unilocular ovary. Only one integument was formed. Vacuolization had started in the middle layer cells and the epidermal cells. (b) Detail of a juncture area of the middle layer cells. Note the cortical arrays of MTs (arrows) before intercellular space formation. (c) Longitudinal section showing the integument at fertilization stage (1 DAA). Note the formation of vacuoles in the outer epidermis and middle layers and the deviating differentiation of the inner epidermis which surrounds the, nucellus and embryo sac. (d) A part of the seed coat showing cytoplasmic differences between inner epidermal and middle layer cells. Parallel arrays of cortical MTs (arrows) were found. (e) Detail of inner epidermis showing an anticlinal wall with numerous MTs running parallel to the cell wall (arrows) and plasmodesmata which were darkly stained by the OsO₄. The cytoplasm is darkly stained because of ribosomes. (f) Oblique section of the wall between the inner epidermis of integument and nucellus. Cuticles had fused (arrow head). Wall thickening was mainly observed at the integument side (electron-dense area). Note the extensive arrays of parallel MTs (arrows). Abbreviations: Ch, chalaza; En, endosperm; ER, endoplasmic reticulum; ES, embryo sac; IE, inner epidermis of integument; In, integument; IS, intercellular space; L, lipid droplet; MC, middle layer cells of integument; Mp, micropyle; N, nucleus; Nc, nucellus; OE, outer epidermis of integument; S, starch grain; V, vacuole; W, wall ingrowth; Zy, zygote.



embryo sac (Fig. 1c). There were no stomata in the outer epidermis, and plastids had differentiated into chloroplasts.

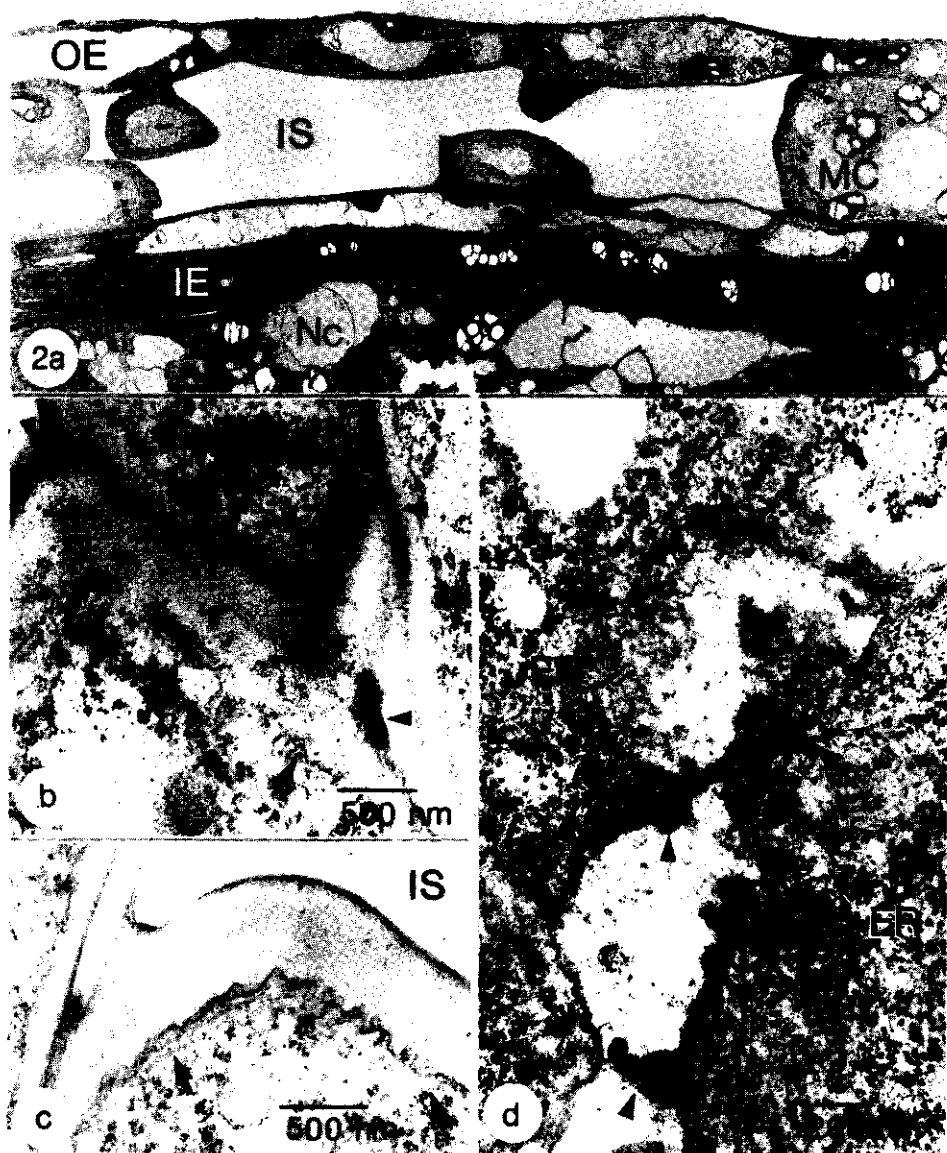
The two or three layers of cells of the middle layer showed large vacuoles now. Numerous electron-dense microfibrils were observed in the cell walls at this stage. Tiny intercellular spaces were frequently observed between the cells of the middle layer at 1 DAA. Cortical MTs were found in parallel arrays in the cells of the inner epidermis and middle layer cells (Fig. 1d).

The cells of the inner epidermis contained much cytoplasm, numerous ribosomes (Figs. 1d, e), small vacuoles and plastids without well developed grana and thylakoid membranes. Plasmodesmata were frequently found in the anticlinal walls (Fig. 1e), not in the outer periclinal walls and only sometimes in the inner periclinal walls. The outer periclinal walls bordering the nucellus thickened and the cuticulae of epidermis and nucellus fused (Fig. 1f). Extensive cortical arrays of MTs were found near the thickening walls.

Stage III (2-5 DAA)

The cells of the integument had enlarged considerably at 5 DAA (Fig. 2a). The outer epidermis consisted of a single layer of elongated and flattened cells that were well attached to each other and characterized by thin walls, the presence of vacuoles and chloro-amyloplasts containing several small starch grains each. From 2 DAA onwards, intercellular spaces enlarged. Cell walls separated from each other at the middle lamella, and the plasmodesmata in the bordering walls disappeared completely. Electron-dense material was regularly found in the corners of the newly formed intercellular spaces, independent of the direction of sectioning (Fig. 2b). Cell walls bordering the intercellular spaces slightly thickened before and during the formation of the intercellular spaces. As the intercellular spaces enlarged, contact between the

Fig. 2. Electron micrographs of the developing seed coat of *R. sceleratus* from 4 (d) and 5 days after anthesis (a-c). (a) Longitudinal section of seed coat. Note the elongated cells of the outer epidermis and the large intercellular spaces in the middle layer. (b-c) Details of the middle layer cells during the formation of intercellular spaces. Electron-dense material was regularly observed in the corners of the enlarging intercellular spaces (arrow head). MTs near the wall exhibited various orientations (arrows). (d) Detail of anticlinal wall of the inner epidermis. Note the large plasmodesmata (arrow heads) and the numerous MTs running near the wall (arrows). See Fig. 1 for explanation of abbreviations.



middle layer cells and the cells of the outer epidermis decreased. In general, less plasmodesmata were observed in the periclinal cell walls of seed coat cells than in the anticlinal cell walls, and more plasmodesmata were found in the anticlinal walls of the inner epidermis than in those of the outer epidermis and middle layer. Cortical MTs were observed in all the cells of the developing seed coat. In the elongating cells they were all found in hoop-like orientations, parallel to each other and perpendicular to the length axis of the cells. When they were found near the separating walls bordering a developing intercellular space, cortical MTs were observed in a less ordered way (Figs. 2b, c). At the end of the stage, the tonoplasts of the central vacuoles in the middle layer cells and the outer epidermal cells degenerated. In such cells, cortical MTs were observed only incidentally.

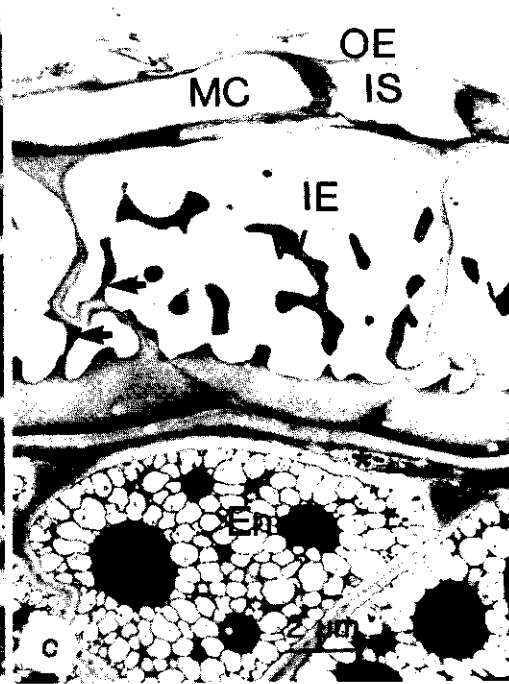
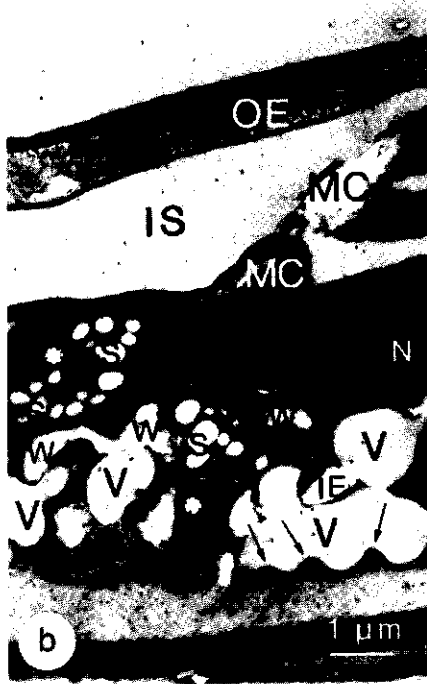
The cells of the inner epidermis were still flattened and contained darkly stained cytoplasm, amyloplasts (Fig. 2a) and numerous ribosomes (Fig. 2d). Large plasmodesmata were found in the anticlinal walls and cortical MTs were observed in their vicinity (Fig. 2d).

Stage IV (6-12 DAA)

At about 7 DAA, wall ingrowth and cell degeneration were observed in the young seed coat (Fig. 3a, b).

The cells of the outer epidermis and the middle layers ceased growing and the cytoplasm became electron-dense and degenerated (Fig. 3b). Degeneration in outer epidermis and middle layer preceded that of the inner epidermal cells. Deterioration of the tonoplast of the central vacuole preceded

Fig. 3. Electron micrographs of the young seed coat of *R. sceleratus* from 7 (a, b) and 25 days after anthesis (c). (a) Onset of wall ingrowth formation at the outer periclinal wall of an inner epidermal cell. Note the membranous vesicle-tube complex (arrows) giving rise to the wall ingrowths. (b) Seed coat showing degenerating outer epidermis and middle layer cells. The inner epidermis formed a thick outer cell wall bearing well developed wall ingrowths (W) surrounding areas with cytoplasm (*). The ridges in the cell wall (arrows) are covered with a thin layer of cytoplasm, in which bundles of parallel MTs were observed at higher magnification. (c) Part of mature seed coat and endosperm. Note the absence of cytoplasm in all cells of the seed coat and the prominent wall ingrowths in the cells of the inner epidermis. Some wall ingrowths are connected to the anticlinal wall (arrows). * = degenerated nucellus. See Fig. 1 for explanation of abbreviations.



that of the cell membrane, and starch grains, nuclei and ER were the last recognizable cell components. Microtubules were not found in the degenerated cells of the outer epidermis and middle layer.

The outer periclinal walls of the inner epidermis continued to thicken and at its inner side cell wall ingrowths were formed (Fig. 3b). Initially, amorphous membranous vesicle-tube complexes appeared in the cytoplasm (Fig. 3a). The vesicle-tube complexes fused with each other and with the plasmalemma. They extended deep into the cell and enlarged, resulting in the formation of many finger-like and smooth-surfaced profiles (Fig. 3b). This occurred as long as eventually degenerating cytoplasm was observed in the inner epidermal cells, *i.e.*, up to 20 DAA. Plasmodesmata were not found in the profiles. Microtubules were observed along the vesicle-tube complex in a random order but there was no association between the membrane complexes and the MTs.

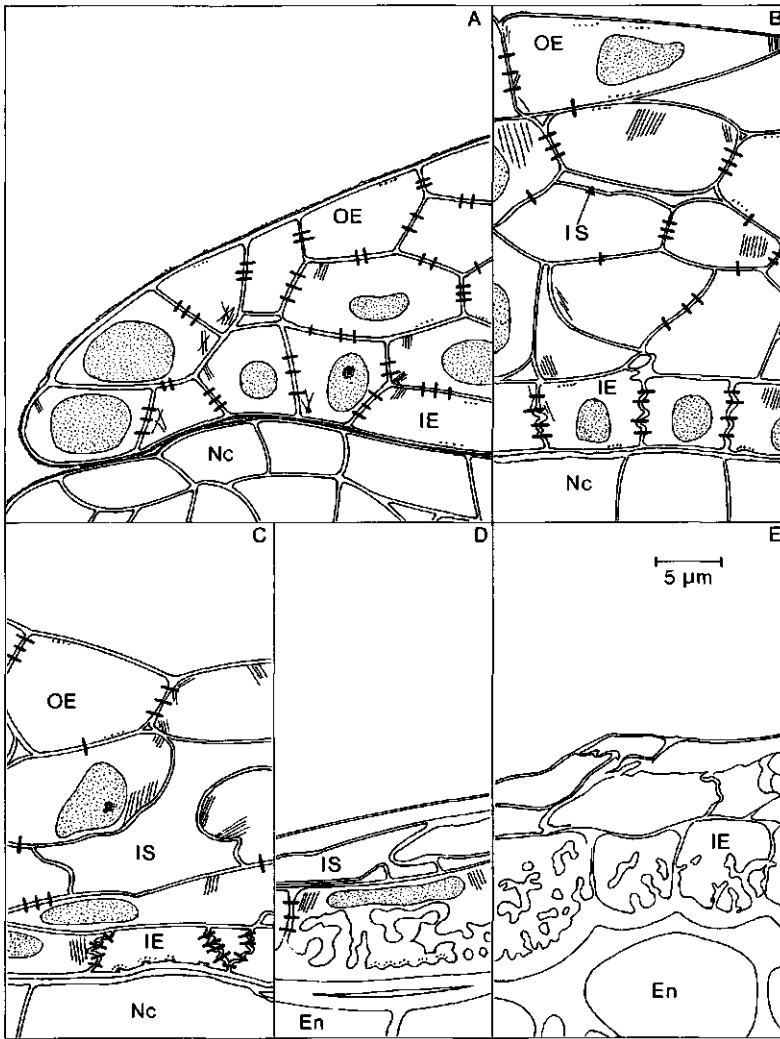
Cortical MTs along the outer wall were observed at particular sites, *i.e.*, at the tips of the undulating cell membrane as indicated by arrows in Fig. 3b (MTs are not visible due to the low magnification). Oblique sections revealed that the MTs ran parallel to these ridges. At the end of the stage, cortical MTs disappeared from the cells of the inner integument. The tonoplasts and other membranous structures degraded and disappeared in the cytosol, and remnants of cytoplasm and degenerated nuclei were observed in the cells. At this developmental stage the nucellus was replaced by endosperm.

Stage V (13-25 DAA)

At the final stage of seed development, the seed coat eventually covered the endosperm directly because the nucellus was compressed and consumed by

Fig. 4. Schematic representation of seed coat development in *R. sceleratus* with plasmodesmata in cell walls and cortical MTs in cytoplasm from 1 day before anthesis up to 25 days after anthesis (a) Stage I; 1 day before anthesis. (b) Stage III (early); 3 DAA. (c) Stage III (late); 5 DAA. (d) Stage IV (late); 12 DAA. (e) Stage V; 25 DAA. Thin short lines in the cytoplasm and dots close to the plasmalemma represent the position and the orientation of microtubules, and thick lines represent the positions and relative frequencies of plasmodesmata in the cell walls. See Fig. 1 for explanation of abbreviations.

Chapter 4. Seed coat development in *Ranunculus*



the endosperm (Fig. 3c). The outer epidermis and the middle layers were stretched and pressed between the inner epidermis and the pericarp. All cytoplasm and plasmodesmata disappeared, leaving only cell walls in the seed coat. However, intercellular spaces remained in the middle layer. The inner epidermis of the integument showed well developed wall ingrowths. It became the mechanical layer of the seed coat, the most prominent structure at this stage (Fig. 3c).

DISCUSSION

The differentiation of outer epidermis, middle layer and inner epidermis of the integument of *R. sceleratus* resulted in three morphologically and functionally different cell layers of the seed coat. As summarized schematically in Fig. 4, morphological changes coincided with various cytological changes such as the change in distribution of plasmodesmata, the change in configuration of MTs, the separation of cells by the formation of intercellular spaces, and the local thickening of cell walls.

The differentiation of plant cells depends on the position of the cell in the tissue and on the presence of symplasmic contact with neighbouring cells by plasmodesmata (Robards and Lucas 1990). Fransz and Schel (1991) reported that during somatic embryogenesis in maize, the embryogenic clusters lack plasmodesmatal connections to the surrounding callus. Symplasmically isolated cells can undergo a different development, rather auto-controlled than imposed by the surrounding tissue, such as that known from studies on embryo-sac formation, pollen development and embryo-endosperm interactions (see e.g. Van Lammeren 1986a, b).

Plasmodesmata show a clear distributional change during seed coat development of *R. sceleratus* (Fig. 4): from an even distribution in the young integument (Stages I and II), to an uneven distribution in the young seed coat (Stage III and IV) and the complete disappearance at maturity (Stage V). The cells of the outer epidermis maintained intensive symplasmic contact by plasmodesmata whereas the contact of these cells with the middle layer cells reduced, because of the formation of intercellular spaces. It was also found that the inner epidermis became isolated symplasmically from adjacent

middle layer cells. Thus, the three layers became isolated from each other to a certain degree and then showed a different development and fate. Because the symplasmic isolation coincided with characteristic development, the distribution of plasmodesmata might serve as an early indicator for cell differentiation.

As a consequence of symplasmic isolation, all cell layers had to be more or less self-supporting. The precursors for the synthesis of the wall ingrowths in the inner epidermis should come from the inner epidermis itself, probably from the starch resources, which indeed disappeared during maturation, and by increased transport from cell to cell within the epidermis. The enlarged plasmodesmata in the anticlinal cell walls of the inner epidermis point to such a possibility. However, it is possible that the apoplasmic and symplasmic transport of storage products from the outer part of the seed coat still existed to some extent.

The extensive intercellular spaces, developed in the middle layer of the seed coat, form a closed system because there are no stomata or other openings in the epidermis, which itself was covered by a cuticle. Little is known about the physical and biochemical characteristics as well as the function of non-stomatal intercellular spaces (Woolley 1983). In mature seeds, intercellular spaces and dead cells function in seed dispersal on water by the reduction of specific gravity of the seeds. At earlier stages of seed coat development, the intercellular space of the photosynthetically active middle layer probably functions as an air/gas exchange and storage accommodation likely filled with a.o. O₂, CO₂ and, in later stages, probably ethylene. The electron-dense material found in various corners of intercellular spaces, might represent remnants of wall material, in this case the middle lamella.

Observations on the cytoskeleton revealed that MTs are found in all seed coat cells until degeneration occurs (Fig. 4). Three typical configurations of cortical MTs were distinguished.

- (1) Parallel arrays of MTs were observed perpendicularly to the length axis of elongating epidermal cells. This phenomenon was also observed, after immunolabelling of MTs in semi-thin sections (unpublished), and probably relates to the method of cell wall formation and expansion,

although the literature is controversial (see Derksen *et al.* 1990; Seagull 1991).

- (2) Extensive arrays of MTs were found at places where cell walls thickened, e.g. the outer wall of the inner epidermis and cell walls of the middle layer that thickened before intercellular space formation. In the latter case their orientation was less ordered.
- (3) The bundles of parallel running MTs, found on the tips of the undulating outer cell wall of the inner epidermis, might well function in the formation of these wall ridges, too, as was shown during the formation of wall thickening in annular vessels of the xylem, and the cell wall thickenings in the mesophyll cells of maize (Apostolakos *et al.* 1991).

Cortical MT configurations remained unchanged during the intercellular space formation in *R. sceleratus*. It thus seems probable that they also assist cell wall thickening at early stages of intercellular space formation and probably do not function directly in space-enlarging, for which the physical force responsible may be generated by the growing epidermis and by the production of metabolic gas which cannot escape from the seed coat.

The extensive cortical MTs, present under the thickening outer walls of the inner epidermis, did not show a clear association with the fusing vesicle-tube complexes of the developing wall ingrowths. At later stages of wall ingrowth formation, cortical MTs were no longer present, although thickening of the wall ingrowths continued until starch grains and cytoplasm had disappeared. Based on those observations, we suggest that cell walls develop in various patterns: Cortical MTs do function when regular wall thickening occurs. However, when wall ingrowths are formed and when wall thickening continues in partly degenerating cells the MTs do not function in the process.

Cell aging in higher plant cells has drawn some attention but, up to now, most of the biochemical processes involved in plant cell aging are unknown (Rodriguez Sanchez 1990). Dawidowicz-Grzegorzewska and Podstolski (1992) observed a decrease of contrast in all cellular membranes in the transmission electron microscope, and regarded this as a symptom of age-induced membrane deterioration. This phenomenon was also observed in the

aging cells of the seed coat of *R. sceleratus*. When the inner epidermal cells degenerated, the ER, nuclei and starch grains were still present in the degrading cytoplasm. The thickening of the profiles of the cell wall ingrowths, however, continued until almost all remnants of the cytoplasm disappeared. This implies that the aging process is asynchronous for normal cell processes and wall synthesis.

Acknowledgements. The authors are indebted to S. Massalt for the photographs, A. Haasdijk for the artwork and Prof. Dr. M.T.M. Willemse for helpful discussion and critical reading of the manuscript. The authors also thank Prof. Dr. J.H.M. Willison and Dr. Zhang Min for providing various facilities for finalizing the manuscript when the first author visited Dalhousie University, Canada.

REFERENCES

- Apostolakis, A., Galatis, B., and Panteris, E. (1991) Microtubules in cell morphogenesis and intercellular space formation in *Zea mays* leaf mesophyll and *Pilea cadieri* epithem. *J. Plant Physiol.* **137**: 591-601.
- Boesewinkel, F.D., and Bouman, F. (1984) The seed structure. In: Johri, B.M. (ed.): *Embryology of Angiosperms*, Springer-Verlag, Berlin. pp. 567-610.
- Dawidowicz-Grzegorzewska, A., and Podstolski, A. (1992) Age-related changes in the ultrastructure and membrane properties of *Brassica napus* L. seeds. *Ann. Bot.* **69**: 39-46.
- Derksen, J., Wilms, F.G.A., and Pierson, E.S. (1990) The plant cytoskeleton: its significance in plant development. *Acta Bot. Neerl.* **39**: 1-8.
- Fransz, P. F., and Schel, J.H.N (1991) Cytodifferentiation during the development of friable embryogenic callus of maize (*Zea mays*). *Can. J. Bot.* **69**: 26-33.
- Robards, A.W., and Lucas, W.J. (1990) Plasmodesmata. *Ann Rev. Plant Physiol. Plant Mol. Biol.* **41**: 369-419.
- Rodriguez, R., and Sanchez, T. (1990) *Plant Aging. Basic and Applied Approaches*. Vol. 186 In: NATO ASI Series A. Life Sciences. Proceedings of a NATO ASI held at Ribadesella, Spain 1989.
- Seagull, R.W. (1991) Role of the cytoskeletal elements in organized wall microfibril deposition. In: Haigler, C.H., and Weimer P.J. (eds.): *Biosynthesis and Biodegradation of Cellulose*, Marcel Dekker Inc. New York. pp. 143-163.
- Sing, B. (1936) The life-history of *Ranunculus sceleratus* L. *Proc. Ind. Acad. Sci.* **4B**: 75-91.
- Spurr, A.R. (1969) A low viscosity epoxy resin embedding medium for electron microscopy. *J. Ultrastruct. Res.* **26**: 31-43.
- Van Lammeren, A.A.M. (1986a) A comparative ultrastructural study of the megagametophytes in two strains of *Zea mays* L. before and after fertilization. Agric. Univ. Wageningen Papers 86-1, pp. 37.
- Van Lammeren, A.A.M. (1986b) Developmental morphology and cytology of the young maize embryo (*Zea mays* L.). *Acta Bot. Neerl.* **35**: 169-188.
- Woolley, J.T. (1983) Maintenance of air in intercellular spaces of plants. *Plant Physiol.* **72**: 989-991.
- XuHan, X., and Van Lammeren, A.A.M. (1993) Microtubular configurations during the cellularization of coenocytic endosperm in *Ranunculus sceleratus* L. *Sex. Plant Reprod.* **6**: 127-132.

Chapter 5

Microtubular Configurations during the Cellularization of Coenocytic Endosperm in *Ranunculus sceleratus* L.¹

Xu XuHan and André A.M. van Lammeren

Department of Plant Cytology and Morphology, Wageningen Agricultural
University, 6703 BD, Wageningen, The Netherlands

¹ Reprinted, with permission, from *Sex. Plant Reprod.* 6: 127-132 (1993).

Abstract. Endosperm cellularization in *Ranunculus sceleratus* was studied in terms of the initiation of cell wall formation in the coenocytic endosperm. The first endosperm cell walls were in an anticlinal position relative to the cell wall of the embryo sac and originated from the cell plates and not from wall ingrowths from the embryo sac wall itself. Alveolar endosperm was formed 3 days after pollination. Microtubules were associated with the freely growing wall ends of the anticlinal walls and were observed in various orientations that generally ranged from angles of 45° to 90° to the plane of the wall. They were absent in the regions where vesicles had already fused. These microtubules may function in maintaining the growth and the direction of growth of the anticlinal wall until cellularization is completed. At the site where three neighbouring alveoli share their freely growing wall ends, remarkable configurations of microtubules were observed: in each alveolus, microtubules ran predominantly parallel to the bisector of the angle formed by the common walls. These microtubules may form a physically stable framework and maintain the direction of growth of the wall edges. It is concluded that the growing edge of the anticlinal endosperm wall and its associated microtubules are a special continuum of the original phragmoplast that gave rise to the anticlinal wall.

Key words: cell wall, cytoskeleton, endosperm cellularization, microtubules, *Ranunculus sceleratus*.

INTRODUCTION

Angiosperms with the nuclear type of endosperm development initially exhibit coenocytic endosperm. Endosperm cell wall formation begins when the endosperm has formed one layer of nuclei lying near the cell wall of the central cell.

The process of wall formation has been studied by electron microscopy in various species. In *Triticum aestivum* it has been reported that cell walls originate, at least in part, from cell wall protrusions (Mares *et al.* 1977; Morrison *et al.* 1978). This has also been found in *Helianthus annuus* (Newcomb 1973; Yan *et al.* 1991), *Arabidopsis thaliana* (Mansfield and Briarty 1990) and *Stellaria media* (Newcomb and Fowke 1973). However, Fineran *et al.* (1982) and Van Lammeren (1988) concluded that endosperm cell walls in *T. aestivum* originate from cell plates. The literature is also contradictory concerning the structure of the growing wall ends. Three types have been described: (1) wall edges without fusing vesicles and microtubules (MTs), (2) wall edges with fusing vesicles but without MTs, and (3) wall edges with both fusing vesicles and MTs (For a review see Fineran *et al.* 1982).

The present paper presents data on the origin of the first endosperm cell walls in *Ranunculus sceleratus*, and on the configuration and function of the MTs associated with the growing wall ends during the initial phase of endosperm cellularization.

MATERIALS AND METHODS

Plants of *Ranunculus sceleratus* L. were grown under greenhouse conditions. Developing ovaries and ovules were excised at various days after anthesis (DAA). For both electron microscopy and conventional light microscopy, samples were fixed at room temperature for 3-12 h in a mixture of 2.5% glutaraldehyde and 2% para-formaldehyde in phosphate buffered saline (PBS: 135 mM NaCl, 2.7 mM KCl, 1.5 mM KH₂PO₄, 8 mM Na₂HPO₄; pH 7.2). After rinsing in the same buffer, samples were post-fixed for 12 h at 4°C in 1-2%

osmium tetroxide in PBS, then rinsed in PBS and dehydrated in a graded ethanol series. The long fixation was necessary to preserve ultrastructure and microtubules. Samples were embedded in low viscosity resin (Spurr 1969). For light microscopy semithin median sections were stained with Toluidine Blue O. For electron microscopy, ultrathin sections were stained with uranyl acetate and lead citrate and analysed using a JEM-1200 EXII transmission electron microscope operating at 80 kV.

For the immunocytochemical staining of MTs, samples were fixed in 4% paraformaldehyde in microtubule stabilizing buffer (MSB: 1 mM EGTA, 4% PEG, 100 mM PIPES; pH 6.9) containing 0.05% Triton X-100 (w/v) for 3 h at room temperature. After rinsing in PBS and infusion with 1 M sucrose for 12 h followed by an infusion with 2.3 M sucrose in PBS for 24 h, samples were cryofixed in liquid nitrogen sludge. Semi-thin cryosections were prepared with a Reichert Jung FC 4D ultra-cryomicrotome, and affixed to poly-L-lysine-coated slides (poly-L-lysine, Sigma, St Louis, M., USA; 0.1% (w/v) in PBS, pH 7.2). The sections were incubated with rabbit polyclonal antitubulin (R229, see Van Lammeren *et al.* 1985) diluted in PBS (1:40), labelled secondly with GaR-FITC (Nordic-Tilburg-Holland) and observed with a Nikon Labophot epifluorescence microscope (for details see Van Lammeren 1988).

The pattern of endosperm development was investigated in median sections of the developing seeds, primarily in the ventral and dorsal regions of the endosperm.

RESULTS

1. Formation of alveolar endosperm

Three days after anthesis a layer of cytoplasm with free endosperm nuclei has formed in the embryo sac. We observed a monolayer of endosperm nuclei in semi-thin, cryosections of an ovule; arrays of MTs radiated from each nuclear envelope. The first nuclear division, which coincided with cell plate formation, occurred in the chalazal part of the endosperm (Fig. 1). The cell plate was aligned perpendicular to the wall of the embryo sac. On one side the cell plate extended towards and fused with the wall of the embryo sac; on the

opposite side it grew towards the central vacuole of the embryo sac and maintained a freely growing end. Thus, a cell wall was formed that was in an anticlinal position relative to the embryo sac wall. More anticlinal walls were formed after successive divisions. These cell walls created an alveolar coenocyte. Each alveolus contained a nucleus but had no cell wall on the side facing the central vacuole (Fig. 2). In general, the nucleus was located near the tonoplast of the central vacuole. Alveolar vacuoles were found between the nucleus and the anticlinal walls.

2. Structure of the anticlinal wall edge

Anticlinal wall edges consisted of numerous small membranous vesicles (Fig. 3). Extensive arrays of MTs were found associated with the wall edges that could only be visualized electron microscopically by prolonged fixation. Generally, the growing wall edge-associated MTs (GWE-MTs) extended more than 5 μm into the surrounding cytoplasm on both sides of the wall plane. Numerous GWE-MTs stopped at the growing wall end in darkly stained areas on the surfaces of membranous vesicles (Fig. 3), some penetrated the wall edge (Fig. 4) and some were observed between the wall edge and the tonoplast of the central vacuole (Fig. 5). The orientation of the GWE-MTs varied. Most GWE-MTs were oriented at a 45° - 90° angle to the plane of the wall edge (Figs. 3-5); however, some were found parallel to the new wall. GWE-MTs were absent in the region where vesicles had fused and had formed smooth plasmalemma (Fig. 5).

3. Cellularization of alveolar endosperm

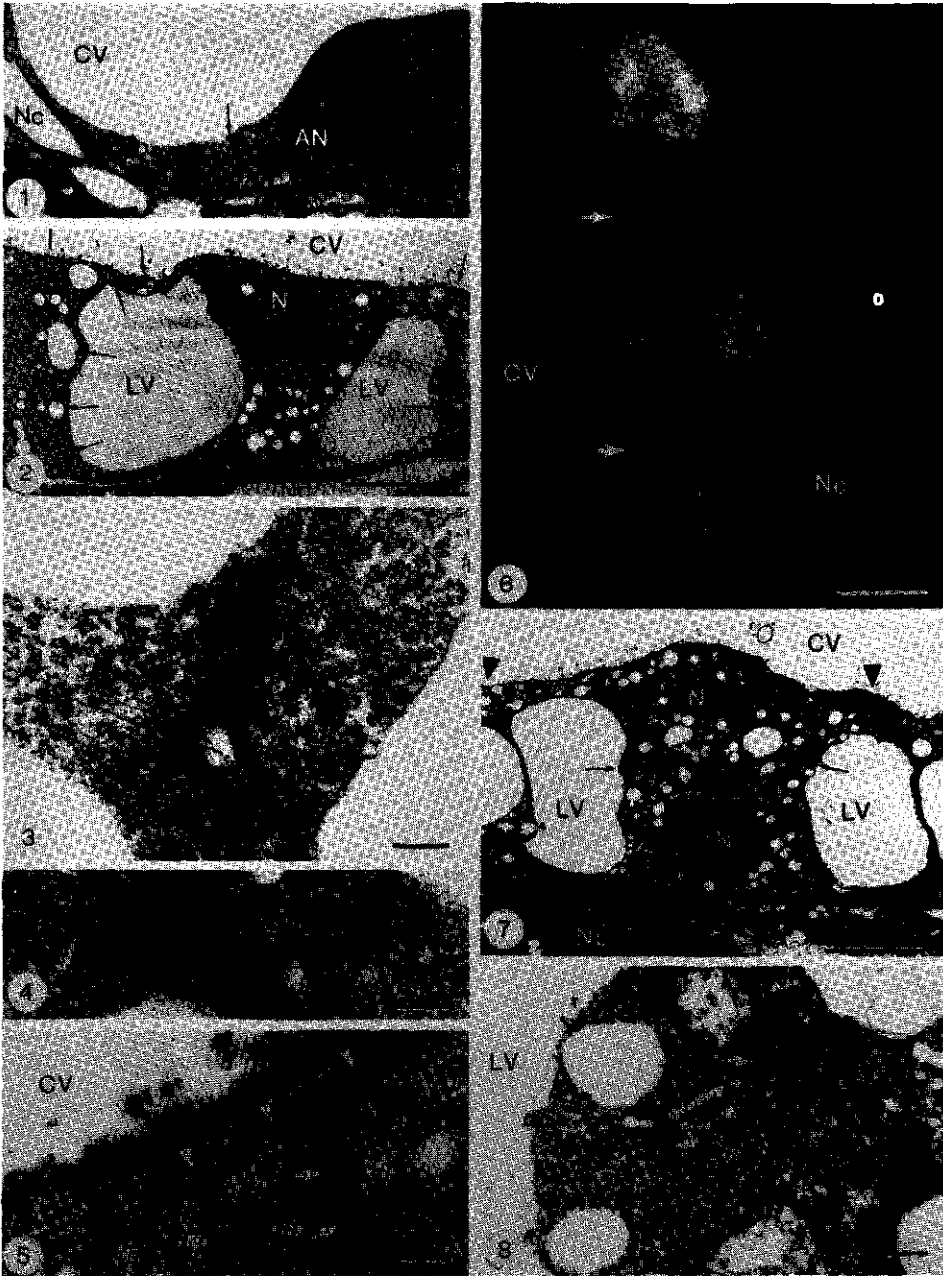
By 4 days after anthesis the nuclei in the alveoli had divided (Fig. 6). The equatorial plate was parallel to the embryo sac wall and cytokinesis had given rise to a layer of uninucleate cells adjacent to the embryo sac wall and a layer of alveoli bordering the central vacuole (Fig. 7). The newly formed periclinal cell plate between two daughter nuclei could not connect with the anticlinal walls immediately (Fig. 7) but had to extend and push the tonoplasts of the lateral vacuoles towards the anticlinal walls. The growing wall edges extended by adding vesicles to their very ends (Fig. 8). Microtubules were associated with the growing wall edge, and the orientation of the MTs was

mainly at an angle between 45° and 90° to the cell wall, while some MTs penetrated the growing edge. In the area where the new wall had been established, perpendicularly oriented MTs were not observed. The following division in the alveoli resulted in a second layer of endosperm cells whereas the alveoli remained. This cellularization continued until alveoli met in the centre of the embryo sac.

4. Microtubular configurations in the contact region of three neighbouring alveoli

Anticlinal wall formation resulted in a regular arrangement of alveoli with a honeycomb appearance. In transverse section, *et al.* parallel to the embryo sac wall, each alveolus appeared to be nearly hexagonal. In the contact region of three neighbouring alveoli the common anticlinal walls had angles of about 120° (Fig. 9). The GWE-MTs which connected with or were near the vertex exhibited a special configuration; in each alveolus they ran parallel to the bisector of the angle formed by the two walls. Microtubules observed further away from the vertex of the three neighbouring alveoli exhibited angles between the wall and the GWE-MTs that gradually increased from about 60° at the vertex to 90° further away (Fig. 9).

Figs. 1-8. AN, Antipodals; CV, central vacuole; EC, endosperm cytoplasm; LV, lateral vacuole; N, nucleus; Nc, nucellus. **Fig. 1.** Light micrograph of nuclear endosperm and antipodals in the chalazal part of the embryo sac of *R. sceleratus*. The endosperm cytoplasm and nuclei lie between the sac wall and the central vacuole. Note the first karyokinesis, which coincides with the formation of the cell plate (arrow). Bar = 20 μm . **Fig. 2.** Electron micrograph of endosperm of *R. sceleratus* at the alveolar stage of development. Note the anticlinal walls (arrows), which separate the nuclei and form the *alveolus*. Bar = 10 μm . **Fig. 3.** Electron micrograph of the growing edges of an anticlinal wall in the alveolar endosperm. Microtubules run along both sides of the growing wall edge (arrows) and connect with the darkly stained surfaces of vesicles. Bar = 200 nm. **Fig. 4.** Electron micrograph of the growing edge of an anticlinal wall in the alveolar endosperm. Some GWE-MTs penetrate the growing edges of an anticlinal wall. Bar = 200 nm. **Fig. 5.** Electron micrograph of the growing edge of an anticlinal wall at the alveolar endosperm stage showing a bundle of MTs (arrowheads) between the growing wall edge (arrows) and the tonoplast of the central vacuole. Bar: 200 nm. **Fig. 6.** Light micrograph of immunohistochemically stained MTs in a semithin cryosection of the endosperm at a late alveolar stage (5 DAA) and just before cellularization by periclinal cell plate formation. Three alveoli with mitotic spindles are shown. The areas of the growing wall edges of the anticlinal walls are indicated by arrows. Bar = 10 μm . **Fig. 7.** Electron micrograph showing the early alveolar-cellular endosperm stage. Two nuclei are present in the alveolus. Cell plate formation (arrows) continues underneath the tonoplasts of the lateral vacuoles and will result in a periclinal cell wall forming an endosperm cell and an aveolus. The freely growing wall ends of the alveolus are indicated by arrowheads. Bar = 5 μm . **Fig. 8.** Detailed view of the edge of the periclinal cell plate as shown in another section in Fig. 7. Note that the MTs are associated with the edge of the cell plate (arrows). Bar = 500 nm.



5. Wall protrusions

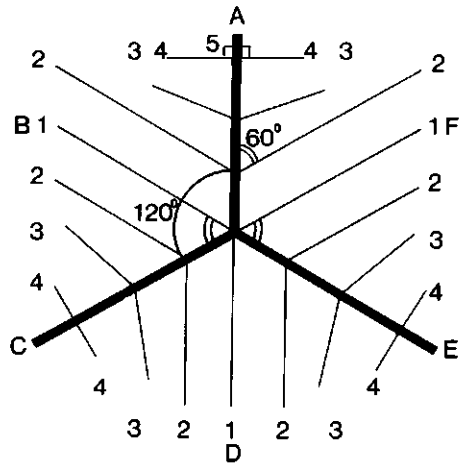
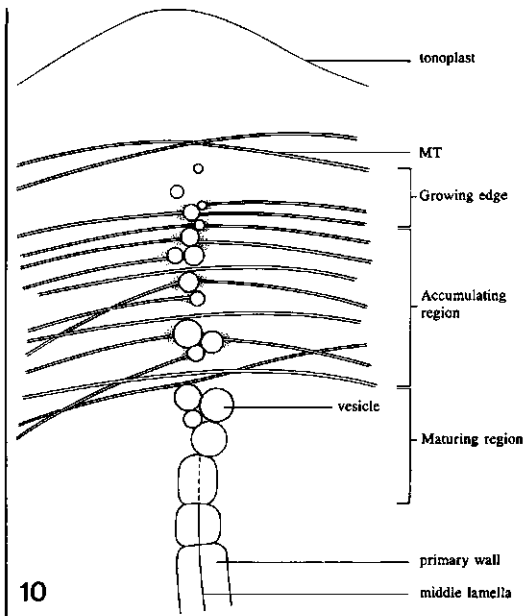
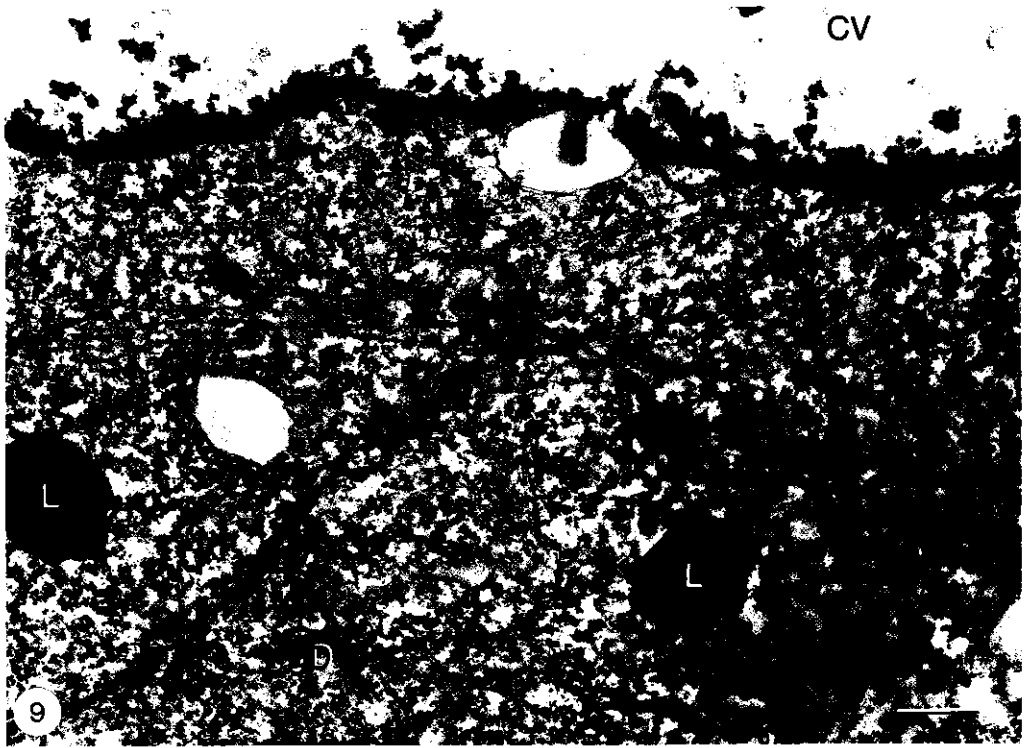
Occasionally small wall protrusions were observed in the embryo sac wall extending into the cytoplasm of the endosperm. They did not form any compartments (*i.e.*, alveoli or cells) in the developing endosperm. Vesicles were not found on the distal edges of the wall protrusions nor were MTs connected to the profiles of the wall protrusions.

DISCUSSION

1. Origin of anticlinal walls

The research presented here shows that anticlinal walls are formed after karyokinesis. Not all of the anticlinal walls formed in the alveolar endosperm can, however, be associated with the spindle apparatus of daughter nuclei. How then are cell walls between non-daughter nuclei established? Based upon our finding that coenocytic endosperm nuclei can be surrounded by radiating MTs, as has also been observed in coenocytic tetrads during microsporogenesis in *Gasteria* (Van Lammeren *et al.* 1985) and in the coenocytic endosperm of wheat at the moment of alveolus formation (Van Lammeren 1988), we suggest that phragmoplasts will be formed in all of the planes where MTs of neighbouring nuclei interact. The resulting cell plates

Figs. 9-11. CV, central vacuole; D, dictyosome; ER, endoplasmic reticulum; L, lateral vacuole. Fig. 9. Electron micrograph of a joining area of the common wall edges among three endosperm alveoli at the alveolar-cellular endosperm stage. Note the GWE-MTs (arrows) that extend parallel to the bisector of the angle of each two adjacent walls. For details see the text and for schematic representation see Fig. 11. Bar = 500 nm. Fig. 10. A simplified diagrammatic illustration of the structure of a growing wall edge of an anticlinal wall. Three zones can be recognized. The distal zone is the *growing edge* where the vesicles add on the end. Microtubules (MT) run in front of the wall end. The second distal zone is the *accumulating region*. Here, more vesicles accumulate, and the GWE-MTs connect to the more or less aligned vesicles. Some vesicles fuse and form an irregularly shaped cell wall. The next zone, adjacent to the normal-shaped primary wall, is the *maturing region*. Here, a more regular and smoother wall has formed, and a middle lamella appears. The GWE-MTs disappear in this region. Fig. 11. A diagrammatic representation of the microtubular configuration in the area of three neighbouring endosperm alveoli. The thick lines A, C and E represent the cell walls. The thin lines represent the MTs and also the bisectors in the case of B, D and F. The curved lines represent the angles, which are 120° between the cell walls. At and near the vertex the angles between most GWE-MTs (MTs no. 1, 2) and the cell walls are 60° (curved double lines). Away from the vertex, GWE-MTs become gradually perpendicular to the wall (MTs no. 3, 4).



will be perpendicular to the axes between the nucleus of one alveolus and the respective nuclei surrounding it. The regularity of the organization of the alveoli thus depends on the regularity in distribution of the nuclei in the cytoplasm along the wall of the embryo sac at the moment of alveolus formation. Thus, our observations confirm those of previous investigations concerning the origin of anticlinal cell walls between daughter nuclei in *R. sceleratus*.

2. The structure of the growing edge of anticlinal walls

The literature presents data on freely growing walls in the alveolar endosperm of *Helianthus annuus* (Newcomb 1973, Yan *et al.* 1991), *Stellaria media* (Newcomb and Fowke 1973) and *Triticum aestivum* (Mares *et al.* 1977, Morrison *et al.* 1978, Fineran *et al.* 1982, Van Lammeren *et al.* 1988). The formation of the anticlinal wall, however, is only discussed in detail by Fineran *et al.* (1982). Data concerning the structure of the wall end of the anticlinal walls are contradictory. In wheat (*Triticum aestivum*), Morrison *et al.* (1978) investigated the distal edges of growing anticlinal walls but did not find GWE-MTs and regarded the wall edges to be wall ingrowths. Mares *et al.* (1977) found both anticlinal wall edges and GWE-MTs but accepted the interpretation of Morrison *et al.* (1978). Fineran *et al.* (1982) thoroughly investigated the timetable of wall initiation in *Triticum aestivum* and observed that regularly arranged MTs and fusing vesicles were associated with the edges.

Only after long pre- and postfixation was this also observed with *R. sceleratus*, and it should probably be considered to be characteristic. The present investigation shows that the growing edge of the anticlinal wall in the endosperm has the same structure as that of the phragmoplast-cell plate complex during periclinal division in an alveolus. Thus, we conclude that the growing edges of the anticlinal walls are a continuum of the original cell plates. They differ from normal phragmoplasts in that they grow continuously and form the walls for more than one pair of daughter cells. A model of the growing edge of the anticlinal wall and its associated MTs is shown in Fig. 10. Three regions of the growing wall edge are distinguished: the growing

edge, the accumulating region and the maturing region. The characteristic microtubular configuration is depicted.

In the present study, the structural differences between the edge of a wall ingrowth and the edge of an anticlinal wall have been clearly defined. Thus, it can be stated that wall ingrowths do not contribute to endosperm cellularization in *R. sceleratus* (See also Fineran *et al.* 1982).

3. Microtubular configurations in the contact region of three neighbouring alveoli

The organization of the MT framework in the contact region of three neighbouring alveoli is schematically represented in Fig. 11. The walls of an alveolus tend to form 120° angles. Generally, phragmoplast MTs are found at about 90° angles to the wall plane, as shown in Fig. 10. At the vertex, however, they are found parallel to the bisector at 60° angles to the wall. This phenomenon must be based on the spatial interference of MTs coming from two walls; by pushing from two sides they will force each other in a direction parallel to the bisector. Further away from the vertex, MTs retain their normal organization. This interaction of MTs most likely maintains the position of the walls at angles 120°.

4. Function of microtubules associated with growing wall ends

Phragmoplast microtubules contribute to the inward flux of vesicles as well as to their alignment during cell plate initiation (Gunning 1982). For phragmoplast formation in wheat endosperm see Morrison and O'Brien (1976), Mares *et al.* (1977) and Fineran *et al.* (1982) for wheat endosperm, Hepler (1982) for lettuce root tip cells and Brown and Lemmon (1991) for orchids pollen. In the present study we observed vesicles between microtubules, but the mechanism of transport is still unknown. Based on the configuration of GWE-MTs in the growing edge of the anticlinal wall as shown in Fig. 10, we suggest that an equilibrium state is provided at each side of the wall plane. Moreover, as shown schematically in Fig. 11, the GWE-MTs form a special configuration in the contact region of three neighbouring alveoli. Together with the growing wall edges they form an equilibrium system

that maintains the condition for alveolus shaping and elongation. Therefore, we conclude that the microtubular framework at the growing wall edge most likely provides physical support for the wall edges and thus determines the shape of alveoli.

Acknowledgments. The authors are indebted to Mr. S. Massalt and Mr. A. Haasijk for the art work, to Prof. Dr. M.T.M. Willemsse for the critical reading of the manuscript and to Mrs. J. Brady reading the English text. The study was granted by a Sandwich Ph.D. Fellowship of the Wageningen Agricultural University.

REFERENCES

- Brown, R.C., and Lemmon, B.E. (1991) Pollen development in orchids. 5. A generative cell domain involved in spatial control of the hemispherical cell plate. *J. Cell Sci.* **100**: 559-566.
- Fineran, B.A., Wild, D.J.C., and Ingerfeld, M. (1982) Initial wall formation in the endosperm of wheat, *Triticum aestivum*: a reevaluation. *Can. J. Bot.* **60**: 1776-1795.
- Gunning, B.E.S. (1982) The cytokinetic apparatus: its development and spatial regulation. In: Lloyd, C.W. (ed) *The cytoskeleton in plant growth and development*. Acad. Press, New York, pp. 230-288.
- Mansfield, S.G., and Briarty, L.G. (1990) Endosperm cellularization in *Arabidopsis thaliana* L. *Arabidopsis Inf. Serv.* **27**: 65-72.
- Mares, D.J., Stone, B.A., Jeffery, C., and Norstog, K. (1977) Early stages in the development of wheat endosperm. II ultrastructural observations on cell wall formation. *Aust. J. Bot.* **25**: 599-613.
- Morrison, I.N., and O'Brien, T.P. (1976) Cytokinesis in the developing wheat grain; division with and without a phragmoplast. *Planta* **130**: 57-69.
- Morrison, I.N., O'Brien, T.P., and Kuo, J. (1978) Initial cellularization of the aleurone cells in the ventral region of developing wheat grain. *Planta* **140**: 19-30.
- Newcomb, W. (1973) The development of the embryo sac of sunflower *Helianthus annuus* after fertilization. *Can. J. Bot.* **51**: 879-890.
- Newcomb, W., and Fowke, L.C. (1973) The fine structure of the change from the free-nuclear to cellular condition in the endosperm of chickweed *Stellaria media*. *Bot. Gaz.* **134**: 236-241.
- Spurr, A.R. (1969) A low viscosity epoxy resin embedding medium for electron microscopy. *J. Ultrastruct. Res.* **26**: 31-43.
- Van Lammeren, A.A.M. (1988) Structure and function of the microtubular cytoskeleton during endosperm development in wheat: an immunofluorescence study. *Protoplasma* **146**: 18-27.
- Van Lammeren, A.A.M., Keijzer, C.J., Willemsse, M.T.M., and Kieft, H. (1985) Structure and function of the microtubular cytoskeleton during pollen development in *Gasteria verrucosa* (Mill.) H. Duval. *Planta* **165**: 1-11.
- Yan, H., Yang, H.-Y., and Jensen, W.A. (1991) Ultrastructure of the developing embryo sac of sunflower (*Helianthus annuus*) before and after fertilization. *Can. J. Bot.* **69**: 191-202.

Chapter 6

Microtubular Configurations during Endosperm Development in *Phaseolus vulgaris*¹

X. XuHan and A.A.M. van Lammeren

Department of Plant Cytology and Morphology, Wageningen Agricultural
University, Arboretumlaan 4, 6703 BD Wageningen, The Netherlands

¹ Reprinted, with permission, from *Can. J. Bot.* 72: 1489-1495 (1994)

Abstract. Microtubular cytoskeletons in nuclear, alveolar and cellular endosperm of bean (*Phaseolus vulgaris*) were analyzed immunocytochemically and by electron microscopy to reveal their function during cellularization. Nuclear endosperm showed a fine network of microtubules between the wide-spaced nuclei observed towards the chalazal pole. Near the embryo, where nuclei were densely packed, bundles of microtubules radiated from nuclei. They were formed just before alveolus formation and functioned in spacing nuclei and in forming internuclear, phragmoplast-like structures that gave rise to nonmitosis-related cell plates. During alveolus formation cell plates extended and fused with other newly formed walls, thus forming the walls of alveoli. Growing wall edges of cell plates exhibited arrays of microtubules perpendicular to the plane of the wall, initially. When two growing walls were about to fuse, microtubules of both walls interacted, and because of the interaction of microtubules, the cell walls changed their position. When a growing wall was about to fuse with an already existing wall, such interactions between microtubules were not observed. It is therefore concluded that interactions of microtubules of fusing walls influence shape and position of walls. Thus microtubules control the dynamics of cell wall positioning and initial cell shaping.

Key words: cell wall, cellularization, endosperm, microtubule, *Phaseolus vulgaris*

INTRODUCTION

In angiosperms with nuclear endosperm, the transition from nuclear endosperm to cellular endosperm was investigated in *Helianthus annuus* (Newcomb 1973), *Triticum aestivum* (Mares *et al.* 1977; Morrison and O'Brien 1976; Morrison *et al.* 1978; Fineran *et al.* 1982; Van Lammeren 1988), *Haemanthus katherinae* (Newcomb, 1978), *Arabidopsis thaliana* (Mansfield and Briarty 1990), *Phaseolus vulgaris* (Brown 1917; Weinstein 1926; Yeung and Cavey 1988), *Nitraria sibirica* (Li *et al.* 1992), *Glycine max* (Dute and Peterson 1992) and *Ranunculus sceleratus* (XuHan and Van Lammeren 1993). Questions, however, still remain as to how nuclear endosperm cellularizes. The alveolus has been proposed to be the functional unit in the cellularization process (Fineran *et al.* 1982; XuHan and Van Lammeren 1993). However, from a mathematical point of view, the number of mitosis-established cell walls (Fineran *et al.* 1982) does not agree with the number of walls needed to complete cellularization. Thus, additional questions arise whether wall ingrowths (Pate and Gunning 1972) contribute to cellularization, new cell walls branch to give rise to additional cell walls, or other mechanisms cause the formation of the nonmitosis-related walls. In alveolar endosperm it was observed that freely growing wall edges (GWE) are always associated with microtubules (MTs) (Van Lammeren 1988; XuHan and van Lammeren 1993). Therefore the freely GWE of the anticlinal wall was defined as the continuum of the original phragmoplast that continuously grows until cellularization is completed (XuHan and Van Lammeren 1993). However, how lateral walls of alveoli fused with each other was not investigated in detail.

Here we question to what level MTs do determine cellularization of endosperm and how MTs influence the site, shape and size of alveoli. Especially we questioned when and how cell wall fusion was influenced by MTs. *Phaseolus vulgaris* is especially suited to study the dynamics of the microtubular cytoskeleton in the process of endosperm cellularization because it exhibits nuclear, alveolar and cellular endosperm simultaneously from the early globular embryo stage until the cotyledonary stage. We present the results of changing microtubular configurations in developing endosperm,

obtained by transmission electron microscopy and by light microscopic observations on excised fertilized embryo sacs and sectioned material.

MATERIAL AND METHODS

Plants of *P. vulgaris* L. var. Groffy were grown under greenhouse conditions (23:18°C, light:dark). For the immuno-cytochemical staining of MTs, developing seeds were excised, immersed in 4% paraformaldehyde in phosphate-buffered saline (PBS, pH 7.0) with 0.1% Triton X-100, and integuments were peeled off for the greater part, using a binocular microscope. Isolated embryo sacs were further fixed for 24h, dehydrated in a graded series of ethanol, and embedded in polyethylene glycol (PEG) for the preparation of semithin (1-2 μm) sections. Fixation in 4% paraformaldehyde, the immuno-cytochemical staining of MTs with polyclonal antitubulin raised against calf brain tubulin (Van Lammeren *et al.* 1985), and the labelling with a second antibody conjugated with fluorescein isothiocyanate (FITC) (GaR-FITC Nordic, The Netherlands) were similar to the procedures described elsewhere (Van Lammeren 1988). Immunolabelling of whole mounts of endosperm was done after dissection of parts of the nuclear and alveolar endosperm. Additional treatment of the endosperm with 1% Triton X-100 for 1-2 h preceded immunolabelling to improve penetration of antibodies. The application of monoclonal anti- α -tubulin (Sigma Chemical Co., St. Louis, Mo.) revealed comparable configurations of fluorescent MTs, although the faint diffuse fluorescence, regularly observed in nuclei and nucleoli after labelling with the polyclonal antibody, was absent in such labelling experiments. Omission of the first antibody and application of preimmune serum served as controls. There was no fluorescence in such sections. Images were recorded with conventional fluorescence microscopy.

For electron microscopy, fixation with 2% paraformaldehyde, 2.5% glutaraldehyde and 1 or 2% osmium tetroxide, embedding in Spurr's resin, ultrathin sectioning, and post-staining were the same as reported previously (XuHan and Van Lammeren 1993).

RESULTS

Microtubular configurations in nuclear, alveolar and cellular endosperm

When the embryo was at the globular to elongated stage, the endosperm already had nuclear, alveolar, and cellular parts (Fig. 1). Microtubules were observed in all the tissues of the seed at this stage. In the nuclear endosperm at the chalazal part of the embryo sac MTs formed a fine reticulate network (Fig. 2). Some MTs radiated from nuclear envelopes. They were interwoven with other MTs in the internuclear area. The arrays of the network consisted of bundles of parallel MTs as was revealed by electron microscopy (Fig. 3). Control experiments in which preimmune serum was applied or in which the first antibody was omitted, no such configurations were observed. In the nuclear endosperm near the embryo, in which alveolus formation was about to start, bundles of MTs radiated from neighbouring nuclei. They were interwoven and formed arrays of bundles between pairs of nuclei (Fig. 4). Such arrays of internuclear MTs (INMTs) would ultimately give rise to phragmoplast-like structures and cell plates by which the alveolar cell walls developed.

The alveolar endosperm was restricted to the region near the apical part of the embryo (see Fig. 1). Alveoli often exhibited irregular shapes because the elongating embryo pushed the endosperm forward. Microtubules were abundantly present in the alveolar endosperm (Fig. 5). They ran from nuclei through the cytoplasm.

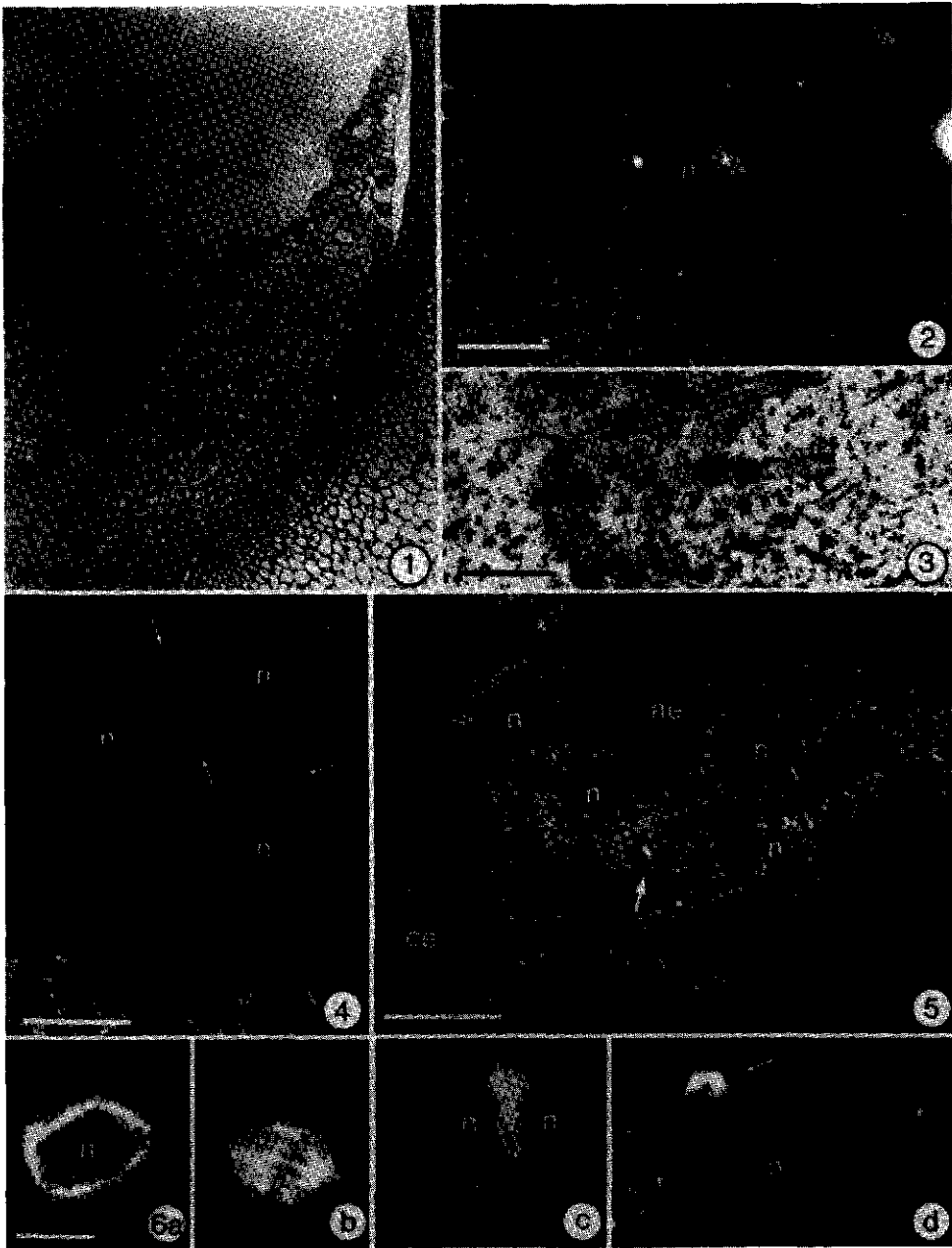
In cellular endosperm karyokinesis was always followed by cytokinesis (Fig. 6). Pre-prophase bands (PPBs) were found in dividing cells whereas PPBs were never observed in the nuclear endosperm. Hereafter, metaphase, anaphase, and telophase MT configurations appeared and at interphase an MT network was present throughout the whole cytoplasm again (Fig. 6).

Configurations of GWE-MTs

In the alveolar endosperm, cell plates were formed in the equatorial planes of the phragmoplast-like structures. The GWEs of cell plates expanded to all sides. The inner GWE grew towards the centre of the embryo sac. The outer GWE grew towards and finally connected to the existing embryo sac wall or to the profiles of the sac wall ingrowths. Lateral GWEs connected to other adjacent endosperm walls. Wall ingrowths themselves never gave rise to anticlinal wall formation. Microtubules, associated with the GWE that fused with the embryo sac wall or with an already thickened endosperm cell wall, showed a perpendicular orientation to the growing wall plane. They maintained this configuration during cell wall fusion (Fig. 7). We regularly observed cortical MTs near thickened endosperm cell walls or near the wall of the embryo sac. They were not involved in the process of cell wall fusion.

A different MT configuration was observed when GWEs grew towards and connected to recently formed cell walls or cell plates that still had associated MTs and in which vesicles were still fusing (Figs. 9, 10). Just before fusion, the GWE and the recently formed cell plate both exhibited MTs in perpendicular orientations. Then the MTs of the approaching GWE as well as those of the approached plate gradually changed their orientations. The original perpendicular orientation of MTs changed into an oblique orientation while the fusion proceeded (Fig. 8). In the fusion area the MTs of the approached plate parted away from either side of the approaching GWE

Fig. 1. Bright-field light micrograph showing a longitudinal semithin section of the micropylar side of the embryo sac of bean with embryo (em) and endosperm. The endosperm consisted of nuclear (ne), alveolar (ae) and cellular endosperm (ce). Embedded in PEG. Scale bar = 100 μm . Fig. 2. Immunofluorescence micrograph of a whole-mount preparation of endosperm showing fluorescent arrays of MTs in the nuclear endosperm in the region towards the chalazal pole. Note the reticulate network of numerous bundles of MTs, some of them running from the nuclear envelope. The faint diffuse labelling in the nucleus is due to fluorescence of out of focus MTs. The labelling in the nucleolus (*) is due to a nonspecific binding. n, nucleus. Scale bar = 20 μm . Fig. 3. Electron micrograph showing bundles of internuclear MTs in the nuclear endosperm. Scale bar = 500 nm. Fig. 4. Immunofluorescence micrograph of semithin PEG section of nuclear endosperm near the embryo showing thick internuclear bundles of MTs (INMTs, arrows). n, nucleus. Scale bar = 10 μm . Fig. 5. Immunofluorescence micrograph of semithin PEG section with cellular (ce) and developing alveolar (ae) endosperm. Compared with Fig. 4, INMTs increase in number and will give rise to phragmoplast-like structures between nuclei (arrow). Scale bar = 10 μm . Fig. 6. Fluorescent MTs in semithin PEG sections of cellular endosperm showing successive stages of normal cytokinesis. (a) Prophase cell with MTs surrounding the nucleus. (b) Metaphase cell with spindle of MTs. (c) Telophase cell with phragmoplast. (d) Late telophase cells showing nearly completed cytokinesis. The phragmoplast still existed at the side towards the central vacuole (arrow). At the right-hand side an interphase cell is partly depicted. n, nucleus. Scale bar = 10 μm .



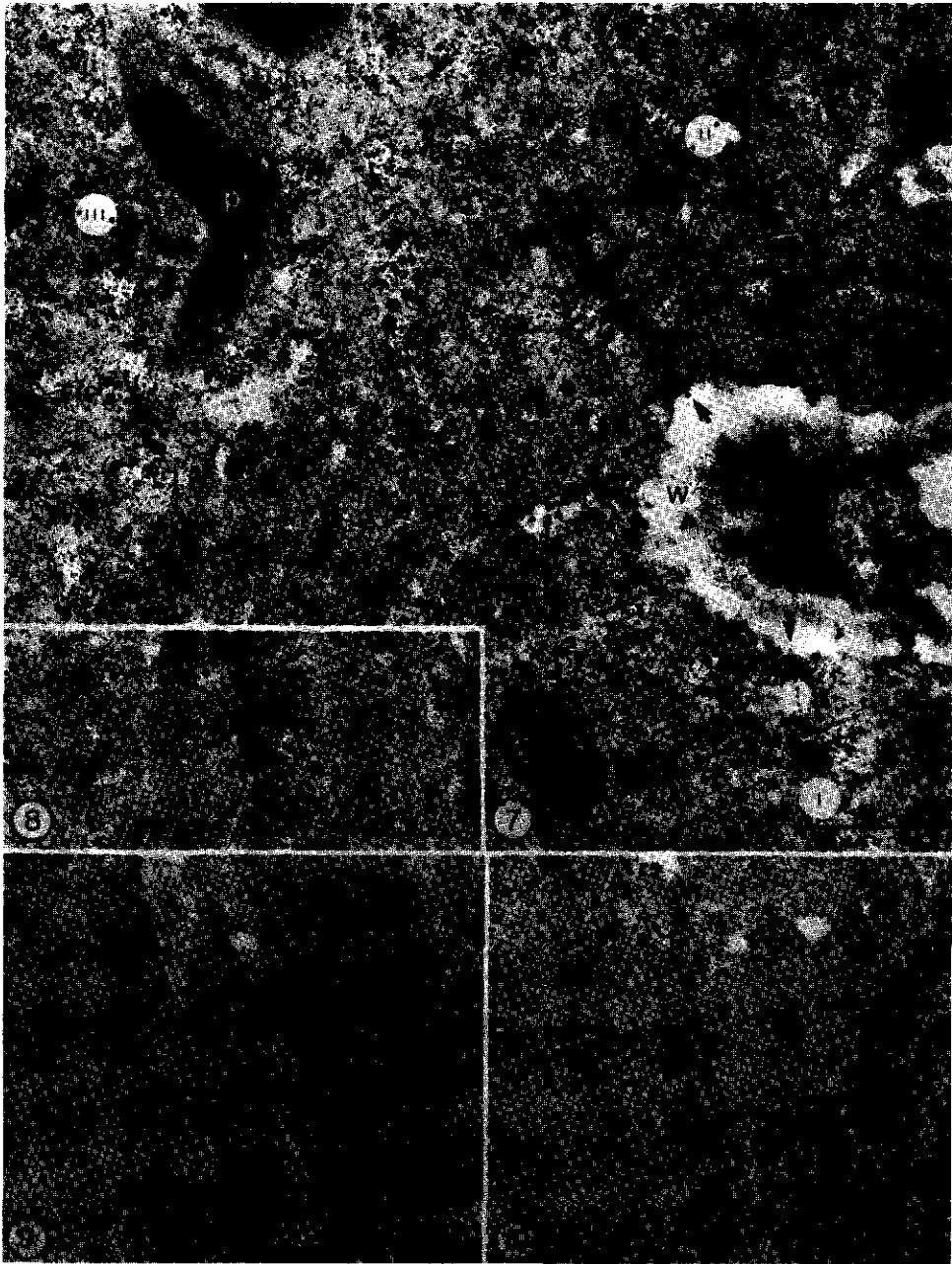
(Figs. 9, 10). The MTs of the approaching GWE formed rather small acute angles to the GWE but maintained mirror symmetric configurations to the GWE. Simultaneously the approached plate bent and formed a bulge towards the approaching GWE and MTs at the fusion site attained parallel orientations to the bisectors of the angles between the plates. At the end of the fusion, a Y-shaped cross of cell plates or walls was formed (Fig. 11). The MTs near the vertex of the Y-shaped cross were parallel to the bisectors of the angles and they formed a Y-shaped configuration, too. Throughout our observations, wall branching processes were not observed.

DISCUSSION

Microtubular configurations in nuclear, alveolar, and cellular endosperm

Compared with the previous work reviewed in the introduction, the present work shows remarkable differences in MT configurations in nuclear, alveolar, and cellular endosperm. In the nuclear endosperm with wide spaced nuclei, MTs run throughout the cytoplasm forming a reticulate network. In nuclear endosperm that is about to form alveoli, MTs radiate from nuclei and bundles of INMTs become prominent. In the alveolar endosperm GWE-MTs form the most remarkable MT arrays. Finally in the cellular endosperm, cortical, PPB, spindle, and phragmoplast MTs appear in a way common to somatic cells.

Fig. 7. Electron micrograph showing endosperm wall joinings. On the lower right and upper right GWEs (I and II) attach to a thickened endosperm wall (W) at the sites indicated by thick arrows. Dotted lines indicate the position of the growing walls. Note that GWE-MTs (small arrows) are perpendicular to the planes of the growing wall edges I and II. On the upper left, a GWE (III), also associated with MTs, approaches. Microtubules in the central area are either associated with GWE II or run in front of GWE III. Scale bar = 1 μ m. **Fig. 8.** Electron micrograph of bean endosperm showing a GWE that is near the fusion site with an other young cell wall still associated with MTs. MTs (arrows) gradually change orientation from perpendicular to the GWE away from the fusion site (lower side) to oblique to the GWE, *i.e.*, parallel to the bisectors of the wall angles near the fusion site (upper side). Orientation of MTs is indicated by arrows. Scale bar = 1 μ m. **Figs. 9 and 10.** Electron micrographs of two serial sections of a stage of wall fusion between a GWE (1) and a recently formed wall or plate (2) in the alveolar region of bean endosperm. Both cell walls exhibit associated MTs. MTs from wall 2 part away from the approaching wall 1 as is indicated by the long arrows at the upper side (Fig. 9) and the long arrows at the lower side (Fig. 10) of the approaching GWE. Note that the recently formed wall or plate (2) exhibits a bulge towards the approaching GWE. Its associated MTs overlap the MTs of the GWE 1 (short arrows) that are pushed back. Scale bar = 1 μ m



Microtubular configurations and cellularization

Microtubules function in cellularization in various ways. Pre-prophase bands (Pickett-Heaps and Northcote 1966) determine new wall planes by fixing the plane of division (Gunning 1982) and spindle, phragmoplast, and GWE-MTs control the position of the cell plate and the direction of cell plate extension in alveolar endosperm (XuHan and Van Lammeren 1993). The configurations of the MT arrays observed in the nuclear endosperm near the embryo of bean evoke considerations as to the function of these arrays.

The first MT configurations related to cellularization were observed in the nuclear endosperm just before alveolus formation. The MTs radiating from the nuclei probably function in the regular spacing of the nuclei first, and later, in the development of cell plates around each nucleus. Those cell plates are restricted to equatorial planes initially and expand from the centre to the periphery following a development as commonly seen during cytokinesis.

Cell plates between daughter nuclei are formed in the phragmoplast after karyokinesis. The other cell plates are formed in the phragmoplast-like structures, developed from the INMTs between nondaughter nuclei and are thus independent from karyokinesis. Thus, cell plates are formed in all the internuclear areas in the alveolar endosperm and nuclei become surrounded by cell walls at their lateral sides, not at the sides directed towards the wall of the central cell and towards the central vacuole of the central cell. Since alveoli are only formed when nuclei are near each other, induction of cytokinesis apparently depends on the distance between the nuclei in the endosperm. Phragmoplast-like structures were not described for *Nitraria sibirica* by Li *et al.* (1992) who only stated that phragmoplasts were a result of normal mitosis. Dute and Peterson (1992) described a different formation of anticlinal walls, rather projecting from the wall of the central cell into the endosperm cytoplasm. This might, however, be the result instead of the onset of anticlinal wall formation.

The extension of the cell plate occurs in three directions, *i.e.*, the GWEs grow towards the embryo sac wall, towards the inner side of the embryo sac, and in lateral directions. The GWEs that grow toward the embryo sac wall fuse with that wall or with profiles of wall ingrowths from the embryo sac in a

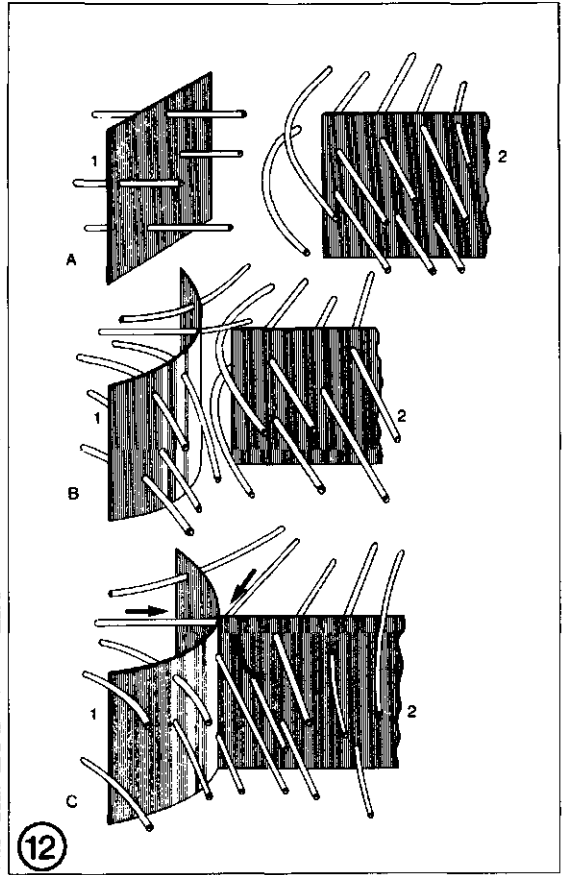
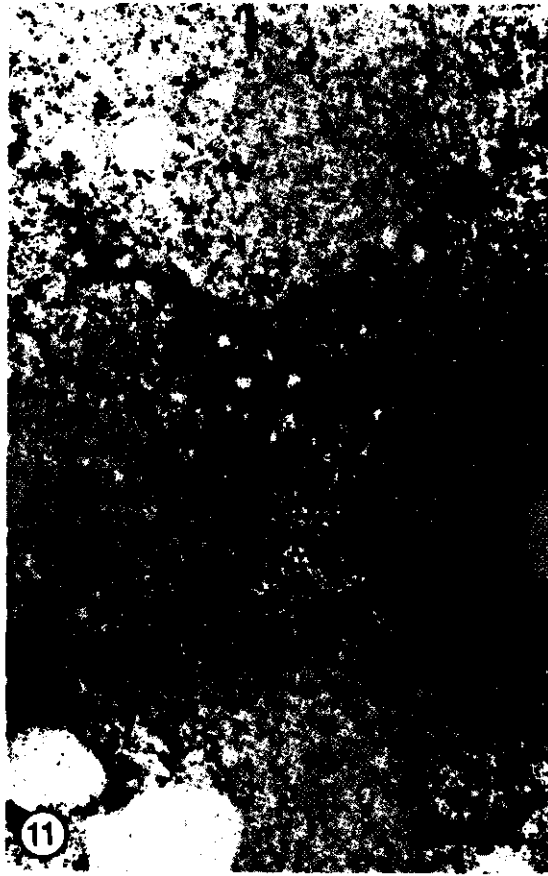


Fig. 11. Electron micrograph of the vertex area of the wall juncture. Note that MTs attain orientations parallel to the future bisectors (arrows). Scale bar = 1 μ m. **Fig. 12.** A diagrammatic illustration of a wall coalescence area showing the changes in microtubular configurations when two growing walls or plates fuse at a right angle. (A) When the GWE of plate (2) is still far away from the recently formed wall or plate (1), each population of MTs exhibits mirror symmetric orientations to each plane of the walls or plates. (B) When the two walls or plates are about to fuse, both population of MTs interact and change their orientations in the fusing area. As a result, wall or plate number 1 changes its shape. (C) When fusion has finished, the three walls and the MTs are separated by the walls or plates in the three alveoli and form Y-shaped crosses but the MTs stagger by half an angle to the wall or plate Y-shaped cross. The MTs on both sides of a common wall or plate are in mirror symmetric configuration. They will disappear when the wall or plate matures. Arrows indicate the bisectors in each newly formed alveolus.

random fashion and do not grow further then. Thus, it is concluded that the anticlinal walls are formed by cell plates that grow and connect to wall profiles or to the embryo sac wall. Existing wall profiles themselves do not form anticlinal walls. The inner GWEs of the anticlinal walls continuously grow towards the central vacuole, forming the walls of the alveoli and the file of cells behind. The lateral sides of the cell plate grow towards the other cell plates or to existing anticlinal cell walls and fuse, forming the alveoli. Wall branching, as suggested in *Arabidopsis thaliana* (Mansfield and Briarty 1990) was never observed in either this species or in *R. sceleratus* (XuHan and Van Lammeren 1993). We observed that anticlinal walls of the bean endosperm are often disturbed in position in the region near the tip of the embryo because the embryo presses against the endosperm. Thus, walls become oblique.

In our studies, as well as in those on soybean (Dute and Peterson 1992), extensive arrays of MTs are associated with GWEs, independent of the directions of growth or of the fusion of the GWEs with other walls. Growing wall edges show the same ultrastructure as normal cell plate edges (Hepler and Jackson, 1968) and should therefore be considered as a continuum of the phragmoplast. When GWEs grow, GWE-MTs form approximate mirror symmetric configurations as seen in mitotic phragmoplasts. These results are in agreement with those of our previous investigation in *R. sceleratus* (XuHan and Van Lammeren 1993).

Function of GWE-MTs

During the cellularization of bean endosperm, GWE-MTs control the direction of wall growth and wall fusion. An interesting phenomenon was observed when the GWE of a growing wall was about to fuse with another recently formed wall. According to mechanics and the interaction of MTs not taken into consideration, the approaching GWE could have pushed the recently formed wall. However, the recently formed wall bends towards the approaching GWE. This can be explained by the model shown in the diagrammatic illustration (Fig. 12). Here it is suggested that the dynamic configuration of the MT frameworks play a role in cell wall fusion and the changing shape of the walls. First the MTs of the two fusing walls do not interact (Fig. 12A). Then the MTs of the approaching wall push aside the

MTs of the opposite wall. By this action the opposite wall bends because the associated MTs change position (Fig. 12B). Ultimately this results in the rearrangement of the fusion site with angles between the walls approaching 120 ° each (Fig. 12C). Microtubules of adjacent walls interfere, and special configuration of MTs then provide an equilibrium in the area of wall junction as was analyzed previously in *R. sceleratus* (XuHan and Van Lammeren 1993). The present results, however, revealed the origin of such configurations. Since TEM studies were not done in the analysis of endosperm cellularization in wheat (Van Lammeren 1988), it might well be that comparable interactions of cell plate associated MTs lead to the hexagonal shape of the alveoli observed in that study.

Acknowledgments. The authors thank Mr. S. Massalt for the photographs, Mr. A. Haasdijk for the artwork, and Mr. F. Vegter for reading the English text. The authors also thank Professor M.T.M. Willemsse for his helpful discussion. The study was granted by a Sandwich Ph.D. Fellowship of the Wageningen Agricultural University.

REFERENCES

- Brown, M.M. (1917) The development of the embryo sac and of the embryo in *Phaseolus vulgaris* Bull. Torrey Bot. Club 44: 535-544.
- Dute, R.R., and Peterson, C.M. (1992) Early endosperm development in ovules of soybean, *Glycine max* (L.) Merr. (Fabaceae). Ann. Bot. 69: 263-271.
- Fineran, B.A., Wild, D.J.C., and Ingerfeld, M. (1982) Initial wall formation in the endosperm of wheat, *Triticum aestivum*: a reevaluation. Can. J. Bot. 60: 1776-1795.
- Gunning, B.E.S. (1982) The cytotkinetic apparatus: its development and spatial regulation. In: Lloyd, C.W. (Ed.) *The cytoskeleton in plant growth and development*. Academic Press, London. pp. 229-293.
- Heppler, P.K., and Jackson, W.T. (1968) Microtubules and early stages of cell-plate formation in the endosperm of *Haemanthus katherinae* Baker. J. Cell Biol. 38: 437-466.
- Li, S.W., Ma, H., and Tu, L.Z. (1992) The ultrastructural study on the early development of endosperm of *Nitraria sibirica*. Acta. Bot. Yunnanica 14: 151-156.
- Mansfield, S.G., and Briarty, L.G. (1990) Endosperm cellularization in *Arabidopsis thaliana* L. Arabidopsis Inf. Serv. 27: 65-72.
- Mares, D.J., Stone, B.A., Jeffery, C., and Norstog, K. (1977) Early stages in the development of wheat endosperm. II. Ultrastructural observations on cell wall formation. Aust. J. Bot. 25: 599-613.
- Morrison, I.N., O'Brien, T.P. (1976) Cytokinesis in the developing wheat grain: division with and without a phragmoplast. Planta 130: 57-67.
- Morrison, I.N., O'Brien, T.P. and Kuo, J. (1978) Initial cellularization and differentiation of the aleurone cells in the ventral region of the developing wheat grain. Planta 140: 19-30.

Chapter 6. Phragmoplast in bean endosperm

- Newcomb, W. (1973) The development of the embryo sac of sunflower *Helianthus annuus* after fertilization. *Can. J. Bot.* **51**: 879-890.
- Newcomb, W. (1978) The development of cells in the coenocytic endosperm of the African blood lily *Haemanthus katherinae*. *Can. J. Bot.* **56**: 483-501.
- Pate, J.S., and Gunning, B.E.S. (1972) Transfer cells. *Ann. Rev. Plant Physiol.* **23**: 173-196.
- Pickett-Heaps, J.D., and Northcote, D.H. (1966) Organization of microtubules and endoplasmic reticulum during mitosis and cytokinesis in wheat meristems. *J. Cell Sci.* **1**: 109-120.
- Van Lammeren, A.A.M., Keijzer, C.J., Willemsse, M.T.M., and Kieft, H. (1985) Structure and function of the microtubular cytoskeleton during pollen development in *Gasteria verrucosa* (Mill.) H. Duval. *Planta* **165**: 1-11.
- Van Lammeren, A.A.M. (1988) Structure and function of the microtubular cytoskeleton during endosperm development in wheat: an immunofluorescence study. *Protoplasma* **146**: 18-27.
- Weinstein, A.I. (1926) Cytological studies on *Phaseolus vulgaris*. *Am. J. Bot.* **13**: 248-263.
- XuHan, X., and Van Lammeren, A.A.M. (1993) Microtubular configurations during the cellularization of coenocytic endosperm in *Ranunculus sceleratus* L. *Sex. Plant Reprod.* **6**: 127-132.
- Yeung, E.C., and Cavey, M.J. (1988) Cellular endosperm formation in *Phaseolus vulgaris*. I. Light and scanning electron microscopy. *Can. J. Bot.* **66**: 1209-1216.

Chapter 7

An Improved Immunolabelling Method for the Microtubular Cytoskeleton in Poplar (*Populus nigra* L.) Free Nuclear Endosperm¹

Xu XuHan, André Souvré, Christel Granier and Michel Petitprez

Laboratoire de Biotechnologie et Amélioration des Plantes, UA INPT/INRA,
INP-ENSAT, 145 Av. de Muret, 31076 Toulouse Cedex, France.

Fax: (33) 61423029

¹ accepted by *Biotech. Histochem.* (1995)

Abstract. A study on the immunocytochemical staining of the microtubular cytoskeleton has been conducted with free nuclear endosperm, a tissue which is particularly difficult to fix. It is suggested that long fixation time, *e.g.* 45 h, is necessary for the preservation of the integrity of the microtubular network with paraformaldehyde-based fixative. The effects of low glutaraldehyde concentration in the fixative and of the routinely used ethanol dehydration method on the loss of β -tubulin antigenicity are not significant, while the former improves preservation of tissue structure. An ethanol-free embedding method is recommended for immunocytochemical studies on ethanol-sensitive target proteins.

Key words: embryo sac, endosperm, fixation, immunolabelling, microtubule, *Populus nigra*

Introduction

For decades, one of the most important subjects in biotechnology has been the search for reliable and easy microscopic methods to reveal cytological and histological events (Curr 1956, Stoward 1973, Juniper and Lawton 1979, Larsson 1988, Marc and Hackett 1989, Bell *et al.* 1989, Baskin *et al.* 1992, Kamo and Griesbach 1993, Dannenhoffer and Shen-Miller 1993). Large, highly cytoplasmic rich or extremely vacuolated tissues are some of the most difficult materials for structural preservation in histo- and cytological research. For immunocytochemical staining it becomes more complex because one has to take into consideration both the post-fixation changes and the antigenicity of target proteins (De Mey *et al.* 1982, Traas *et al.* 1987, Sonobe and Shibaoka 1989, Harold and Harold 1992, Larsson 1988). In plant materials, an Angiosperm-specific tissue, endosperm, exhibits all the above characteristics. In most cases, endosperm exists as a delicate tissue surrounding an extremely large vacuole, *i.e.* the central vacuole of the formal central cell. Moreover, this tissue, at early developmental stages, is a "liquid" coenocyte enveloped by a poorly permeable embryo sac wall as found in *Populus* and in other Angiosperms belonging to the Free Nuclear Type endosperm class (Li *et al.* 1982, XuHan and Van Lammeren 1993, for review see Vijayaraghavan and Prabhakar 1984). Thus, it is difficult to use immunocytochemical methods to visualize cytological events in this tissue, especially at whole tissue level, and that may account for the fact that there has only been a very limited amount of work dealing with the immunolabelling of the microtubular cytoskeleton in the coenocytic endosperm (Van Lammeren 1988, Webb and Gunning 1990, XuHan and Van Lammeren 1993, 1994, Brown *et al.* 1994).

In the work presented in this paper, we tested the effects of three parameters on the preservation of β -tubulin antigenicity and tissue structure: glutaraldehyde in paraformaldehyde-based fixative, duration of fixation, and omission of ethanol in sample processing. To achieve the last aim, an ethanol-free embedding method is used.

MATERIALS AND METHODS

Developing ovaries at 20 to 30 days after anthesis were collected from naturally grown *Populus nigra* plants. Nucelli were manually isolated by peeling off the integument tissue in the fixatives. In some cases, endosperm was further isolated manually in the fixatives.

For immunocytochemical staining of microtubules (MTs), samples were fixed in 4% paraformaldehyde (w/v) in 0.1 M phosphate buffered saline (PBS tablet, Sigma Chemical Co. France), pH 7.0, plus 0.1% Triton X-100 (w/v), or the same fixative solution plus 0.1% glutaraldehyde (v/v), or plus 0.5% glutaraldehyde. The length of fixation was tested at 3 h, 11 h, 24 h, and 45 h at room temperature.

Samples were embedded with two methods. (1) They were dehydrated in serial ethanol of 30%, 50%, 70%, 85%, 95% and 100% (v/v) (30 min each) at room temperature, and then transferred to a polyethylene glycol mixture of 4000 and 1500 (PEG4000, PEG1500, Merck-Schuchardt, Germany) (1:3, w/w) dissolved in ethanol, 3:1, 1:1, and 1:3 (v/v) at 50 °C (50 min each). The samples were then infiltrated three times in the PEG mixture without ethanol at 57°C (30 - 60 min each), and solidified in the PEG mixture at room temperature. (2) Samples were dehydrated in serial PEG2000 (Aldrich-Chemie S. à. r. l., France) solutions of 30%, 50%, 70% (w/w) in PBS (1 - 3 h each, can be overnight) at room temperature, and then three times in pure PEG2000 or PEG3000 (Merck-Schuchardt, Germany) (30 - 60 min each) at 57°C, and solidified in the PEG at room temperature. To dissolve or melt PEG, heating is necessary.

The embedded samples used for the present work were stored in small plastic pots at room temperature for less than two weeks, though we did not find antigenicity loss in checked samples stored for three months in these conditions (data unshown). All the samples were sectioned at 1.5 µm with an LKB 2218 Historange microtome. Sections were mounted on poly-L-lysine-coated slides (poly-L-lysine, Sigma, St. Louis, MO, USA; 0.1% (w/v)) using a small loop with PEG1500 water solution in appropriate concentrations

(adjusted by the user to permit the sections to stretch properly). After three washes in PBS for 10 min each, sections were treated with 5% normal goat serum (Amersham Intl. plc, UK) for 0.5 h at 30°C to reduce non-specific labelling. Immunolabelling was performed using a monoclonal anti- β -tubulin (Amersham Intl. plc, UK) as the first antibody at 1:500 dilution for 1 h, and fluorescein isothiocyanate (FITC) linked sheep anti-mouse IgG (Amersham Intl. plc, UK) as the secondary antibody at 1:100 dilution for 1 h, both at 35°C. Three washes for 10 min each in PBS followed each labelling. Controls were made by omission of the first antibody. Sections were further stained with 4,6-diamidino-2-phenylindole (DAPI, Sigma Chimie, France) added in mounting Citifluor (Link Analytical, UK) with final concentration about 0.02% (w/v) to reveal nuclei and DNA-carrying organelles. Observations and microphotographs were taken on a Leitz Laborlux 12 microscope with a Wild Photoautomat MPS45 exposure system, using TMAX P3200 films.

RESULTS

1. Duration of fixation

Fixation treatments for four different lengths of time were compared (Table 1). A fixation duration of 3h did not reveal any photo-recordable MT arrays in the coenocytic endosperm, except that occasionally, a few, individual and very thin, short fluorescent lines were seen, this however was recorded as "no labelling" though in the anti- β -tubulin-omitted control, all the sections appeared dark brown (labelling silence).

Prolonged fixation resulted in an increase of fluorescence of the MT arrays stained by anti- β -tubulin and FITC linked secondary antibody. After 11 h fixation, a few parts of the MT network were sometimes visible. After 24 h fixation, an uncompleted MT network was observed in the endosperm. In the last case, doubling the concentrations of both antibodies did not enhance labelling and increased noise at a low level. These results suggested testing a

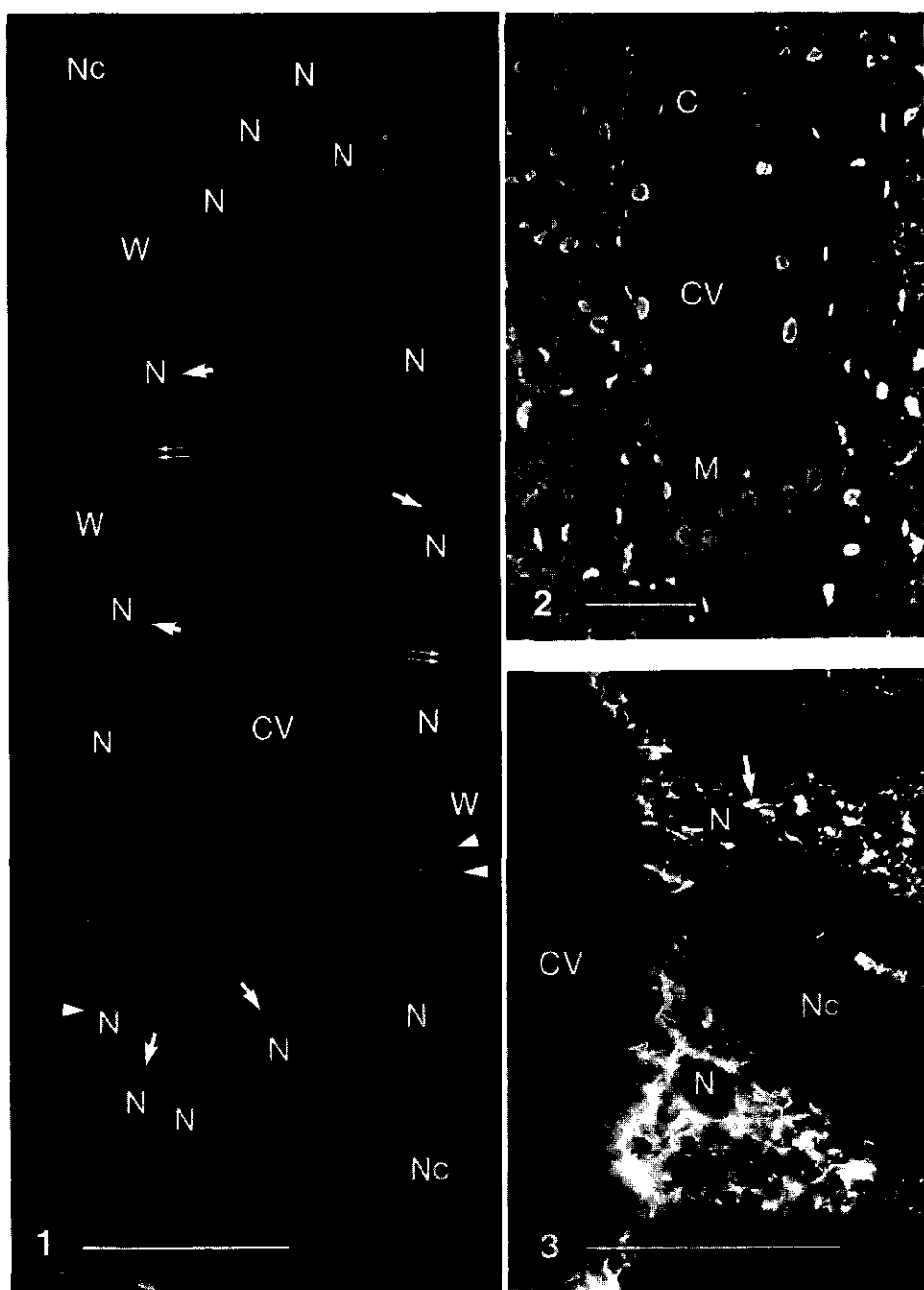
longer period of fixation. Thus, further tests of 45 h fixation were carried out comparing the effects of 0.1% and 0.5% glutaraldehyde (Table 1).

After 45 h fixation, a huge MT network was visualized in the endosperm, although in a few cases the staining of the network was not effectual for the whole endosperm, *e.g.* in the micropylar part where the embryo was present. However, as a rule, images of long and thick bundles and small and short arrays of MTs interweaving into an integral framework in the endosperm tissue were easily obtained (Fig. 1). Compared with the DAPI staining (Fig. 2), it was clear that the vacuoles and nuclei were not stained (Figs. 1, 3). In the MT framework as shown in Figs. 1 and 3, three populations of MTs were visualized, *i.e.* perinuclear arrays of MTs including the arrays radiating from the surfaces of the nuclei, cytoplasmic arrays of MTs that were interwoven in internuclear spaces and were the main constituent of the MT network, and some cortical MTs close to the embryo sac wall. The MTs were more extensive where the nuclei were close to each other, *e.g.* in the micropylar or chalazal part. The outer tissue, *i.e.* the nucellus, sometimes exhibited loss of tubulin antigenicity after 45 h fixation.

2. Glutaraldehyde

Glutaraldehyde did neither distinguishably decrease MT specific labelling nor increased non-specific labelling in the concentrations tested in the present

Fig. 1. Fluorescence micrograph of the poplar nuclear endosperm immunocytochemically stained with monoclonal anti- β -tubulin and FITC conjugated secondary antibody, showing an overview of the microtubular framework in the endosperm in a longitudinal section. Note the three populations of microtubules in the framework: radiating arrays (arrows) from the nuclear surfaces; cytoplasmic arrays (double arrows) in the internuclear areas; and a few cortical arrays (arrowheads) near the cell wall of the embryo sac. Endosperm was fixed for 45 h in 4% paraformaldehyde and 0.5%-glutaraldehyde and processed via the ethanol-mediated PEG procedure. CV: central vacuole; N: nucleus of endosperm; Nc: nucellus tissue; W, embryo sac wall. Bar = 50 μ m. **Fig. 2.** Fluorescence micrograph at a low magnification showing nuclear position in the same section as in Fig. 1. DAPI staining. C, chalazal part; M, micropylar part; V, central vacuole of the formal central cell. Bar = 50 μ m. **Fig. 3.** Fluorescence micrograph of microtubular cytoskeleton of the endosperm in an oblique section showing the radiating arrays of MTs and the orientations of the cytoplasmic MTs. Arrow points a possible MT nucleation. Endosperm was fixed for 45 h in 4% paraformaldehyde and 0.5%-glutaraldehyde and processed via the ethanol-mediated PEG procedure. CV, central vacuole; N, nucleus of endosperm; Nc, nucellus tissue. Bar = 50 μ m.



work, nor did it significantly contribute to the preservation of MTs compared with glutaraldehyde-absent fixation. Prolonged duration of fixation also did not bring about any obvious effects of the glutaraldehyde on specific or non-specific labelling in the conditions tested. However, at the level of overall structure of sectioned tissue, we found that glutaraldehyde preserved the integrity of the endosperm and other tissues. This effect occurred with 0.5% glutaraldehyde at 24 h fixation in ethanol-free embedding and was further enhanced with a prolonged fixation time of 45 h. The same effect was also seen in the normal embedding procedure at 0.1% glutaraldehyde and 45 h fixation (Table 1). Sections tended to keep tissue integrity during mounting sections to slides when the samples were fixed with glutaraldehyde for 24 and 45 h. To avoid tissue compression, it was also found necessary to leave the section in the mounting PEG solution in the loop for some time, *e.g.* 15 sec, until the solution reached equilibrium before the section was affixed to the slide.

3. Ethanol-mediated and ethanol-free embedding

Ethanol, used in dehydration and transition to various PEG types, did not produce an MT-labelling loss in the overall MT configuration compared with the ethanol-free processing method (Table 1).

As described in materials and methods, a graded PEG-PBS solution series was used instead of ethanol-mediated transfer to embedding PEG. We found that PEG at molecular weights of 2000 and 3000 were suitable, because their 70% solutions were still of low viscosity at room temperature. A regime of 30%, 50%, 70% PEG-PBS solutions at room temperature and pure PEG at 57°C was adopted because samples did not show structural compression when omitting intermediate steps, *e.g.* 80% and 90% PEG-PBS solutions. However, when isolated young nucelli or endosperm was used, infiltration in PEG-PBS solutions led to compression of the tissue, which started even at the beginning in 7% PEG solution. In general, the infiltration is slower than the ethanol-mediated regime.

Samples could stay overnight in the PEG solution at any step (before the warm PEG) without antigenicity loss of β -tubulin. In pure PEG, at least two changes were necessary to maintain the hardness of the embedded block for 1 to 3 μ m sectioning at room temperature.

| Fixation time (h) | Glutaraldehyde concentration in fixatives (%) | | | | |
|----------------------|---|-------|-----|------------------------|---------|
| | 0 | 0.1 | 0.5 | 0 | 0.5 |
| | Normal embedding | | | Ethanol-free embedding | |
| 3 | - | - | - | - | - |
| 11 | * | + | + | + | + |
| 24 | ++ | ++ | * | ++ | ++ # |
| 45 | * | +++ # | * | * | +++ # # |

Table 1. Effects of duration of fixation, glutaraldehyde concentration in paraformaldehyde-based fixative, and ethanol- and non-ethanol- involved embedding procedures on immunocytochemical labelling of microtubules and tissue structure preservation in the free nuclear endosperm of poplar. -, no labelling; *, test undone; +, poor labelling; ++, unsatisfactory labelling; +++, good labelling; #, improved tissue structure preservation; ##, further improved tissue structure preservation.

DISCUSSION

The greatest change in the concept and techniques of fixation (e.g. Curr 1956) lies in the modification from lethal to semi-lethal or non-lethal fixation in order to preserve properties of proteins such as antigenicity for immunohistochemical studies. Proper *in situ* immunolabelling of MTs depends on optimizing various parameters during sample processing. Compared with previous work, the method optimized in the present work results in good images of the MT framework in the nuclear endosperm of Angiosperms at a sectioned whole tissue level.

In this work, we still use Triton to enhance fixative penetration, whereas to simplify the test of fixation parameters, we avoided using ethylene glycol-bis(2-aminoethyl ether)-N,N,N',N'-tetraacetic acid (EGTA) piperazine-N,N'-bis[2-ethanesulfonic acid] (PIPES) involved MT stabilizing buffer (Traas *et al.* 1987, XuHan and Van Lammeren 1993) and aldehyde reducing agents such as sodium cyanoborohydride (NaBH_3CN) (Barney *et al.* 1990, Mattson *et al.* 1990). Although those chemicals may play roles in the immunolabelling of MTs, the present method yields clear images of MT arrays which are even sharper than the images revealed using the cryosection-method which we obtained from the small coenocytic endosperm of *Ranunculus sceleratus* (XuHan and Van Lammeren 1993). Because ethanol and long time fixation, especially involving glutaraldehyde, were thought to be responsible for losses of antigenicity in general, cryosectioning avoiding ethanol and glutaraldehyde was used in that research. However the present results indicate that either the routinely used ethanol dehydration and transition to embedding medium, or the glutaraldehyde-added fixatives does not affect antigenicity of β -tubulin at a distinguishable level in the endosperm.

The ethanol-free procedure reported in this paper shows no advantage with regard to the visualization of MTs compared with the ethanol-mediated method. It can, however, be used in the cases when target proteins would be ethanol sensitive, and the timing of the processing is less critical.

The mechanisms of aldehyde function in fixatives are discussed by Jones (1973) and Hopwood (1973). The sharp image of MTs in the present work is mainly due to the prolonged fixation that both preserves the structure of the tissue and preserves the antigenicity of the β -tubulin. The reason that the antigenicity of β -tubulin is preserved during the long-time fixation used in the present work could be that within the time of fixation, a very limited quantity of aldehydes penetrates the tissue, and most of that, that does penetrate, is bound by the other elements in the tissue. We estimate that the maximal fixation time is close to 45 h because the surrounding nucellar tissue has started to loss antigenicity of β -tubulin at this time, suggesting that it would soon occur in the endosperm.

In the samples fixed for 45 h in glutaraldehyde-added fixatives, we observed that the cytoplasmic MTs run throughout the cytoplasm of the poplar nuclear endosperm. Although interconnecting with the radiating and cortical MTs, they form a rather independent population. Little attention has been paid so far to the cytoplasmic population, and the population has not been properly classified as done for other kinds of microtubular organizations in plant cells (Goddard *et al.* 1994). The present results indicate that the cytoplasmic population of MTs can be an independent type of organization as its analogue in animal cells (Ingber *et al.* 1994). This organization stands next to the radiating arrays, the preprophase band, the cortical arrays, the spindle, and the phragmoplast organizations. Poor fixation might have led to ignorance of the phenomenon. The cytoplasmic MTs were also noticed by Baskin *et al.* (1992) in plant cells with an improved methacrylate embedding method, suggesting importance of improving immunocytochemical techniques.

Acknowledgments. We thank Dr. André A. M. van Lammeren for helpful discussion, Ms. Joanne Ariss for reading the English text and Mr. Georges Alliaume for the photographs.

REFERENCES

- Barney, C.I., Huber, F.W., and McCarthy, J.R. (1990) A convenient synthesis of hindered amines and α -trifluoromethylamines from ketons. *Tetrahedron Lett.* 31: 5547-5550.
- Baskin, T.I., Busby, C.H., Fowke, L.C., Sammut, M., and Gubler, F. (1992) Improvements in immunostaining samples embedded in methacrylate: localization of microtubules and other antigens throughout developing organs in plants of diverse taxa. *Planta* 187: 405-413.
- Bell, P.B., Lindroth, M., Fredriksson, B.-A., and Liu, X.-D. (1989) Problems associated with the preparation of whole mounts of cytoskeletons for high resolution electron microscopy. *Scan. Microscopy Suppl.* 3: 117-135.
- Brown, R.C., Lemmon, B.E., and Olsen, O.-A. (1994) Endosperm development in barley: microtubule involvement in the morphogenetic pathway. *Plant Cell* 6: 1241-1252.
- Curr, E. (1956) *A Practical Manual of Medical and Biological Staining Techniques*. Leonard Hill, London. (for main objects of fixation, see pp. 4-5)
- Dannenhoffer, J.M., and Shen-Miller, J. (1993) Evaluation of fixative composition, fixative storage, and fixation duration on the fine structure and volume of root-cell nucleoli. *Biol. Cell* 79: 71-79.
- De Mey, J., Lambert, A.M., Bajer, A.S., Moeremans, M., and De Brabander, M. (1982) Visualization of microtubules in interphase and mitotic plant cells of *Haemanthus endosperm* with the immuno-gold staining method. *Proc. Natl. Acad. Sci. USA* 79: 1898-1902.

Chapter 7. Microtubules in poplar nuclear endosperm

- Goddard, R.H., Wick, S.M., Silflow, C.D., and Snustad, P. (1994) Microtubule components of the plant cell cytoskeleton. *Plant Physiol.* **104**: 1-6.
- Harold, R.L., and Harold, F.M. (1992) Configuration of actin microfilaments during sporangium development in *Achlya bisexualis*: Comparison of two staining protocols. *Protoplasma* **171**: 110-116.
- Hopwood, D. (1973) Theoretical and practical aspects of glutaraldehyde fixation. In: Stoward, P.J. (ed.) *Fixation in Histochemistry*. Chapman and Hall, London. pp. 47-83.
- Ingber, D.E., Dike, L., Hansen, L., Karp, S., Liley, H., Maniotis, A., McNamee, H., Mooney, D., Plopper, G., Sims, J., and Wang, N. (1994) Cellular tensegrity: exploring how mechanical changes in the cytoskeleton regulate cell growth, migration, and tissue pattern during morphogenesis. *Int. Rev. Cytology* **150**: 173-223.
- Jones, D. (1973) Reactions of aldehydes with unsaturated fatty acids during histological fixation. In: Stoward, P.J. (ed.) *Fixation in Histochemistry*. Chapman and Hall, London. pp. 1-45.
- Juniper, B.E., and Lawton, J.R. (1979) The effect of caffeine, different fixation regimes and low temperature on microtubules in the cells of higher plants: evidence for diversity in their response to chemical and physical treatments. *Planta* **145**: 411-416.
- Kamo, K.K., and Griesbach, R.J. (1993) Evaluation of DAPI as a fluorescent probe for DNA in viable *Petunia* protoplasts. *Biotech. Histochem.* **68**: 350-359.
- Larsson, L.-I. (1988) *Immunocytochemistry: Theory and Practice*. CRC Press, Inc., Boca Raton, Florida.
- Li, W.-D., Fan, L.-W., and Mai, X.-L. (1982) Embryological observations on the seed development of *Populus simonii* Carr. *Sci. Silv. Sin.* **18**: 113-119.
- Marc, J., and Hackett, W.P. (1989) A new method for immunofluorescent localization of microtubules in surface cell layers: application to the shoot apical meristem of *Hedera*. *Protoplasma* **148**: 70-79.
- Mattson, R.J., Pham, K.M., Leuck, D.J., and Cowen, K.A. (1990) An improved method for reductive alkylation of amines using titanium (iv) isopropoxide and sodium cyanoborohydride. *J. Org. Chem.* **55**: 2552-2554.
- Sonobe, S., and Shibaoka, H. (1989) Cortical fine actin filaments in higher plant cells visualized by rhodamine-phalloidin after pretreatment with m-maleimidobenzoyl n-hydroxysuccinimide ester. *Protoplasma* **148**: 80-86.
- Stoward, P.J. (1973) *Fixation in Histochemistry*. Chapman and Hall, London.
- Traas, J.A., Doonan, J.H., Rawlins, D.J., Shaw, P.J., Watts, J., and Lloyd, C.W. (1987) An actin network is present in the cytoplasm throughout the cell cycle of carrot cells and associated with the dividing nucleus. *J. Cell Biol.* **105**: 387-395.
- Van Lammeren, A.A.M. (1988) Structure and function of the microtubular cytoskeleton during endosperm development in wheat: an immunofluorescence study. *Protoplasma* **146**: 18-27.
- Vijayaraghavan, M.R., and Prabhakar, K. (1984) The endosperm. In: Johri, B.M. (ed.) *Embryology of Angiosperms*. Springer-Verlag, Berlin, Heidelberg. pp. 319-376.
- Webb, A.C., and Gunning, B.E.S. (1990) The microtubular cytoskeleton during development of the zygote, proembryo and free-nuclear endosperm in *Arabidopsis thaliana* (L.) Heynh. *Planta* **184**: 187-195.
- XuHan, X., and Van Lammeren, A.A.M. (1993) Microtubular configurations during the cellularization of coenocytic endosperm in *Ranunculus sceleratus* L. *Sex. Plant Reprod.* **6**: 127-132.
- XuHan, X., and Van Lammeren, A.A.M. (1994) Microtubular configurations during endosperm development in *Phaseolus vulgaris*. *Can. J. Bot.* **72**: 1489-1495.

Chapter 8

Development of Coenocytic Endosperm in Poplar (*Populus nigra* L.): Two Kinds of Microtubular Configurations Constitute One Alveolar Phragmoplast during Alveolation

X. XuHan^{1,3}, W.-D. Li², A. Souvré³ and A. A. M. van Lammeren¹

¹ Department of Plant Cytology and Morphology, Wageningen Agricultural University, Arboretumlaan 4, 6703 BD Wageningen, The Netherlands.
Fax: (31) 837085005

² Biology Department, Chinese Academy of Forestry, Beijing 100091, China.
Fax: (86) 102581937

³ Laboratoire de Biotechnologie et Amélioration des Plantes, Ecole Nationale Supérieure Agronomique de Toulouse, Institut National Polytechnique, 145 Av. de Muret, F-31076 Toulouse Cedex, France.
Fax: (33) 61423029

Abstract. Phragmoplast patterning and growth patterning were investigated in the coenocytic endosperm of poplar (*Populus nigra*) by light and electron microscopy. In nuclear endosperm, free nuclei position regularly in the cytoplasm along the embryo sac wall. Microtubules (MTs) form a widespread network throughout the cytoplasm. Nucleation sites, which often appear as microtubule converging centers, develop on nuclear envelopes and form MTs that radiate from the nuclei into the cytoplasm. In areas with densely packed nuclei, these MTs may function in the initiation of alveolation.

During the initial phase of endosperm cellularization, formation and fusion of anticlinal walls result in the formation of alveoli. Cortical MTs are rare in alveoli, but numerous MTs are associated with the freely growing edges of the anticlinal walls. The MTs at the wall edges form a phragmoplast complex, the alveolar phragmoplast (a-phragmoplast) consisting of two kinds of microtubular organizations. In the non-junction wall edges, the a-phragmoplast MTs exhibit mirror symmetric configurations. In the junction wall edges, they show axial symmetric configurations. These two populations of microtubules are the basic elements of the a-phragmoplast which functions as a huge dynamic frame in the patterning of wall growth during the alveolation of the coenocytic endosperm. It is suggested that a-phragmoplasts exist in all angiosperm species that have alveolar endosperms.

Besides alveoli with one nucleus, multinuclear alveoli are observed. In both kinds of alveoli, nuclei tend to maintain a central position with regard to the anticlinal walls. Translocation of nuclei to the region bordering the central vacuole of the embryo sac occurs. Microtubular bundles running along the cytoplasm strand may function in that nuclear translocation.

Key words: cellularization, endosperm, microtubule, *Populus nigra*, phragmoplast

INTRODUCTION

In Angiosperms, zygotic embryos develop in a $3n$ endosperm environment. Since both the embryo and the endosperm are products of double fertilization, and besides the endosperm being either a supernumerary embryo (Sargent 1900, Friedman 1990, 1994) or a mimic of female gametophyte of Gymnosperms (Thomas 1907), their developmental patterns differ from each other and their fates are programmed differently. In general, embryo development lacks the coenocytic phase, with exception of Paeoniaceae (Johri *et al.* 1992), whereas in the three so far known types of endosperm formation, *i.e.*, Helobial Type, Nuclear Type and Cellular Type, the Helobial and Nuclear Types do include coenocytic phases. Although the first division of the fertilized central cell is completed by cytokinesis in the Helobial Type, one of the sister cells undergoes only nuclear division before it finally enters the cellular phase. In the Nuclear Type, endosperm initially lacks any cell wall formation, and later, develops walls and enters the alveolar and then the cellular phase.

A landmark for nuclear endosperm development is the transition from the nuclear phase to the cellular phase via alveolation. For a good understanding of endosperm development, cellularization of nuclear endosperm has long been subject to investigations (Newcomb and Fowke 1973, Mares *et al.* 1975, Morrison and O'Brien 1976, Morrison *et al.* 1978, Mares *et al.* 1977, Van Lammeren 1988, XuHan and Li 1990, Fineran *et al.* 1982, Chamberlin and Horner 1993, see also Vijayaraghavan and Prabhakar 1984, Lopes and Larkins 1993 for reviews). However, the process of cellularization still remains in discussion. Morrison and O'Brien (1976) propose that furrowing inward walls, derived from embryo sac wall ingrowths, lead to cellularization, and the cellularization is completed by wall branching and meeting at the side nearest the central vacuole of the embryo sac. Mares *et al.* (1975, 1977) postulate an alveolation process in which "alveoli are formed by centripetal growth of wall projections arising on the central cell wall". Fineran *et al.* (1982) suggest a mitosis-derived alveolation pattern for nuclear endosperm cellularization. Van Lammeren (1988), XuHan and Van Lammeren (1993, 1994) confirm that the alveolus is the functional unit of nuclear endosperm

cellularization, but argue that alveolar walls are not totally mitosis-derived. Recently, supporting Morrison and O'Brien (1976), Brown *et al.* (1994) state that in barley, nuclear endosperm cellularization follows a way other than alveolation, in which wall formation occurs all around the free nuclei, and they provide evidence that the microtubular cytoskeleton is involved in the morphogenesis.

Despite the conflicting models described above, there is a general agreement about the involvement of microtubules (MTs) in the processes of cellularization (Mares *et al.* 1977, Fineran *et al.* 1982, Van Lammeren 1988, XuHan and Van Lammeren 1993, 1994; Brown *et al.* 1994). Recently, models of two populations of MTs were postulated for the freely growing wall edge associated MTs (GWE-MTs) in celery-leaved buttercup endosperm (XuHan and Van Lammeren 1993). This has been found true in bean endosperm (XuHan and Van Lammeren 1994) and sunflower endosperm (XuHan 1994). If the putative models of the two microtubular configurations are proved in phylogenetically distant plant species, it would indicate that the phragmoplast contains more configurations rather than the one known until now.

This study is focused on the endosperm development of poplar which has the Nuclear Type of endosperm development. Poplar embryogeny was studied previously by Li *et al.* (1982), Li and Zhu (1989), and XuHan and Li (1990). Our concerns are addressed to the pattern of poplar endosperm development at the coenocytic stage, especially to the cytological events involved such as the microtubular configurations and nuclear behaviour in relation to alveolation.

MATERIALS AND METHODS

Catkins were sampled from naturally grown poplar (*Populus nigra* L.) plants each week after anthesis. Ovules and young seeds were immersed in fixative, and nucelli were manually isolated from seeds by peeling off the integument tissue .

Electron microscopy and conventional light microscopy

Samples were fixed at room temperature for 24 h in a mixture of 4% glutaraldehyde (v/v) and 1% paraformaldehyde (w/v) in phosphate buffered saline (PBS: 135 mM NaCl; 2.7 mM KCl; 1.5 mM KH_2PO_4 ; 8 mM Na_2HPO_4 ; pH 7.0). After rinsing in the same buffer, they were post-fixed for 12 h at 4°C in 0.5% osmium tetroxide in PBS, then rinsed in PBS and dehydrated in a graded ethanol series. Samples were embedded in low viscosity resin (Spurr 1969). Ultrathin sections were stained with uranyl acetate and lead citrate, and were analyzed using a JEM-1200 EXII transmission electron microscope operating at 80 kV. Semithin sections were stained with Toluidine Blue for light microscopy.

Statistic analysis

Serial 4- μm sections were collected from select samples at the monolayer alveolar stage. Then, median sections of the embryo sacs and tangential sections through the middle part of the alveoli were selected (Fig. 1). Numbers of nuclei per alveolus were determined from 15 serial sections of one seed. Data on alveolar wall numbers were obtained from the tangential sections of 4 seeds and only one section was used from each seed. Data of frequency of different types of alveoli were obtained from observation of 100 alveoli in 13 longitudinal serial semithin sections (with a few ultrathin sections in between) in monolayer alveolar endosperm.

Immunocytochemistry

The fixation conditions of the samples have been optimized for the nuclear endosperm of poplar (XuHan *et al.* accepted). Briefly, the samples were fixed in 6% paraformaldehyde (v/v) and 0.5% glutaraldehyde (w/v) in PBS containing 0.1% Triton X-100 (w/v) for 45 h at room temperature, and were embedded in polyethylene glycol 2000 and sectioned with an LKB 2218 Historange microtome. Sections of 1.5 μm were mounted on poly-L-lysine-coated slides (poly-L-lysine, Sigma, 0.1% (w/v)) and after washing in PBS,

they were treated by 5% normal goat serum for 0.5 h at 30°C to reduce background. Immunofluorescent labeling of MTs was performed using a monoclonal anti- β -tubulin (Amersham Intl. plc) as the first antibody at 1:100 dilution for 1 h, and fluorescein isothiocyanate (FITC) linked sheep anti-mouse IgG (Amersham Intl. plc) as the second antibody at 1:100 dilution for 1 h, both at 35°C. Three-time washes in PBS were followed by each labeling. Omission of the first antibody was applied as control. Nuclei and DNA-carrying organelles were stained by 0.02% (w/v) 4,6-diamidino-2-phenylindole (DAPI, Sigma) added to Citifluor (Link Analytical) when sections were mounted. Observations and microphotography were done on a Leitz Laborlux 12 microscope with a Wild Photoautomat MPS45 exposure system, using Kodak Ektachrome 1600HC and TMAX P3200 films.

RESULTS

1. Nuclear endosperm

In the nuclear endosperm of *P. nigra*, all free nuclei were positioned in a layer of cytoplasm between the central vacuole of the embryo sac and the embryo sac wall, and regularly spaced (Fig. 2). Long bundles of cytoplasmic MTs, orienting in various directions, formed a wide-spread network throughout the cytoplasm. Cortical MTs were rare. Some short arrays of MTs radiating from nuclear envelopes were developed. This radiating population was interwoven with the cytoplasmic MT network. In the micropylar part, more radiating arrays of MTs had developed from the surfaces of the nuclei (Fig. 3). Regularly, microtubule converging centers (MTCCs) were observed here and the converging tips were oriented to the nuclear surface. In this area of the endosperm, the nuclei became closer to each other and cellularization would first be initiated here (Li and Zhu 1989, XuHan and Li 1990). Cone-like microtubular arrays, *i.e.*, MTCCs, were not often observed in the endosperm with wide-spaced nuclei. DAPI-stained organelles exhibited a collectively even distribution throughout the nuclear endosperm. (Fig. 2b).

2. Alveolation of coenocytic endosperm

Alveolation started about 25 days after anthesis by the formation of anticlinal walls arising in most internuclear areas of the cytoplasm surrounding the central vacuole of the central cell (Fig. 4). Each alveolus contained one or more nuclei (Figs. 5, 6), and was bordered by walls at its lateral sides, by the embryo sac wall at its outer side, and by the tonoplast of the central vacuole at its inner side (Fig. 5). The endosperm remained coenocytic because the alveoli were not bordered by walls at the inner sides. Alveoli elongated by growth of the edges of the anticlinal walls towards the central vacuole.

2.1 Alveolar walls and nuclei

In tangential sections of the monolayer of alveoli (Fig. 1), anticlinal walls exhibited a polygonous configuration (Fig. 9). The pattern of anticlinal walls

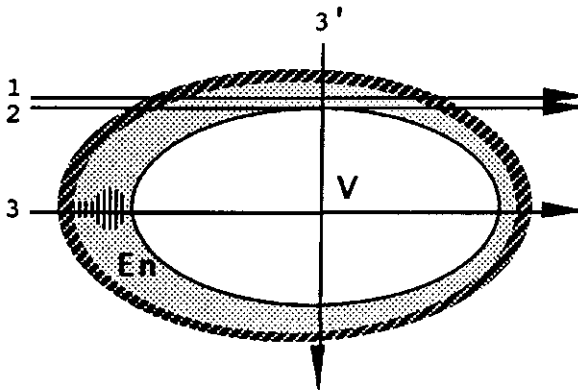
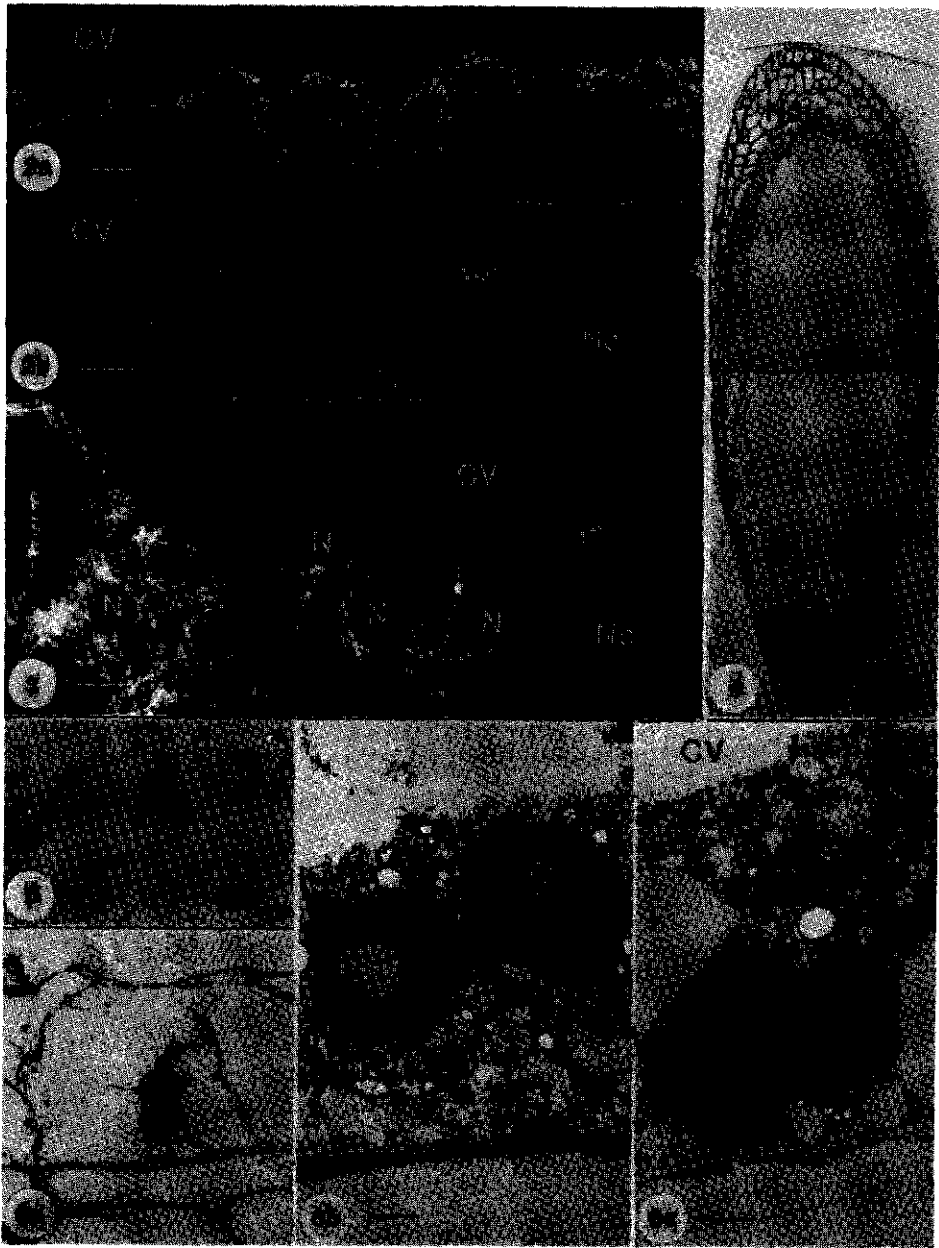


Fig. 1. A diagrammatic representation showing the section positions of the embryo sac. (1) Median tangential section through the middle of endosperm giving rise to cross section of alveoli. Anticlinal wall number is counted in such sections. (2) Tangential section through the inner side of the endosperm producing end views of anticlinal wall edges. Wall junctions and axial symmetric phragmoplast can be best seen in such sections. (3) Median section through the major axis of the embryo sac producing longitudinal sections of alveoli. Side views of anticlinal wall edges are regularly observed in such sections. (3') Median section through the short axis of the embryo sac producing longitudinal sections of alveoli. Side views of anticlinal wall edges are also regularly observed in such sections. En, endosperm; V, central vacuole of the embryo sac.

was analyzed in 100 alveoli. The number of walls ranged from 4 to 9 per alveolus with an average of 6 (Fig. 7). In longitudinal sections, both mononuclear and multinuclear alveoli were observed. Mononuclear alveoli often bore their nuclei near the tonoplast of the central vacuole (Fig. 5). Multinuclear alveoli bore their nuclei in a central strand of cytoplasm running from the outer side towards the inner side of the alveolus, here called the "central strand" (Figs. 5, 6). According to observations on serial semithin sections and their adjacent ultrathin sections, the central strand appeared in 66% of the alveoli of which most (56%) were multinuclear (Fig. 8). There was a tendency that most nuclei were positioned at the inner side of alveoli when one nucleus was present in an alveolus (mononuclear alveolus), whereas nuclei were positioned in the central strands when more nuclei were present in an alveolus (multinuclear alveolus). Because the well elongated mononuclear alveoli usually bore their nuclei at the inner side, it is likely that the nuclei were translocated from outer side of alveolus to the inner side along the central strands. Some multinuclear alveoli showed mononucleolar nuclei far from each other (Fig. 5), other showed mononucleolar nuclei close to each other (Figs. 6a, b). Some mononuclear alveoli contained a large nucleus with two nucleoli of equal size (Fig. 6c). Comparison of the volume of nuclei in mononuclear and binuclear alveoli and taken the number of nucleoli taken into account, it cannot be excluded that nuclei fuse in the central strand.

Fig. 2. (a) Immunocytochemical micrograph of the nuclear endosperm in a median longitudinal section (Fig. 1, section position 3) showing MT configurations in the endosperm in the middle part of the embryo sac. (b) The same section stained by DAPI, showing even distribution of DNA-carrying organelle and the position of free nucleus. CV, central vacuole; N, nucleus; Nc, nucellus. Bar = 10 μ m. **Fig. 3.** Immunocytochemical micrograph of the nuclear endosperm in a tangential section of the micropylar part showing enhancement of the MT labeling before cellularization. Note the MT nucleation sites shaped in cone-like MTCCs (arrows). CV, central vacuole; N, nucleus; Nc, nucellus. Bar = 10 μ m. **Fig. 4.** Light micrograph showing an overview of the alveolar endosperm in longitudinal section (Fig. 1, section position 3). CV, central vacuole; En, endosperm; Nc, nucellus. Bar = 200 μ m. **Fig. 5.** Conventional light micrograph showing alveolar endosperm (Fig. 1, section position 3). In the left alveolus, an oblique central strand (arrow) includes three nuclei. In the middle alveolus, central strand contains two nuclei (only one is in the section). In the right hand alveolus, a nucleus is positioned at the inner side of the alveolus. Also note the freely growing edges of anticlinal walls (arrowheads). CV, central vacuole; En, endosperm; Nc, nucellus. Bar = 2 μ m. **Fig. 6.** Electron micrograph of alveolar endosperm (Fig. 1, section position 3) showing the process of the alveolar nucleus fusion in the central strand. Note the interphase nucleoli in all the nuclei. (a) Two nuclei positioned in a multinuclear alveolus. Bar = 10 μ m. (b) Two nuclei in close position. Bar = 2 μ m. (c) Nucleus contains two nucleoli. Bundles of MTs (arrows) in the central strand run towards to the nucleus. CV, central vacuole. Bar = 2 μ m.



2.2 MTs and Phragmoplasts

Extensive MTs were present in the cytoplasm bordering the tonoplast of the central vacuole of the alveolar endosperm, some in the central strands of alveoli, and less in cortical cytoplasm (Fig. 10). In the central strands, long bundles of MTs were observed along the central strand and close to the nuclear envelope (Fig. 6c).

Intensive microtubular arrays were observed at the inner edges of the anticlinal walls of the alveoli. They formed phragmoplasts associated with the growing wall edges in each alveolus (Figs. 10, 11). Because the growing wall edges of all alveoli had fused to a kind of honey-comb system (see Fig. 9), the phragmoplasts of all individual cell plates connected, and their MTs were interwoven and formed a huge network, the alveolar-phragmoplast. In the alveolar phragmoplast, some Mts run from the growing wall edges to the

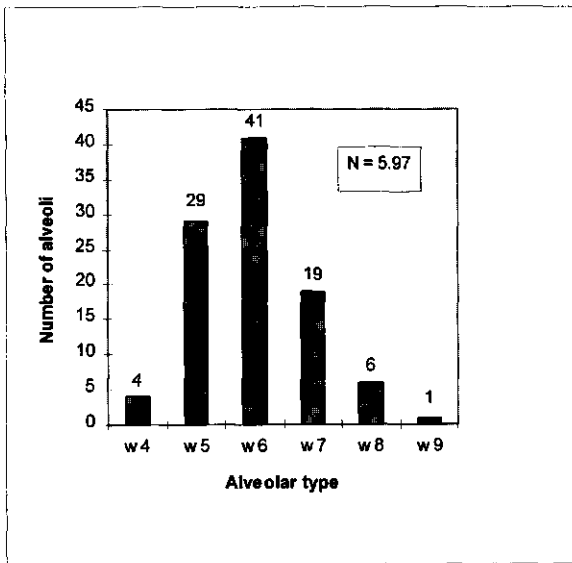


Fig. 7. Frequency of distribution of alveoli in relation to anticlinal wall number per alveolus in monolayered alveolar endosperm counted in the median tangential sections (see Fig. 9) of 4 embryo sacs. In "Alveolar type" axis (X axis), the number attached with "w" indicates how many anticlinal walls per alveolus. N, average number of anticlinal walls per alveolus among 100 alveoli counted in 4 seeds.

cytoplasm and directed to the endoplasmic reticulum (ER) and other organelles (Fig. 12). Two kinds of microtubular organizations were observed in the alveolar phragmoplast (Figs. 13, 14). One was associated with non-junction wall edges. Here most MTs were perpendicular to the wall edge. Some MTs near the very end of the wall edge were oblique. Collectively, this population of the MTs exhibited a mirror symmetric configuration (Fig. 11). The other kind was associated with junction wall edges, and the population of

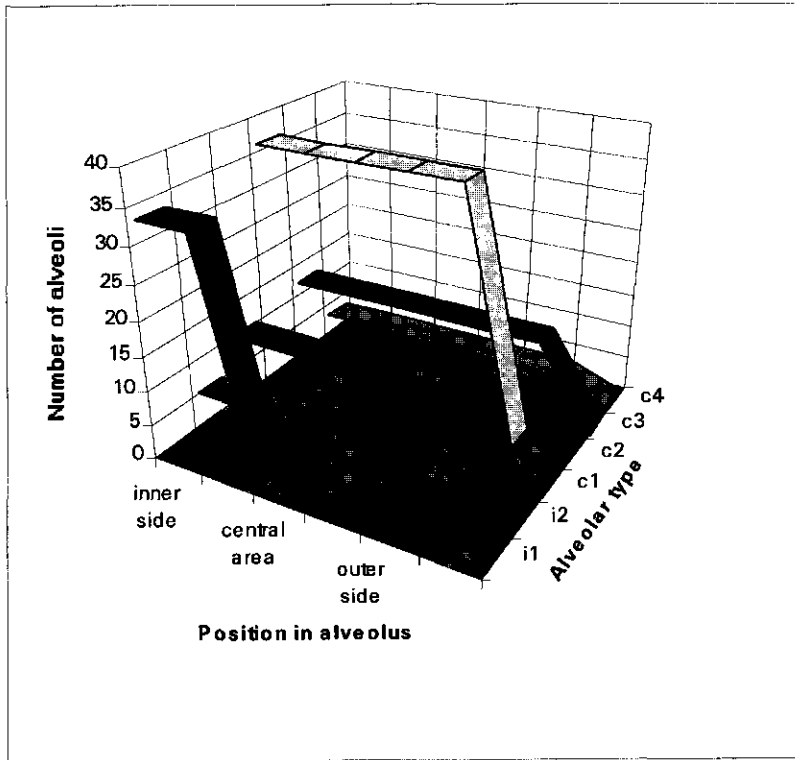


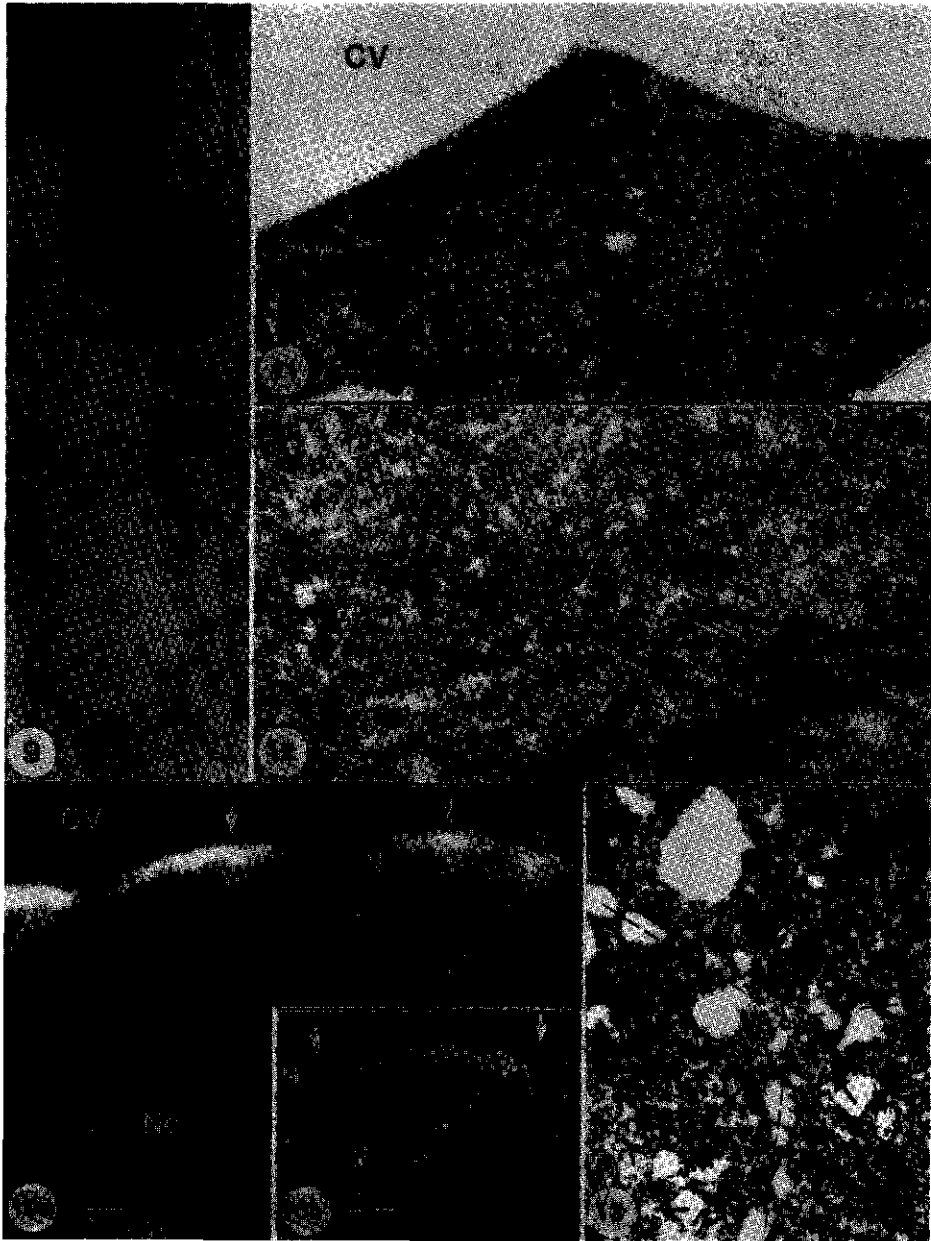
Fig. 8. Frequency of distribution of different types of alveoli in monolayered alveolar endosperm in relation to the positioning of alveolar nuclei. In "Alveolar type" axis (Y axis), i, alveolus with inner side positioned nucleus/nuclei; c, alveolus with nucleus/nuclei positioned in the central strand. The number attached with "i" or "c" indicates the number of nuclei per alveolus. 100 alveoli with 174 nuclei were counted in serial longitudinal sections (see Fig. 1, position 3).

the MTs collectively exhibited an axial symmetric configuration (Fig. 13). At such sites, junctions of three anticlinal walls were commonly observed and the phragmoplast MTs tended to be parallel to the bisectors of the angles formed by the walls. Away from the wall junction, the MTs changed gradually to be perpendicular to the wall edge, *i.e.*, they transformed from the axial symmetric to the mirror symmetric configuration.

2.3 Organelles

DAPI-stained organelles were present throughout the cytoplasm of the alveoli but more abundant in the inner areas between the nucleus and the growing wall edges and in the areas surrounding the nucleus (Fig. 10b). In the growing wall edge areas where intensive phragmoplast MTs were present, the DAPI-stained organelles were almost absent (Fig. 10b). Electron microscopy revealed that the DAPI-stained organelles were plastids and mitochondria, and that they were collectively absent in both mirror symmetric (Fig. 11) and axial symmetric microtubular organization areas of the alveolar phragmoplast (Figs. 12-13).

Fig. 9. Light micrograph showing monolayer alveolar endosperm (En) at tangential section (Fig. 1, section position 1). Note that the alveolar nuclei are surrounded by anticlinal walls and tend to position in the center of the alveoli. Nc, nucellus. Bar = 50 μ m. **Fig. 10.** Longitudinal section (Fig. 1, section position between 2 and 3). (a) Immunocytochemical micrograph of the elongated alveoli showing MT labeling in the phragmoplasts in the freely growing wall edges (arrows) and the wall junction (double arrow). Very few cortical MTs are present in the alveoli compared with those in nucellus cells (Nc). (b) The same section stained by DAPI, showing the distribution of DNA-carrying organelles in the cytoplasm of one alveolus in (a) where the nucleus (N) in the central strand is present in the section. Note the DNA-carrying organelles are collectively absent in the alveolar phragmoplasts (arrowheads). CV, central vacuole of endosperm. Bar = 10 μ m. **Fig. 11.** Electron micrograph of alveolar endosperm in a longitudinal section (Fig. 1, position 3) showing MTs of mirror symmetric configuration in the a-phragmoplast associated with the freely growing wall edge of an anticlinal wall. Note that plastids and mitochondria are not present in the alveolar phragmoplast. CV, central vacuole of the endosperm. Bar = 500 nm. **Fig. 12.** Electron micrograph of alveolar endosperm in a longitudinal section (Fig. 1, position 3) showing peripheral area of alveolar phragmoplast. Note the extensive phragmoplast MTs "pushing" the organelles out of the phragmoplast. ER, endoplasmic reticulum. M, mitochondrion; P, plastid. Bar = 500 nm. **Fig. 13.** Electron micrograph of alveolar endosperm in a tangential section (Fig. 1, position 2) showing MTs in axial symmetric configuration in the a-phragmoplast. Fusing wall vesicles form a Y-shaped wall configuration as shown by dotted lines. The bisectors of the wall angles are indicated by arrows. Bar = 500 nm.



Discussion

1. Alveolation

This work allows us to confirm the pattern of alveolus development as postulated for celery-leafed buttercup (XuHan and Van Lammeren 1993), and bean (XuHan and Van Lammeren 1994). In general, alveolation includes (1) cell plate formation in internuclear spaces, (2) cell plate fusion at the lateral sides of the alveoli, and (3) elongation of alveoli by growth of the freely growing wall edges of the anticlinal walls at the inner sides of alveoli. These processes result in the formation of a layer of alveoli surrounding the central vacuole of the embryo sac. Each alveolus is shaped as a tetra- to nono-gonous column of walls with an opened inner side. Understanding phragmoplast formation (see XuHan and Van Lammeren 1993) is a prerequisite for understanding the presently described alveolar growth pattern. On the other hand, understanding the alveolar growth pattern is prerequisite for the characterization of the alveolar-phragmoplast.

Alveolus formation in the nuclear endosperm of wheat was reported by Mares *et al.* (1977) and Fineran *et al.* (1982). Newcomb (1978) found alveolus formation in the nuclear part of the Helobial endosperm of African blood lily. In celery-leafed buttercup (XuHan and Van Lammeren 1994) and bean (XuHan and Van Lammeren 1994), we postulate detailed models for morphogenesis in endosperm cellularization, which are applicable to poplar. Cellularization patterns as reported by Morrison *et al.* (1978) for the nuclear endosperm of wheat and by Brown *et al.* (1994) for the nuclear endosperm of barley, differ from the findings in this species, wheat (Mares *et al.* 1977, Fineran *et al.* 1982, Van Lammeren 1988), celery-leafed buttercup (XuHan and Van Lammeren 1993), sunflower (XuHan 1994), and bean (XuHan and Van Lammeren 1994).

The present work reveals the presence of growing alveoli not only with one nucleus but also with more nuclei. This finding raises the question if anticlinal wall deposition initially is not synchronous in all the internuclear

spaces of the nuclear endosperm in poplar. Such phenomenon should lead to multinuclear alveoli. Multinuclear alveoli could also develop by division of the alveolar nucleus without following cytokinesis. Such division has, however, never been observed.

2. Phragmoplasts

The pattern of mirror symmetric organization of MTs has been known to exist in the phragmoplast formed during normal cell division. Such mitosis-cytokinesis or meiosis-cytokinesis related phragmoplast is called m-phragmoplast here. In the alveolar endosperm, MTs exhibit the greatest density at the growing wall edges of the anticlinal walls forming two organizational patterns, a mirror symmetric configuration and an axial symmetric configuration. The MTs in mirror symmetric organization exhibit the same configuration as in the m-phragmoplast. The axial symmetric configuration of MTs, however, does not exist in the m-phragmoplast. The MTs in both mirror symmetric and axial symmetric configurations interconnect and form an integrated network covering the whole honey-comb like surface of the alveolar endosperm. They function as one phragmoplast system. We suggest to term this phragmoplast system the alveolar-phragmoplast (a-phragmoplast) versus the mitotic-phragmoplast (m-phragmoplast). The a-phragmoplast translocates forwards during wall edge extension, while cellularization in the alveoli occurs. Thus, a file of cells are formed behind the wall edges (Mares *et al.* 1977, XuHan and Van Lammeren 1993, 1994). We conclude that the a-phragmoplast differs from the m-phragmoplast in its compound configuration, and in having a long lasting growth pattern leading to the formation of common walls for more than two cells.

The growing wall edge associated MTs (GWE-MTs) found in celery-leaved buttercup exhibit mirror symmetric and axial symmetric configuration that were analyzed from a point of view of mechanics (XuHan and Van Lammeren 1993). Investigations in bean proved again the presence of the mirror symmetric and axial symmetric microtubular configurations, and elucidated

the origin of the axial symmetric configuration (XuHan and Van Lammeren 1994). The present paper reveals the relationship between the two kinds of microtubular configurations, confirms that both organizations of MTs are the only elements of the a-phragmoplast, and elucidates that they concurrently function in controlling the growth of the freely growing wall edges in the alveolar endosperm (Fig. 14). We presume that the a-phragmoplast also functions in alveolations, such as observed in *Araucaria araucana* (Hodcent 1969), in wheat (Van Lammeren 1988), *Ranunculus sceleratus* (XuHan and Van Lammeren 1993), and in sunflower (XuHan 1994).

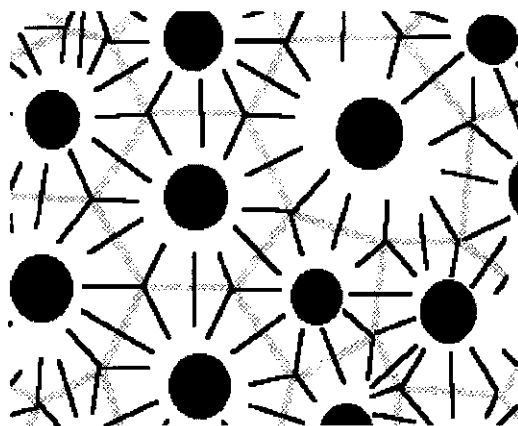


Fig. 14. A diagrammatic representation showing microtubular configurations at an end view (Fig. 1 position 2) of a part of the alveolar phragmoplast associated with the freely growing edges of the anticlinal walls in the alveolar endosperm.

3. Nuclei, organelles, and MTs

The MTCC, a structural unit instrumental for the reorganization of interphase and mitotic microtubular arrays in plant cells (Smirnova and Bajer 1994), is also observed in the present research. Cone-like microtubular arrays are noticed in the nuclear endosperm. They are gradually enhanced when nuclei are positioned more compact just before alveolation. It is possible that the MTCCs in the nuclear endosperm are involved in initiating endosperm

alveolation by enhancing MTs in the nuclear domain. The transformation of the radiating and internuclear MTs to phragmoplast MTs is discussed for the free nuclear endosperm of wheat (Van Lammeren 1988), celery-leafed buttercup (XuHan and Van Lammeren 1993), bean (XuHan and Van Lammeren 1994), and barley (Brown *et al.* 1994).

The MTs radiating from nuclear surfaces probably account for the positioning of nuclei (Brown *et al.* 1994). Cytoskeletons involved in organelle movement and nuclear positioning have been investigated in lower and higher plants (Beckerle and Porter 1983, Menzel and Schliwa 1986a, b; McNaughton and Goff 1990, Chen and Li 1991). At the early stage of the nuclear endosperm, the nuclei spread rapidly all over the thin layer of cytoplasm and become regularly spaced. Interaction between the radiating MTs and the cytoplasmic MT network may generate mechanical forces for nuclear positioning, where the radiating populations serve as an "anchor" for the nucleus and the cytoplasmic microtubular network forms the dynamic tracks. It has been scarcely found in vacuolated plant cells that the nuclei have a central position in the cell. In poplar endosperm, however, most alveolar nuclei exhibit a central position in both mononuclear and multinuclear alveoli. In the latter case, the nuclei align in the central strands. The mechanism for the patterning requires further research. However, the radiating MTs as discussed above may function in the positioning of the nuclei.

Based on structural and developmental analysis, the present paper reveals the translocation processes of the nucleus from the outer and central area to the inner side of the alveolus. Because we observed alveoli with two mononucleolar nuclei in immediate vicinity, and mononuclear alveoli with larger nuclei exhibiting two nucleoli, fusion of nuclei in alveoli can not be excluded. Although there is a lack on data on ploidy levels in poplar endosperm, the possibility of the nuclear fusion might lead to variation of the endosperm ploidy in poplar. In *Erythronium sibiricum* it has been observed that differences in ploidy level in the endosperm are caused by chromatic

agglutination (Petrova 1969). There, nuclear fusion occurred during mitosis, whereas the data from poplar point to nuclear fusion at interphase.

The MTs found parallel to the moving track of the nuclei in the central strand may function in nuclear translocation either directly in the way known for chromosome transport or indirectly through interaction with microfilaments. This population of MTs in poplar is less dense than phragmoplast MTs and rather independent from phragmoplast MTs. In celery-leafed buttercup, the a-phragmoplast MTs persist during the whole mitotic cycle, also when alveoli undergo peripheral cytokinesis (XuHan and Van Lammeren, 1993).

It is found that the DNA-carrying organelles are extensively distributed in the area between the growing wall edges and the nucleus. Very few of them are present in the areas of the a-phragmoplast (Figs. 10-13). We therefore conclude that the MTs of the a-phragmoplasts have the same characteristic as found in m-phragmoplasts, and that they collectively expel the organelles from the areas of wall growth (see also Pickett-Heaps and Northcote 1966, Hepler and Jackson 1968).

CONCLUDING REMARKS

As a conclusion, alveolation is a typical growth pattern of early cellularization in nuclear endosperm. Alveolation and subsequent mitosis-derived cytokinesis are the unique processes in the cellularization of coenocytic endosperm. This has been proved in several phylogenetically distant Angiosperms, and is expected to be true in cellularization processes occurring in the nuclear part of Helobial endosperm and in the Gymnosperm female gametophyte as well. At present, two phragmoplast types have been found in the plant kingdom, the m-phragmoplast and the a-phragmoplast. The term "phragmoplast", which has been used for m-phragmoplast, should be maintained as a general term for both types. The main characteristics of phragmoplasts are summarized in Table 1.

Table 1. A summary of the characteristics of a-phragmoplast compared with m-phragmoplast.

| Phragmoplast type | Origin | MT configuration | Function | Cell plate/wall growth pattern | Organelle distribution | Presence |
|------------------------|---|--|--|--|---|---|
| m-phragmoplast | <ul style="list-style-type: none"> mitotic/meiotic cytokinesis | <ul style="list-style-type: none"> mirror symmetric | <ul style="list-style-type: none"> disk-like cell plate formation in mitotic or meiotic cytokinesis | <ul style="list-style-type: none"> terminated after a pair of daughter nuclei are separated by the wall | <ul style="list-style-type: none"> absence of DNA-carrying organelles presence of ER and vesicles | <ul style="list-style-type: none"> all higher plant species |
| a-phragmoplast | <ul style="list-style-type: none"> mitotic cytokinesis, transformation of internuclear MTs of nondaughter nuclei | <ul style="list-style-type: none"> mirror symmetric | <ul style="list-style-type: none"> disk-like cell plate formation, growth of freely growing wall edges of endosperm alveolar walls at non-junction areas | <ul style="list-style-type: none"> terminated at outer and lateral sides where fusion with other walls occurs, but interminated at inner side after 2 nuclei are separated by the anticlinal walls | <ul style="list-style-type: none"> absence of DNA-carrying organelles presence of ER and vesicles | <ul style="list-style-type: none"> <i>Helianthus annuus</i>¹ <i>Phaseolus vulgaris</i>² <i>Populus nigra</i>³ <i>Ranunculus sceleratus</i>⁴ |
| axial symmetric domain | <ul style="list-style-type: none"> fusion of freely growing wall edges | <ul style="list-style-type: none"> axial symmetric, commonly exhibits a "Y" cross | <ul style="list-style-type: none"> growth of freely growing wall edges of endosperm alveolar walls at wall junctions | <ul style="list-style-type: none"> terminated at outer side where fusion with other walls occurs, but interminated at inner side after 3 nuclei are separated by the anticlinal wall | <ul style="list-style-type: none"> absence of DNA-carrying organelles presence of ER and vesicles | <ul style="list-style-type: none"> <i>Phaseolus vulgaris</i>² <i>Populus nigra</i>³ <i>Ranunculus sceleratus</i>⁴ |

1. XuHan (1994), 2. XuHan and Van Lanmeren (1994), 3. The present paper, 4. XuHan and Van Lanmeren (1993).

Acknowledgments. The authors thank Prof. T. Hong for taxonomic assistance, Prof. M.T.M. Willemse for helpful discussion, Mr. A. Haasdijk and Mr. S. Massart for the art work. The study was granted by a Ph.D. fellowship from the Wageningen Agricultural University, Wageningen, The Netherlands, and partially by a research fellowship from Laboratoire de Biotechnologie et Amélioration des Plantes, INP-ENSAT, Toulouse, France, and a visiting research grant from the Chinese National Natural Science Foundation.

REFERENCES

- Beckerle, M. C., and Porter, K. R. (1983) Analysis of the role of microtubules and actin in erythrocyte intracellular motility. *J. Cell Biol.* **96**: 354-362.
- Brown, R.C., Lemmon, B.E., and Olsen, O.-A. (1994) Endosperm development in barley : microtubule involvement in the morphogenetic pathway. *Plant Cell* **6**: 1241-1252.
- Chamberlin, M.A., and Horner, H.T. (1993) Nutrition of ovule, embryo sac, and embryo in soybean: an anatomical and autoradiographic study. *Can. J. Bot.* **71**: 1153-1168.
- Chen, S.-T., and Li, C.-W. (1991) Relationships between the movements of chloroplasts and cytoskeletons in diatoms. *Bot. Marina* **34**: 505-511.
- Fineran, B. A., Zild, D. J. C., and Ingerfeld, M. (1982) Initial wall formation in the endosperm of wheat, *Triticum aestivum*: a reevaluation. *Can. J. Bot.* **60**: 1776-1795.
- Friedman, W. (1990) Double fertilization in *Ephedra*, a nonflowering seed plant: its bearing on the origin of angiosperms. *Science* **247**: 951-954.
- Friedman, W. (1994) The evolution of embryogeny in seed plants and the developmental origin and early history of endosperm. *Am. J. Bot.* **81**: 1468-1486.
- Hepler, P.K., and Jackson, W.T. (1968) Microtubules and early stages of cell-plate formation in the endosperm of *Haemanthus katherinae* Baker. *J. Cell Biol.* **38**:437-466.
- Hodcent, E. (1969) Recherch sur les facteurs entrant en jeu lors de l'alvéolization des prothalles femelles de l'*Araucaria araucana*. *Rev. Cytol. et Biol. Vég.* **32**: 155-164.
- Johri, B.M., Ambegaokar, K.B. and Srivastava, P.S. (1992) Paeoniaceae. In: Johri, B.M., Ambegaokar, K.B., and Srivastava, P.S. (eds.) *Comparative Embryology of Angiosperms*. Springer-Verlag, Berlin. Vol. 1. pp. 325-328.
- Li, W.-D., Fan, R.-W., and Mai, X.-L. (1982) Embryological observations on the seed development of *Populus simonii* Carr. *Sci. Silv. Sin.* **18**: 113-119.
- Li, W.-D., and Zhu, T. (1989) Fertilization and embryo development in *Populus euphratica* Oliv. *Forest Res.* **2**: 1-8.
- Lopes, M.A., and Larkins, B.A. (1993) Endosperm origin, development, and function. *Plant Cell* **5**: 1383-1399.
- Mares, D.J., Norstog, K., and Stone, B.A. (1975) Early stages in the development of wheat endosperm. I The change from free nuclear to cellular endosperm. *Aust. J. Bot.* **23**: 311-326.
- Mares, D.J., Stone, B.A., Jeffery, C., and Norstog, K. (1977) Early stages in the development of wheat endosperm. II ultrastructural observations on cell wall formation. *Aust. J. Bot.* **25**: 599-613.

- McNaughton, E. E., and Goff, L. J. (1990) The role of microtubules in establishing nuclear spatial patterns in multinucleate green algae. *Protoplasma* 157: 19-37.
- Menzel, D., and Schliwa, M. (1986 a) Motility in the siphonous green alga *Bryopsis*. I. Spatial organization of the cytoskeleton and organelle movements. *Eur. J. Cell Biol.* 40: 275-285.
- Menzel, D., and Schliwa, M. (1986 b) Motility in the siphonous green alga *Bryopsis*. II. Chloroplast movement requires organized arrays of both microtubules and actin filaments. *Eur. J. Cell Biol.* 40: 286-295.
- Morrison, I.N., O'Brien, T.P.(1976) Cytokinesis in the developing wheat grain: Division with and without a Phragmoplast. *Planta* 130: 57-69.
- Morrison, I.N., O'Brien, T.P., and Kuo, J. (1978) Initial cellularization of the aleurone cells in the ventral region of developing wheat grain. *Planta* 140: 19-30.
- Newcomb, W. (1978) The development of cells in the coenocytic endosperm of the african blood lily *Haemanthus katherinae*. *Can. J. Bot.* 56: 483-501.
- Newcomb, W., and Fowke, L.C. (1973) The fine structure of the change from the free-nuclear to cellular condition in the endosperm of chickweed *Stellaria media*. *Bot. Gaz.* 134: 236-241.
- Petrova, T.F. (1969) L'agglutination de la chromatine au cours des mitoses dans l'albumen chez *Erythronium sibiricum*. *Rev. Cytol. Biol. Vég.* 32: 391-369.
- Pickett-Heaps, J.D., and Northcote, D.H. (1966) Organization of microtubules and endoplasmic reticulum during mitosis and cytokinesis in wheat meristems. *J. Cell Sci.* 1: 109-120.
- Sargant, E. (1900) Recent work on the results of fertilization in angiosperms. *Ann. Bot.* 14 :689-712.
- Smirnova, E.A., and Bajer, A.S. (1994) Microtubule converging centers and reorganization of the interphase cytoskeleton and the mitotic spindle in higher plant *Haemanthus*. *Cell Motil. Cytoskeleton* 27: 219-233.
- Spurr, A.R. (1969) A low viscosity epoxy resin embedding medium for electron microscopy. *J. Ultrastruct. Res.* 26: 31-43.
- Thomas, E.N. (1907) Some aspects of "double fertilization" in plants. *Sci. Progress* 1: 420-426.
- Van Lammeren, A.A.M. (1988) structure and function of the microtubular cytoskeleton during endosperm development in wheat: an immunofluorescence study. *Protoplasma* 146: 18-27.
- Vijayaraghavan, M.R., and Prabhakar, K. (1984) The endosperm. In: Johri, B.M. (ed.) *Embryology of Angiosperms*. Springer-Verlag, Berlin, Heidelberg. pp. 319-376.
- XuHan X. (1994) Microtubular configurations in higher plant embryogenesis and applications of microtubular configurations to the selection of somatic embryogenic cultures. In: *94-Symposium for Young Chinese Developmental Biologists*. Beijing, China. pp. 66-67.
- XuHan, X., and Li, W.-D. (1990) Experimental study on the embryology of the intergeneric cross between *Populus simonii* and *Salix matsudana*. *Forest Res.* 3: 29-33.
- XuHan, X. Souvré, A., Granier, C., and Petitprez, M. An improved immunolabelling method for microtubular cytoskeleton in poplar (*Populus nigra* L.) free nuclear endosperm. *Biotech. Histochem.* (accepted).
- XuHan, X., and Van Lammeren, A.A.M. (1993) Microtubular configurations during the cellularization of coenocytic endosperm in *Ranunculus sceleratus* L. *Sex. Plant Reprod.* 6: 127-132.
- XuHan, X., and Van Lammeren, A.A.M. (1994) Microtubular Configurations during Endosperm Development in *Phaseolus vulgaris* L. *Can. J. Bot.* 72: 1489-1495.

Chapter 9

General Discussion

Xu XuHan

Department of Plant Cytology and Morphology, Wageningen Agricultural
University, Arboretumlaan 4, 6703 BD, Wageningen, The Netherlands

Zygotic embryogeny in Angiosperms varies highly in developmental pattern, and the relation between the embryo and its surrounding tissue is of great importance for the seed formation (Johansen 1950, Maheshwari 1950, Johri 1984, Johri *et al.* 1992). The present work focuses on the cytomorphogenesis during seed development in celery-leafed buttercup (*Ranunculus sceleratus* L.), bean (*Phaseolus vulgaris* L.), and poplar (*Populus nigra* L.).

ZYGOTIC EMBRYOGENY

The zygotic embryogeny of the three species studied in the present work all belong to the Onagrad Type. In this type, the zygote divides transversally. Then the apical cell divides longitudinally and gives rise to the embryo proper, whereas the basal cell divides transversally and gives rise to the embryo suspensor (Johansen 1950, Natesh and Rau 1984). As analyzed in celery-leafed buttercup (Chapter 2), however, the embryo proper is derived from both the apical cell and the sub-apical cell. This result suggests that the Onagrad Type may include modifications.

The cleavage planes of the embryonic cells observed at the three-celled embryo stage remained discernible in later developmental stages (Chapter 2). This is also true in bean, in which the embryo clearly exhibits cytomorphological zones corresponding to the cleavage planes (Chapter 3). However, the bean embryo suspensor shows more cytodifferentiation than that of celery-leafed buttercup, which is likely related to the nutrient supply and the mature seed constitution in the two species. The embryo of celery-leafed buttercup is small and the endosperm is persistent, whereas the bean embryo is large and the endosperm does not exist in the mature seed any more. Based on the morphology, there are two important nutrient pathways to the embryo: one via the suspensor and one via the chalazal part of the ovule. As analyzed in the Chapters 2 and 4, the chalazal part of the ovule, in particular the region from the nucellar stalk to the antipodal cells, is the main nutrient transport pathway to the embryo sac in celery-leafed buttercup. This is indicated by (1) the gradient in distribution of the starch and lipid in the nucellar stalk, (2) by the wall ingrowths of the transfer cell type in the antipodal cells, and (3) by the degeneration of the endosperm surrounding the

embryo proper. The embryo suspensor of celery-leafed buttercup is small, without special differentiation, and therefore a less important nutrient transport pathway. Most tissues of the seed coat do not function in the transfer of storage products. This is deduced from the distribution of plasmodesmata and storage materials, and the formation of the intercellular spaces in the seed coat. This differs significantly from the case of bean. There, the seed coat does function in the transport of metabolites (Offler and Patrick 1984). Nutrient transport studies reveal that the suspensor is the main transfer route both by electron microscopy and by ^{14}C -sucrose autoradiography (Yeung 1980). The present work on the ultrastructure of the bean suspensor indicate that there are two zones in the suspensor: the neck zone and the basal zone. From the studies on the embryo suspensor in Chapter 3, it can be concluded: (1) the suspensor functions in absorbing the nutrients transferred from the integument and the surrounding endosperm. This conclusion is based on polar distribution pattern of wall ingrowths of the transfer cell type. (2) The suspensor might function in synthesizing metabolites, such as hormones, e.g. gibberellic acid (Alpi *et al.* 1975, 1979), because of the abundance of endoplasmic reticulum (ER), plastids and mitochondria, and its large nuclei. (3) Most probably, the suspensor neck zone further transfers nutrients and metabolites to the embryo proper because of its polar distribution of wall ingrowths, the border widened by the wall ingrowths with the embryo proper, and the abundance of plasmodesmata on the bordering walls.

The analysis of the microtubular cytoskeleton in relation to embryo development in bean reveals that this cytoskeleton is highly involved in the differentiation of the suspensor and the embryo proper, and the transition of the embryo from globular to cotyledon stage (Chapter 3). The MTs exhibit configurations regularly associated with certain type of cytomorphogenesis, e.g. parallel cortical MT arrays were observed perpendicular to the length axis of elongating cells. The results of the microtubular configurations obtained from the present work are quite constant in embryogenesis and seed coat development, and they are also in agreement with those previously observed in other plant tissues (see reviews Lloyd 1982, Derksen *et al.* 1990). However, the study on cell aging related microtubular configurations, as analyzed in Chapter 4, reveals disorganization of the microtubular cytoskeleton prior total cell senescence, and thus, provides a novel way to

study the microtubular cytoskeleton in relation to degeneration (XuHan *et al.* 1994).

ENDOSPERM DEVELOPMENT

In higher plants, the coenocytic phase of a tissue is commonly a transient step in development. Examples can be found such as Gymnosperm female gametophytes, Angiosperm female gametophytes and nuclear endosperm. The endosperm development of the three species studied in this work all belong to the Free Nuclear Type, in which the division of the primary endosperm nucleus is not accompanied by cytokinesis, resulting in the formation of free nuclei in the fertilized central cell (Vijayaraghavan and Prabhakar 1984). It has been hypothesized that the cellularization of the free nuclear endosperm is (1) performed by cell wall ingrowths of the central cell wall (Morrison and O'Brien 1976, Mares *et al.* 1977, Morrison *et al.* 1978), or (2) performed by mitotic cytokinesis (Fineran *et al.* 1984). Van Lammeren (1988) questioned both modes, particularly the cell wall formation between non-daughter nuclei. The present work has also focused on the questions of the onset of cellularization, and the process of the cellularization. To solve the problem, it was necessary to find markers to distinguish cell wall ingrowths from cell plates. Microtubular configurations were found specific for cell wall formation, and thus, suitable to be a marker.

As studied in the Chapters 2, 3, 4 and 5, cell wall ingrowths of both transfer cell type and non-transfer cell type exhibited microtubular configurations different from the configurations of cell plate associated microtubules, *i.e.* phragmoplast MTs. Based on these results, the freely growing wall edges of the anticlinal endosperm walls are modeled (Chapter 5). The model is in agreement with the structural characters of the cell plate (Chapters 5, 6, Hepler and Jackson 1968), and thus, the microtubular configuration can be used as a structural marker not only for cell wall formation, but also for the direction of the cell wall growth. That is of importance for the finding and analysis of the alveolar phragmoplast which will be discussed later.

Cellularization is initiated by mitotic cytokinesis, in which one of the free nuclei exhibits karyokinesis followed by cell plate formation in the free

nuclear endosperm (Chapter 5). Therefore, at the very beginning, cellularization is asynchronous. The density of the free nuclei plays a role in the onset of endosperm cellularization. When enough free nuclei are formed in the endosperm, the distance between nuclei becomes quite short and internuclear MTs appear in more dense arrangements mimicking a phragmoplast (Chapters 5). The studies on bean endosperm provide proof for this hypothesis. As revealed in Chapter 6, only that part of the endosperm with a higher density of the free nuclei starts cellularization whereas the portion with fewer nuclei does not (also see Yeung and Cavey 1988). It is likely that mitotic cytokinesis first occurs at that site and triggers the transformation of the already formed extensive internuclear MTs in the endosperm portion with densely compacted free nuclei to a phragmoplast configuration (seen as “phragmoplast-like structure”, Chapter 6). This hypothesized process is represented diagrammatically in Fig. 1.

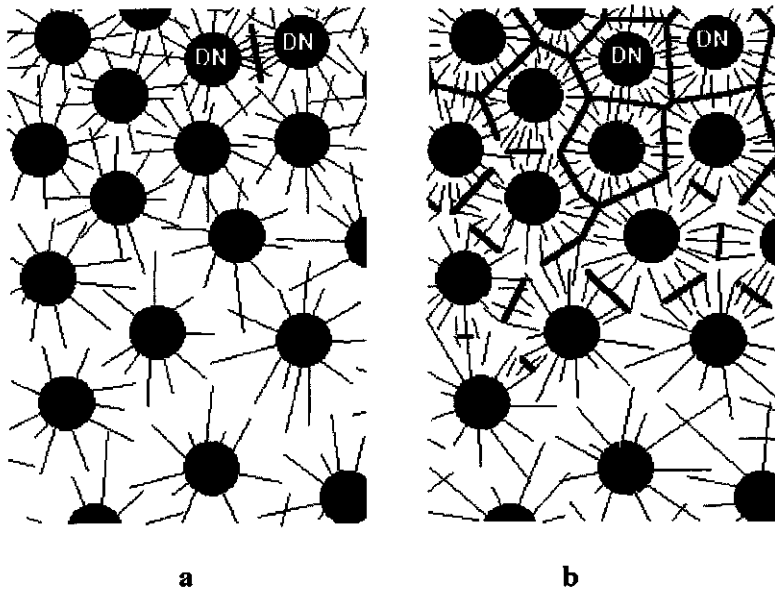


Fig. 1. A diagrammatic representation of the free nuclear endosperm showing the onset of the cellularization. (a) In the upper part, the free nuclei are densely packed whereas in the lower part, the internuclear distance is still long. MTs, radiating from the nuclear surfaces, extend to the internuclear spaces forming the internuclear microtubular domains which mimic phragmoplasts in the upper part of the endosperm. A mitotic cytokinesis gives rise to a pair of daughter nuclei (DN) separated by a cell plate/wall. (b) Cell plate/wall formation spreads to all the phragmoplast-like structures but not in the lower part which has fewer nuclei. The cell plates/walls fuse at lateral sides forming alveoli.

As a result of lateral wall fusion among each other and with the embryo sac wall, alveoli will be formed (Chapter 6), and freely growing edges will only remain at the inner side of the endosperm. The wall edge associated MTs form one single network covering all the growing wall edges underneath the tonoplast of the central vacuole of the endosperm. This network of phragmoplasts is termed the "alveolar phragmoplast" (a-phragmoplast) (Chapter 8). During the alveolation, the a-phragmoplast guides the growth of all freely growing wall edges. The freely growing wall edges at the wall junctions are associated with axial symmetric microtubular organizations, and the non-junction growing wall edges are associated with mirror symmetric microtubular organizations. This has been found in all the three species studies in this thesis. Detailed comparison of the a-phragmoplast and the mitotic (or meiotic) cytokinesis derived phragmoplast, termed in this thesis as "m-phragmoplast", reveals that they have partially different microtubular organizations (Chapter 7), though both phragmoplasts function as a mechanical support system for cell plate growth. Therefore, terminologically, "phragmoplast" should be a general term for both a- and m-phragmoplast, later on.

The cellularization of nuclear endosperm includes two more steps: alveolus elongation and endosperm cell formation, which are studied in the Chapters 5, 6, 8. Based on the already presented internuclear MTs, cell plate formation immediately spreads to the whole area with densely packed nuclei, giving alveolation a morphologically synchronous look. The term "alveolus" is used to describe that the nucleus and some cytoplasm are surrounded by cell walls, but at one side, *e.g.* the side facing to the central vacuole of the embryo sac, the alveolus is left open. The process of alveolus formation has been termed "alveolation" (Hodcent 1969). As studied in detail in the Chapters 5 and 8, depending on the synchrony that happens either among all the free nuclei or only among a part of them (leaving the other part of the free nuclear endosperm uncellularized), the free nuclear endosperm is replaced by alveolar-cellular endosperm, or by concurrent free nuclear-alveolar-cellular endosperm, respectively. It should be denoted that the term "free nuclear" is different from "coenocytic". The latter also includes the alveolar status. Therefore, three components are in fact included in the cellularizing endosperm: the free nuclear part, the alveolus and the endosperm cell. Their

combinations construct three different sub-types of endosperm development in the Free Nuclear Type of endosperm:

(1) The **Peripheral Type** In this type, the developmental pattern can be formulated as:

"peripheral free nuclei \Rightarrow peripheral alveoli \Rightarrow outer layer cells + inner layer alveoli (Fig. 2) \Rightarrow cells".

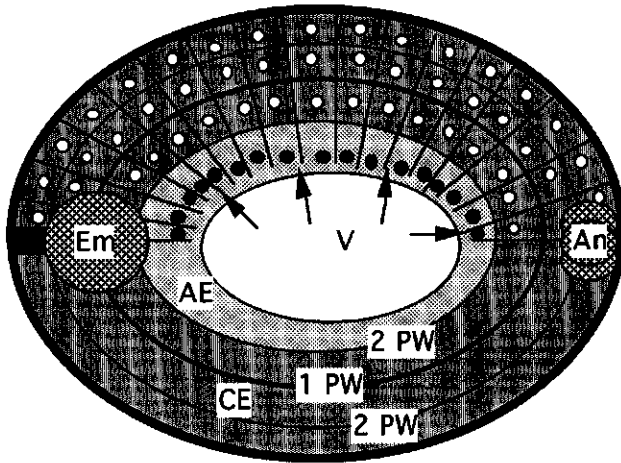


Fig. 2. A diagrammatic representation of the coenocytic endosperm cellularization in celery-leaved buttercup. Only a longitudinal half of the embryo sac is drawn. Note the Peripheral Type of the endosperm development. The nuclei of the alveoli are drawn in black color. The anticlinal walls grow centripetally at the inner wall edges (arrows). An, antipodal cells; Em, embryo; AE, alveolar endosperm; CE, cellular endosperm; 1 PW, the first periclinial walls formed by anticlinal divisions of alveoli at monolayered stage; 2 PW, the second periclinial walls formed by anticlinal divisions of the daughter alveoli and endosperm cells. V, central vacuole.

As seen in *e.g.*, wheat (Mares *et al.* 1977, Fineran *et al.* 1982, Van Lammeren 1988), celery-leaved buttercup (Chapter 5), and in poplar (Chapter 8), the free nuclear endosperm starts to form anticlinal walls all along the embryo sac periphery. Thus, the free nuclear endosperm is replaced by

alveolar endosperm. Freely growing wall edges of the anticlinal walls extend towards the center of the embryo sac. Anticlinally directed mitotic cytokinesis forms the first periclinal wall in alveoli by which one layer of true endosperm cells is created at the outer side. The remaining alveoli at the inner side will again divide and form a second layer of endosperm cells bordering the first layer, thus files of cells are formed behind the freely growing wall edges. Alveolation comes to the end when the front edges of the freely growing walls fuse in the central area of the embryo sac (Chapter 2).

(2) **The Lingering Type** In this type, the developmental pattern can be formulated as:

“peripheral free nuclei \Rightarrow micropylar zone cells + middle zone alveoli + chalazal zone free nuclei (Fig. 3) \Rightarrow cells”.

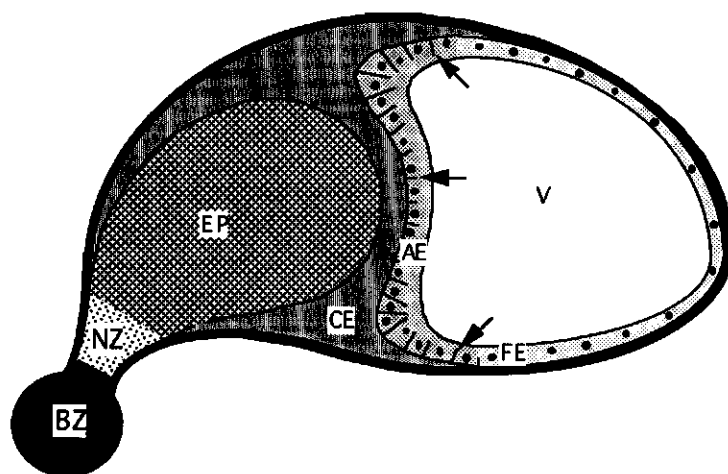


Fig. 3. Schematic representation of the developing embryo sac of bean. Note the Lingering Type of endosperm development. The nuclei are drawn only in the alveolar and free nuclear portions. Arrows point to some freely growing wall edges. AE, alveolar endosperm; BZ, suspensor basal zone; CE, cellular endosperm; EP, embryo proper; FE, free nuclear endosperm; NZ, suspensor neck zone; V, central vacuole.

As seen in bean (Yeung and Cavey 1988, Chapter 6) and *Iberis amara* (Vijayaraghavan and Prabhakar 1984), free nuclear endosperm extends to the embryo sac periphery. The site of the endosperm alveolation moves from the

micropylar part towards the chalazal part while the chalazal endosperm maintains its free nuclear status until cellularization completes.

(3) The **Linear Type** In this type, the developmental pattern can be formulated as:

“micropylar zone free nuclei \Rightarrow micropylar zone alveoli \Rightarrow micropylar zone cells + middle zone alveoli (Fig. 4) \Rightarrow cells”.

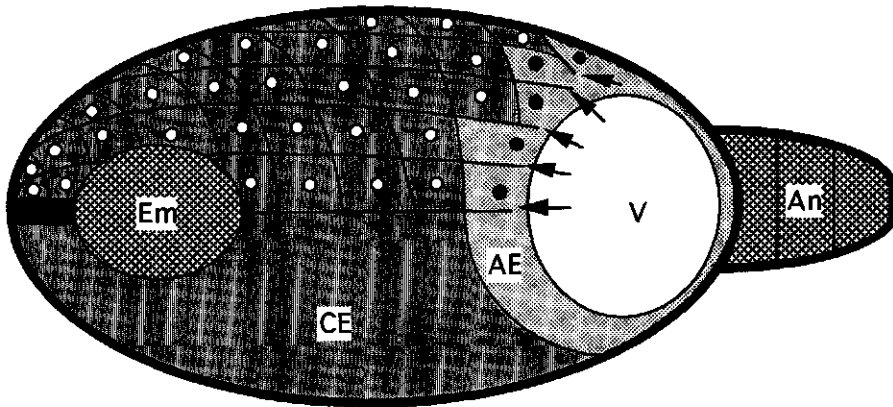


Fig. 4. A diagrammatic representation of the coenocytic endosperm cellularization in sunflower. Only a longitudinal half of the embryo sac is drawn. Note the Linear Type of endosperm development. The nuclei of the alveoli are drawn in back. The freely growing wall edges (arrows) grow towards the chalazal pole. An, antipodal cells; Em, embryo; AE, alveolar endosperm; CE, cellular endosperm; V, central vacuole.

As seen in sunflower (Newcomb 1973, Yan *et al.* 1991, XuHan 1994), the free nuclei of the endosperm do not move to the chalazal part of the embryo sac and cell wall formation soon starts among the micropylarly located free nuclei. Freely growing wall edges extend towards the chalazal part of the embryo sac and cellular endosperm rapidly fills all the embryo sac.

In the three development types mentioned above, the Peripheral and Linear Types are synchronous cellularization types, and the Lingering Type is an asynchronous type. Although tissue development proceeds differently among the three types, the endosperm components commonly include free nuclei,

alveoli and cells. Each component is associated with specific microtubular configurations and those configurations are similar in the three types in the plants studied here (Chapters 5, 6, 8). Particularly, the microtubular organizations associated with the freely growing wall edges exhibit constant but specific characters.

PERSPECTIVES

The present thesis questions the Onagrad embryogeny type of *R. sceleratus* although it exists in a large group of taxa in Angiosperms (Johri *et al.* 1992). A statistic investigation on the variety of this type will hopefully contribute to our understanding of embryogenesis. The knowledge on zygotic embryogenesis, the nutrient supply, the interaction between embryo and endosperm, will be useful in the work on somatic embryogenesis *in vitro*. Although there is now a substantial body of information on the development of the free nuclear endosperm, there is still a need to obtain knowledge as to how the other cytoskeletal elements are involved in the free nuclear endosperm cellularization, and about the molecular basis of the trigger for the cellularization. It is also left open if the a-phragmoplast exists in other coenocytes in higher plants, *e.g.* Gymnospermic female gametophyte. It is obvious that the results in the present work do not bring about a stop, but the onset.

REFERENCES

- Alpi, A., Tognoni, F., and D'Amato, F. (1975) Growth regulator levels in embryo and suspensor of *Phaseolus coccineus* at two stages of development. *Planta* **127**: 153-163.
- Alpi, A., Lorenzi, R., Cionini, P.G., Bennici A., and D'Amato, F. (1979) Identification of gibberellin A₁ in the embryo suspensor of *Phaseolus coccineus*. *Planta* **147**: 225-228.
- Derksen, J., Wilms, F.H.A., and Pierson, E.S. (1990) The plant cytoskeleton: its significance in plant development. *Acta Bot. Neerl.* **39**: 1-8.
- Fineran, B.A., Zild, D.J.C., and Ingerfeld, M. (1982) Initial wall formation in the endosperm of wheat, *Triticum aestivum*: a reevaluation. *Can. J. Bot.* **60**: 1776-1795.
- Hepler, P.K., and Jackson, W.T. (1968) Microtubules and early stages of cell-plate formation in the endosperm of *Haemanthus katherinae* Baker. *J. Cell Biol.* **38**: 437-466.
- Hodcent, E. (1969) Recherch sur les facteurs entrant en jeu lors de l'alvéolization des prothalles femelles de l'*Araucaria araucana*. *Rev. Cytol. Biol. Vég.* **32**: 155-164.

- Johansen, P. (1950) *Plant Embryology*. Chronica Botanica Co. Waltham.
- Johri, B.M. (1984) *Embryology of Angiosperms*. Springer-Verlag, Berlin, Heidelberg.
- Johri, B.M., Ambegaokar, K.B., and Srivastava, P.S. (1992) *Comparative Embryology of Angiosperm*. Springer-Verlag, Berlin.
- Lloyd, C.W. (1982) *The cytoskeleton in Plant Growth and development*. Academic Press, London.
- Mares, D.J., Stone, B.A., Jeffery, C., and Norstog, K. (1977) Early stages in the development of wheat endosperm. II Ultrastructural observations on cell wall formation. *Aust. J. Bot.* **25**: 599-613.
- Maheshwari, P. (1950) *An Introduction to the Embryology of Angiosperms*. McGraw-Hill, New York.
- Morrison, I.N., and O'Brien, P.T. (1976) Cytokinesis in the developing wheat grain; Division with and without a Phragmoplast. *Planta* **130**: 57-69.
- Morrison, I.N., O'Brien, T.P., and Kuo, J. (1978) Initial cellularization of the aleurone cells in the ventral region of developing wheat grain. *Planta* **140**: 19-30.
- Natesh, S., and Rau, M.A. (1984) The embryo. In: Johri, B.M. (ed.) *Embryology of Angiosperms*. Springer-Verlag, Berlin, Heidelberg. pp. 377-443.
- Newcomb, W. (1973) The development of the embryo sac of sunflower *Helianthus annuus* after fertilization. *Can. J. Bot.* **51**: 879-890.
- Offler, C.E., and Patrick, J.W. (1984) Cellular structures, plasma membrane surface areas and plasmodesmatal frequencies of seed coat of *Phaseolus vulgaris* L. in relation to photosynthate transfer. *Aust. J. Plant Physiol.* **11**: 79-99.
- Van Lammeren, A.A.M. (1988) structure and function of the microtubular cytoskeleton during endosperm development in wheat: an immuno-fluorescence study. *Protoplasma* **146**: 18-27.
- Vijayaraghavan, M.R., and Prabhakar, K. (1984) The endosperm. In: Johri, B.M. (ed.) *Embryology of Angiosperms*. Springer-Verlag, Berlin, Heidelberg. pp. 319-376.
- XuHan, X. (1994) Microtubular configurations in higher plant embryogenesis and applications of microtubular configurations to the selection of somatic embryogenic cultures. In: *94-Symposium for Young Chinese Developmental Biologists*. Beijing. pp. 66-67.
- XuHan, X., Souvré, A., Roustan, J.-P., Petitprez, M., and Fallot, J. (1994) Cell-aging related configurations of cortical microtubules in carrot (*Daucus carota* L.) suspension cells. *Cytologia* **59**: 51-57.
- Yan, H., Yang, H.-Y., and Jensen, W.A. (1991) Ultrastructure of the developing embryo sac of sunflower (*Helianthus annuus*) before and after fertilization. *Can. J. Bot.* **69**: 191-202.
- Yeung, E.C. (1980) Embryogeny of *Phaseolus*: the role of the suspensor. *Z. Pflanzenphysiol. Bd.* **96**: 17-28.
- Yeung, E.C., and Cavey, M.J. (1988) Cellular endosperm formation in *Phaseolus vulgaris*. I. Light and scanning electron microscopy. *Can. J. Bot.* **66**: 1209-1216.

Acknowledgements

"In June 1990, being invited by Dr. Jan Schel, Professor Michel Willemse, Professor Jac van Went and Drs. Alfred Munting, I visited the Department of Plant Cytology and Morphology, Wageningen Agricultural University. I soon started my Ph.D. program under the supervision of Professor Willemse. The subject of the thesis was chosen in a meeting among Professor Willemse, Dr. André van Lammeren, Dr. Schel, and me, in a sunny afternoon..."

Xu XuHan «Great men, ordinary lives» 1990

The thesis presented here is completed today. I would like to take this opportunity to express my sincere appreciation to all the people who supported me in preparing this thesis. My acknowledgement first goes to my promoter, Professor Dr. Michiel Willemse. Without his understanding and support, I could not have finished this thesis. I very much appreciate all the wise guidance, critical comments, and indispensable help of my co-promoter, Dr. André van Lammeren. I will never forget those days and nights we worked together.

I am deeply indebted to Dr. Jan Schel. I greatly appreciate his encouragement and invitation which provided me an opportunity to start my research in the Netherlands. I am also very grateful to Professor Dr. van Went, with him the discussion is always interesting and helpful for me. Special thanks go to Siep Massalt for the photographs, Alex Haasdijk and Paul van Snippenburg for the artwork, Ning Ma and Henk Kieft for computer assistance, Adriaan van Aelst for electron microscope assistance, Gerrit van Geerenstein and Casper Pillen for greenhouse work, and Truus van de Hoef-van-Espelo and Regina van de Brink-de Jong for the secretarial help. My appreciation is also extended to my colleagues in the Department, Dr. Anne-Mie Emons, Dr. Coos Keijzer, Dr. Han Magendans, Dr. Gerd Hause and Dr. Bettina Hause, Dr. Alfred Munting, Ing. Norbert de Ruijter, Ir. Peter Wittich, Ir. Folbert Bronsema, Carmen Reinders, Tiny Franssen-Verheijen, Hetty Leferink-ten Klooster, Ir. Kees Straatman, Ir. Marja Thijssen for all the good

Acknowledgements

time I had with them in Wageningen. I acknowledge Wageningen Agricultural University for the financial support as well as many facilities provided.

I am very grateful to Professor Dr. J. H. Martin Willison for his invitation for me to work in Biology Department of Dalhousie University, Halifax, Canada. The precious stay of three months in his laboratory enabled me to finish one chapter, and also gave me a wider approach to do experiment. I am also thankful to Professor Dr. André Souv re at ENSAT, Toulouse, France, where I have an opportunity to study biotechniques which are of importance both for the thesis and for my scientific career.

The most sincere thank goes to my parents, to my brother, and especially to my wife Hui Yu. Their love accompanies me wherever forever.

June 1995

X. XuHan

Samenvatting

Ontwikkeling van zaden in *Phaseolus vulgaris* L., *Populus nigra* L. en *Ranunculus sceleratus* L. met speciale aandacht voor het microtubulaire cytoskelet

Zaden spelen een belangrijke rol bij de geslachtelijke voortplanting van planten. Een zaad bestaat uit een embryo en endosperm omgeven door een zaadhuid. Het embryo is de nieuwe generatie van de plant. Om de vorming, de differentiatie en de rijping van zaden te begrijpen zijn drie plantesoorten geselecteerd voor een vergelijkende cytologische en immunocytochemische studie. Hiervoor zijn de blaartrekkende boterbloem (*Ranunculus sceleratus* L.), de boon (*Phaseolus vulgaris* L.) en de populier (*Populus nigra* L.), gekozen. Bij dit onderzoek is speciaal aandacht besteed aan de ontwikkeling van embryo en endosperm en aan de microtubulaire configuraties die bij deze ontwikkeling optreden.

De embryogenese van de blaartrekkende boterbloem behoort tot het Onagrad type. In deze studie is echter een ontwikkelingspatroon gevonden dat daar van afwijkt. De basale cel van een driecellig, lijnvormig embryo vormt een meercellige suspensor die zich slechts beperkt ontwikkelt. De middelste cel en de topcel vormen het eigenlijke embryo. Dit houdt in dat het eigenlijke embryo niet alleen door de topcel gevormd wordt, maar ook door de subapicale cel. Dit is afwijkend van het Onagrad patroon. Het endosperm neemt het grootste deel van het zaad in beslag en is gevuld met zetmeel en vet. De endospermcellen die de suspensor omgeven, blijven bestaan gedurende de ontwikkeling, terwijl de endospermcellen die het eigenlijke embryo omgeven degenereren. Hieruit blijkt dat er een plaatsafhankelijke interactie tussen embryo en endosperm bestaat.

De verdeling van wandingroeiingen zoals voorkomend in "transfer"-cellen en de verdeling van multivesiculaire structuren is onderzocht in relatie tot het transport van metabolieten. Wandingroeiingen komen voor in antipoden en wijzen op de overdracht van metabolieten van de apoplast van de sporofyt naar de symplast van de megagametophyt (Hoofdstuk 2). Als de zaadhuid differentieert, vertoont het microtubulaire cytoskelet een verscheidenheid aan

configuraties die van belang is voor de vormgeving van de cellen, en voor de vorming van wandingroeiingen die niet tot het "transfer"-type behoren. Gedurende de veroudering van de zaadhuid raakt de microtubulaire organisatie verstoord in de cellen van de zaadhuid (Hoofdstuk 4).

Het embryo van de boon heeft drie cytomorfologische zones te weten het eigenlijke embryo, de suspensor-nekzone en de basale zone van de suspensor. De ultrastructuur en de microtubulaire cinguraties zijn in deze zones onderzocht. De resultaten geven aan dat de ontwikkeling van de structuur gerelateerd is aan de ontwikkeling van de functie van de drie embryogedeelten. Ook is het microtubulaire cytoskelet betrokken bij de ontwikkeling van de structuur in de drie zones. In het bijzonder is het van belang voor de ontwikkeling van de vorm van het eigenlijke embryo en de suspensor. Als gekeken wordt naar de distributie van wandingroeiingen in het embryo, is het ook vanuit structureel oogpunt verklaarbaar dat de embryosuspensor een taak heeft bij het transport van voedingsstoffen vanuit de integumenten en de nucellus naar het eigenlijke embryo (Hoofdstuk 3).

Het endosperm van de blaartrekkende boterbloem (Hoofdstuk 5), de boon (Hoofdstuk 6) en de populier (Hoofdstuk 7 en 8) behoren tot het vrij - nucleaire type. Dit type is gekenmerkt door een coenocytische beginfase waarin vrije kernen verdeeld zijn over het cytoplasma van de bevruchte centrale cel. De coenocytische fase wordt opgevolgd door een fase van celvorming. Het proces van celvorming kan op 3 manieren gestalte krijgen te weten een Perifeer type zoals te zien is in de blaartrekkende boterbloem, een Traag ontwikkelend type dat voorkomt bij bijvoorbeeld de boon, en een Lineaire type zoals te zien is bij bijvoorbeeld de zonnebloem. Bij het "perifere type" omgeven de kernen de centrale vacuole en geven daar aanleiding tot de vorming van alveoli. Het proces van cellularisatie verloopt hier centripetaal. Bij het "traag ontwikkelende type" vormen de vrije kernen alleen alveoli in het micropylaire gebied terwijl aan de chalazale zijde de vrije kernen blijven bestaan. De cellularisatie verloopt vanaf de micropylaire zijde naar de chalazale zijde. In het "lineaire type" liggen al de vrije kernen in het micropylaire gebied en daar geven ze aanleiding tot de vorming van alveoli. De cellularisatie verloopt hier vanaf de micropylaire zijde naar de chalazale zijde. De endospermontwikkeling is onderzocht waarbij speciaal aandacht is gegeven aan de cellularisatie. Het Perifere en het Lineaire type zijn beide

synchroon terwijl het "trage ontwikkelingstype" asynchroon is (Hoofdstuk 9). Hoewel de weefselontwikkeling verschillend verloopt bij de drie typen, start het proces van cellularisatie altijd met de vorming van alveoli. Vervolgens treedt celvorming op terwijl de alveoli blijven bestaan. De vorming van alveoli wordt wel alveolatie genoemd en bestaat uit drie stappen te weten: (1) de ontwikkeling van celplaten in de internucleaire ruimten. De celplaat kan gevormd zijn tussen twee dochterkernen na een kerndeling of tussen twee niet-dochter kernen, (2) versmelting van celplaten aan de laterale zijden van de alveoli en fusie van celplaat-uiteinden met de celwand van de bevruchte centrale cel en (3) verlenging van de alveoli door groei van de vrij-groeiende uiteinden van de anticlinale celwanden in de richting van de centrale vacuole van de centrale cel. De cellularisatie van het endosperm stopt als de wanden van de alveoli elkaar ontmoeten in het centrum van de centrale cel waar oorspronkelijk de centrale vacuole lag.

Tijdens de alveolatie van het endosperm zijn de uiteinden van de vrij-groeiende anticlinale wanden geassocieerd met microtubuli die een spiegel-symmetrische configuratie vertonen met betrekking tot het vlak van de celwand. Op de plaatsen waar celplaten fuseren, worden gewoonlijk Y-vormige wandvergroeiingen waargenomen. De microtubuli verlopen hier parallel aan de bissectrice van de hoek waaronder de wanden staan. Zo vormen zij ook een Y-vormige, ofwel axiaal-symmetrische configuratie die alterneert met die van de celwanden (Hoofdstuk 6). De microtubuli in de spiegel-symmetrische en axiaal-symmetrische configuraties vormen een fragmoplast die al de uiteinden van de vrij-groeiende anticlinale celwanden bedekt. Deze totale fragmoplast wordt in dit proefschrift de alveolaire fragmoplast (a-fragmoplast) genoemd. Hij functioneert als een mechanisch ondersteunend netwerk bij de groei van de celplaat gedurende de alveolatie. De a-fragmoplast en de mitose-cytokinese gerelateerde fragmoplast, in dit proefschrift m-fragmoplast genoemd, worden gekarakteriseerd als functioneel verschillende structuren. Er wordt voorgesteld om de term fragmoplast te handhaven als een algemene term voor beide typen (Hoofdstuk 8).

Summary

Seed plays an important role in the sexual reproduction of higher plants. A seed consists of a seed coat enveloping the endosperm and the embryo which is the new generation of the plant. To understand seed formation, differentiation, and maturation, three species, i.e. celery-leaved buttercup (*Ranunculus sceleratus* L.), bean (*Phaseolus vulgaris* L.), and poplar (*Populus nigra* L.), were selected for comparative cytological and immunocytochemical investigations. Special attention has been paid to embryo and endosperm development and to the configurations of the microtubular cytoskeleton during these processes.

The embryogeny of celery-leaved buttercup belongs to the Onagrad Type. However in this study, the pattern of embryo development appeared different from the Onagrad Type. From three-celled linear proembryos, the basal cell gave rise to a multicellular suspensor that exhibited limited development, whereas the middle and upper cells formed the embryo proper. Therefore, the embryo proper is not only formed by the apical cell but also by the sub-apical cell. The endosperm occupies the greater part of the mature seed, and is filled with lipid and starch. Endosperm cells surrounding the embryo suspensor persist whereas those surrounding the embryo proper degenerate, indicating a site-specific interaction between the endosperm and the embryo. The distributions of wall ingrowths of the transfer type and multivesicular structures are analyzed in relation to metabolite transport. Wall ingrowths are abundant in the antipodal cells and point to the transfer of metabolites from the apoplast to the symplast of the megagametophyte (Chapter 2). During the process of seed coat differentiation the microtubular cytoskeletons of the seed coat cells exhibit various configurations, functioning in cell and in the formation of wall ingrowths of a non-transfer-type. During cell aging microtubular organizations became disturbed in the seed coat cells (Chapter 4).

In bean, the embryo exhibits three cytomorphological zones: the embryo proper, the suspensor neck zone and the suspensor basal zone. The ultrastructure, including microtubular cytoskeleton, was analyzed. The results indicate that the structural differentiation of the embryo zones is related to the

functional differentiation of the three zones. Also the microtubular cytoskeleton is involved in the structural differentiation of the three zones. In particular, it functions in the development of the shape of the embryo proper and the suspensor. Taken the distribution of wall ingrowths in the embryo into account, it is plausible from the structural point of view, too, that the embryo suspensor functions in the transport of nutrients from the integuments and nucellus cells towards the embryo proper (Chapter 3).

The endosperms of celery-leaved buttercup (Chapter 5), bean (Chapter 6) and poplar (Chapters 7 and 8), all belong to the Free Nuclear Type which is characterized by an initial coenocytic phase in which free nuclei are distributed throughout the cytoplasm of the fertilized central. The coenocytic phase is followed by cellularization, studied in detail in this work. In the process of cellularization, three sub-types of developmental patterns are distinguished, i.e., the Peripheral Type as seen in e.g., celery-leaved buttercup and poplar, the Lingering Type as seen in e.g., bean, and the Linear Type as seen in e.g., sunflower. In the Peripheral Type, the free nuclei of the endosperm surround the central vacuole and give rise to alveoli all around. Cellularization proceeds centripetally. In the Lingering Type, the free nuclei surround the central vacuole but the endosperm only forms alveoli in the micropylar area, whereas the chalazal area remains free nuclear. Cellularization proceeds from the micropylar side towards the chalazal side. In the Linear Type, the free nuclei are only present in the micropylar area where they gave rise to alveoli. Cellularization proceeds from here towards the chalazal side. Endosperm development is investigated with special attention to the process of cellularization. The Peripheral and Linear Types belong to the synchronous cellularization type, and the Lingering Type is an asynchronous type (Chapter 9).

Although tissue development proceeds differently, the process of the nuclear endosperm cellularization starts with the formation of alveoli, and proceeds by both alveolus formation and cell formation. The formation of alveoli, termed *alveolation*, includes three steps: (1) mitosis-cytokinesis derived and non-mitosis-cytokinesis derived cell plate formation in internuclear spaces, (2) fusion of cell plates at the lateral sides of the alveoli, and fusion of the extending cell plates with the wall of the fertilized central cell, and (3) elongation of alveoli by the extension of the freely growing wall

edges of the anticlinal walls at the side towards the central vacuole of the central cell. Cellularization of the endosperm ends when the elongating alveoli meet in the central part of the original central vacuole of the central cell.

During the endosperm alveolation, the freely growing edges of the anticlinal walls are associated with extensive MTs with mirror symmetric organization with the respect of the wall plane. In the areas where cell plates fuse, Y-shaped junctions of walls are usually formed. Here, populations of microtubules run well parallel to the bisectors of the wall angles, forming an axial symmetric, Y-shaped organization, too, staggering with the Y-shaped walls (Chapter 6). The microtubules in mirror symmetric and axial symmetric configurations form one phragmoplast covering the freely growing wall edges of all the alveoli. Such phragmoplast is termed *alveolar phragmoplast* (*a-phragmoplast*) in this thesis. It functions as a mechanically supporting framework for cell plate growth throughout the process of alveolation. The *a-phragmoplast* and the mitosis-cytokinesis related phragmoplast, termed *m-phragmoplast* in this thesis, are characterized as functionally different structures. It is suggested that the term phragmoplast should be maintained as a general term for both types of phragmoplasts (Chapter 8).

Résumé

Développement de la graine chez *Phaseolus vulgaris*, *Populus nigra*, et *Ranunculus sceleratus*. Etude particulière du cytosquelette microtubulaire

La graine est l'expression finale de la reproduction sexuée chez les Plantes supérieures. Elle comprend trois parties : l'enveloppe, l'albumen et l'embryon qui représente la nouvelle génération. Dans le but de comprendre la formation, la différenciation et la maturation de la graine, trois espèces, *i.e.* la Renoncule scélérate (*Ranunculus sceleratus* L.), le Haricot (*Phaseolus vulgaris* L.), et le Peuplier (*Populus nigra* L.), ont été utilisés pour effectuer des comparaisons cytologiques et immunocytologiques.

L'embryogenèse de la R. scélérate est définie par les auteurs comme étant de type Onagre. Cependant le mode d'embryogenèse que nous avons observé diffère du type Onagre. La cellule basale des proembryons tricellulés forme le suspenseur multicellulaire qui a un développement limité. La cellule moyenne et la cellule supérieure forment l'embryon proprement dit. L'albumen engorgé en lipides et en amidon occupe la majeure partie de la graine. Les cellules de l'albumen qui entourent le suspenseur persistent alors que celles qui entourent l'embryon dégénèrent ; ce qui signifie qu'il existe une interaction albumen-embryon dépendante de la position. Les invaginations des parois des cellules du type cellule de transfert et les structures multivésiculaires ont été analysées en relation avec le transfert de métabolites. Dans les cellules antipodales de nombreuses invaginations de parois se mettent en place parallèlement au transfert de métabolites de l'apoplaste vers le symplaste (Chapitre 2). Pendant le développement de l'embryon, le tégument de la graine se différencie et devient mature ; simultanément le cytosquelette montre des configurations différentes liées au développement des invaginations pariétales des cellules du type non cellule de transfert et à la morphogénèse des cellules. Pendant la sénescence cellulaire l'organisation microtubulaire des cellules se désorganise (Chapitre 4).

Chez le Haricot, l'embryon présente trois zones distinctes cytomorphologiquement : l'embryon proprement dit, la zone apicale du suspenseur et la zone basale du suspenseur. Les microtubules du cytosquelette sont impliqués dans la différenciation des structures des trois zones pendant les modifications de forme de l'embryon proprement dit et du suspenseur. Le suspenseur joue un rôle dans le transport de nutriments (Chapitre 3).

L'albumen de la R. scélérate (Chapitre 5), du Haricot (Chapitre 6) et du Peuplier (Chapitre 7 et 8) est caractérisé par une phase de développement initiale cénocytique où les noyaux sont libres dans le cytoplasme de la cellule centrale fécondée (*Type noyaux libres*). La phase cénocytique est suivie d'une phase de cellularisation que nous avons étudiée de façon approfondie. Au cours de la cellularisation, nous distinguons trois sous-types de développement: le *type périphérique* de la R. scélérate et du Peuplier, le *type lent* du Haricot et le *type linéaire* du Tournesol.

Chez le type périphérique, l'albumen cénocytique qui entoure la vacuole centrale s'alvéolise en position distale pendant que la cellularisation progresse de façon centripète. Chez le type lent, les noyaux libres sont distribués autour de la vacuole centrale mais l'albumen ne forme des alvéoles que dans la zone micropylaire et la cellularisation progresse de la zone micropylaire vers la zone chalazienne. Chez le type linéaire, les noyaux libres sont situés uniquement dans la zone micropylaire où se forment les alvéoles ; la cellularisation progresse comme dans le type lent. Une attention particulière a été donnée à la cellularisation pendant l'étude du développement de l'albumen. La cellularisation est synchrone chez les types périphérique et linéaire, elle est asynchrone chez le type lent (Chapitre 9).

Alors que le développement tissulaire s'effectue de façon différente chez les trois types, par contre la cellularisation de l'albumen nucléaire commence toujours par la formation d'alvéoles et se poursuit par la formation simultanée des alvéoles et des cellules. La formation des alvéoles, ou *alvéolisation*, comprend trois étapes : 1) la formation dans les espaces inter-nucléaires des plaques cellulaires qui s'intercalent entre les noyaux fils et de celles qui s'intercalent entre les noyaux non fils, 2) la fusion des plaques cellulaires formant les côtés de l'alvéole et la fusion des plaques cellulaires allongées avec la paroi du sac embryonnaire, et 3) l'agrandissement des alvéoles

résultant de l'allongement des bords des parois anticlinales du côté de la vacuole centrale.

Pendant l'alvéolisation de l'albumen, les bords libres des parois anticlinales en croissance sont associés avec de nombreux microtubules disposés de façon symétrique par rapport au plan de la paroi (symétrie bilatérale). Dans les zones où les plaques cellulaires fusionnent, les parois formées se rejoignent pour former un Y et les microtubules s'orientent parallèlement aux bissectrices des angles formés par les parois. Ils sont disposés suivant un axe de symétrie passant par le point de jonction des parois, formant également une figure en Y qui s'intercale avec le Y formé par les parois cellulaires (Chapitre 6).

Les microtubules disposés en symétrie bilatérale et en symétrie axiale forment une sorte de réseau phragmoplastique couvrant l'ensemble des bords libres en croissance de toutes les alvéoles. Cette disposition est appelée phragmoplaste alvéolé (*phragmoplaste-a*). Il joue un rôle mécanique de maintien des plaques cellulaires en croissance pendant l'alvéolisation de l'albumen. Le phragmoplaste-a et le phragmoplaste lié à la mitose-cytocinèse, dénommé *phragmoplaste-m*, ont été caractérisés (Chapitre 8). Nous proposons que le terme de **phragmoplaste** soit conservé pour les deux types de phragmoplaste.

菜豆，欧洲黑杨和芹叶毛茛的种子发育及其微管骨架

(摘要)

种子在高等植物有性生殖中起着重要作用。它由种皮及其包被的胚乳和胚构成，其中胚是新一代的植物个体。本文以毛茛，菜豆和欧洲黑杨为材料，对种子的产生，分化和成熟过程进行了细胞学和免疫细胞化学的比较研究。

芹叶毛茛的胚胎发育属柳叶菜形。但本文报道了一种不同于柳叶菜型的胚胎发育类型。自三细胞胚起，基细胞发育成多细胞构成的胚柄，而顶细胞和中间细胞共同发育为胚本体。因此胚本体不仅由顶细胞构成，而且亦由中间细胞参与构成。这与传统的顶细胞单独发育成胚本体的模式不同。在成熟的芹叶毛茛种子中，胚乳占据了绝大部分空间，并贮有大量脂类和淀粉。胚乳细胞在胚柄处保存完好，但在胚本体周围消耗，衰败。这显示了胚和胚乳相互作用中的位点特异性。本文还对传递细胞型细胞壁内生和多泡体结构与代谢物的运输之间的关系进行了研究。在反足细胞中，大量的细胞壁内生显示了代谢物在质外体和共质体之间的运输关系（第二章）。种皮在胚乳发育期间分化，成熟。其间，微管骨架呈现出多种构型，并作用于非传递细胞型细胞壁的内生和细胞的形态建成。细胞在衰老过程中，微管骨架的组织形式遂失去常态并最终消失（第四章）。

菜豆的胚呈现出三个细胞形态不同的区域：胚本体，胚柄颈区和胚柄基区。对其超微结构包括微管构型的研究表明，胚胎结构的分化与这三个区的功能紧密相关。微管骨架参与这三个区的结构分化，其中，本文特别对在传递细胞型细胞壁内生的过程中以及在胚本体和胚柄在形态转变中的微管构型进行了研究。菜豆胚柄的超微结构显示了其具营养物传递的功能（第三章）。

芹叶毛茛，菜豆和欧洲黑杨的胚乳发育皆属于游离核型。在其共核体的初始期，胚乳游离核逐渐遍布于胚乳的周缘。细胞化过程随之开始。本文对胚乳的细胞化进行了重点研究。游离核型胚乳的发育可

分为三个亚型：向心型（例如芹叶毛茛和欧洲黑杨），延迟型（例如菜豆）和线型（例如向日葵）。向心型的胚乳细胞化过程是围绕中央液泡的胚乳产生蜂窝状细胞壁并向心生长。延迟型则是蜂窝状细胞壁只在珠孔端产生而合点端的胚乳保持游离核状态，细胞化过程由珠孔端向合点端发展。线型的胚乳细胞化过程是胚乳游离核只分布在珠孔端并就地产生蜂窝状细胞壁；细胞化由珠孔端向合点端发展。向心型和线型属于同步细胞化型，而延迟型属非同步化型（第九章）。上述三种胚乳细胞化类型的共同点是细胞化都以蜂窝状细胞壁形成而产生蜂窝状细胞做为开端。这一过程称为“蜂窝化”。它包括三个步骤：（1）有丝细胞分裂及非有丝细胞分裂所产生的细胞板在核间区形成；（2）这些细胞板向周围延伸生长并于相邻的细胞板融合，导致产生蜂窝状细胞；（3）这些融合后的细胞板形成垂直于胚囊壁的垂周壁并在胚囊内侧向心或向合点区生长。这些垂周壁的自由生长端仍然处于细胞板状态。胚乳的细胞化过程以垂周细胞壁在胚囊内侧的自由生长端于胚囊中央或合点端融合而告结束。

在胚乳蜂窝化过程中，垂周壁的自由生长端伴有大量密集的微管。这些微管形成以细胞壁自由生长端的面而成镜像对称的构型。在相邻三个蜂窝状细胞的垂周壁结合部，“Y”型的细胞壁形成。此处微管群平行于“Y”型壁的角平分线，并在总体上形成轴向对称的“Y”字构型，但与“Y”型细胞壁交错 $1/2$ 个角度（第六章）。上述两种构型的微管群交互结合在所有垂周细胞壁生长端上，形成一个蜂窝状成膜体——本文命名为“A型成膜体”。A型成膜体作为一个垂周细胞壁生长端的机械支撑网络在整个游离核胚乳蜂窝化过程中起作用。与A型成膜体相对应，有丝细胞分裂中的成膜体在本文中被称作“M型成膜体”。其产生，组织形式和功能都与A型成膜体有别。鉴于此，“成膜体”一词今后应作为A型及M型成膜体的统称而不应仅指M型成膜体。

Curriculum Vitae

Han XU (徐涵, English name in references as **X. XuHan**) was born in Qingdao City, Shandong Province of the People's Republic of China on 10 April 1961. After 11 years basic education in elementary and middle school, he entered in the Biology Department of Shandong University in 1980. He received his Bachelor of Science with his thesis titled "A study on callose fluorescence in the development of leaf stomata in several *Brassica* species" in July 1984. Then he conducted a 3-year post-graduate study in Forest Research Institute of Chinese Academy of Forestry in Beijing, under the supervision of Professor Wen-Dian Li, and was honored by the degree of Master of Agricultural Science, after defending his thesis on experimental study on the embryology of the intergeneric cross between *Populus simonii* and *Salix matsudana* in July 1987. He worked, thereafter, as a editor in Chinese Science and Technology Press in Beijing for three years, in the meantime he continued his research in Chinese Academy of Forestry. In June 1990 he was accepted in a sandwich Ph.D. program in the Department of Plant Cytology and Morphology, Wageningen Agricultural University, the Netherlands, under the supervision of Professor Dr. Michiel T.M. Willemse, and Dr. André A.M. van Lammeren. A qualifying examination for starting the Ph.D program was done successfully in Wageningen at April 24, 1991. The research focused on morphogenesis and the microtubular cytoskeleton during angiosperm seed development. During his sandwich program, he also worked as a visiting scientist for three months in Biology Department, Dalhousie University in Halifax, Canada where he did research on ultrastructural changes of carrot cells under freezing stress. From January 1992 till present he has been working on sunflower somatic embryogenesis, gene delivery to sunflower zygotic and somatic embryos, and ultrastructural and immunocytochemistry of carrot and sunflower embryogenic and aging calli, in Laboratoire de Biotechnologie et Amélioration des Plantes, École Nationale Supérieure Agronomique de Toulouse, Institut National Polytechnique de Toulouse, France.